



THE HONG KONG
POLYTECHNIC UNIVERSITY

香港理工大學

Pao Yue-kong Library

包玉剛圖書館

Copyright Undertaking

This thesis is protected by copyright, with all rights reserved.

By reading and using the thesis, the reader understands and agrees to the following terms:

1. The reader will abide by the rules and legal ordinances governing copyright regarding the use of the thesis.
2. The reader will use the thesis for the purpose of research or private study only and not for distribution or further reproduction or any other purpose.
3. The reader agrees to indemnify and hold the University harmless from and against any loss, damage, cost, liability or expenses arising from copyright infringement or unauthorized usage.

IMPORTANT

If you have reasons to believe that any materials in this thesis are deemed not suitable to be distributed in this form, or a copyright owner having difficulty with the material being included in our database, please contact lbsys@polyu.edu.hk providing details. The Library will look into your claim and consider taking remedial action upon receipt of the written requests.

THE HONG KONG POLYTECHNIC UNIVERSITY

INSTITUTE OF TEXTILES AND CLOTHING

A Smart Temperature Responsive Polymeric System for Textile Materials

YANG Hengrui

A Thesis Submitted

in Partial Fulfilment of the Requirements

for the Degree of Doctor of Philosophy

April 2012

CERTIFICATE OF ORIGINALITY

I hereby declare that this thesis is my own work and that, to the best of my knowledge and belief, it reproduces no material previously published or written, nor material that has been accepted for the award of any other degree or diploma, except where due acknowledgement has been made in the text.

----- (Signed)

----- YANG Hengrui ----- (Name of student)

Abstract

*Stimuli-responsive polymeric materials can adapt to various surrounding environments, convert chemical and biochemical signals into optical, electrical and thermal signals, or change wettability and adhesion upon external stimuli. In this thesis, a cotton fabric was modified with a thermo-responsive polymer, Poly(*N*-isopropylacrylamide) (PNIPAAm).*

For low grafting efficiency sample, ^1H solid-state NMR techniques were used to characterize the molecular structure and dynamics of the PNIPAAm brushes, while still grafted on the cotton fabric surfaces, avoiding the destructive cleaving procedures. The results demonstrate that the motion of the grafted PNIPAAm brushes is restricted as the temperature rises above the low critical solution temperature (LCST), which was estimated to be ~ 34 °C. Variable temperature (VT) experiments were used to investigate the nature of the hydrophilic-hydrophobic transitions of the grafted polymer. The ^1H solid-state NMR techniques used in this study was proved to be an extremely sensitive and precise way to probe in-situ the LCST transition of the PNIPAAm brushes.

The grafting efficiency of the polymer on the cotton surface has been greatly improved after a short-time UV pretreatment coupled with a room temperature immobilization method. The modified cotton fabric was characterized by FTIR, XPS, NMR, TGA, SEM and OM. It was shown that the

cotton fibers were covered with PNIPAAm brushes with a high grafting efficiency. The PNIPAAm molecular brushes were cleaved from the cotton substrate and characterized by GPC to determine the molecular weight (M_n), molecular weight distribution (PDI) and grafting efficiency. The surface of the temperature responsive cotton fabric is superhydrophobic with a water contact angle (CA) up to 140° at 40°C , and superhydrophilic with a water CA of 0° at room temperature, and this conversion was repeated many times in a short time period and a fully reversible transition was observed. More interestingly, this smart cotton fabric surface can capture moisture from atmosphere at lower temperature and release water at higher temperature. This concept may provide a new insight into solutions for fresh water conversion and purification.

This study presents a valuable synthesis and analysis route towards stimuli-responsive cotton fibers which may be of exceptional applications as novel intelligent fabrics for the textile related industries. On the other hand, this smart PNIPAAm modified may also be used to exploit water from dew and mist, and it may pave the way for solving the problem of water crisis in deserts or arid areas.

Publications

Academic Journal Papers

1. **Hengrui Yang**, Haijin Zhu, M.M.R.M. Hendrix, N.J.H.G.M. Lousberg, G. de With, A.C.C. Esteves*, John H. Xin*, *Temperature triggered collection and release of water from fogs by a sponge-like cotton fabric*. (Accepted by **Advanced Materials**)
2. **Hengrui Yang**, A. Catarina C. Esteves, Haijin Zhu, Dujin Wang, and John H. Xin*, *In-situ study of the structure and dynamics of thermo-responsive PNIPAAm grafted on a cotton fabric*. **Polymer**, 2012, 53 3577-3586
3. Bin Fei, Zongyue Yang, **Hengrui Yang**, Zhigang Hu, Ronghua Wang, John H. Xin*, *Schizophrenic copolymer from natural biopolymer by facile grafting*, **Polymer**, 2010, 51 890–896
4. Xianqiong Chen, Yuyang Liu, Haifeng Lu, **Hengrui Yang**, Xiang Zhou and John H. Xin*, *In-situ growth of silica nanoparticles on cellulose and application of hierarchical structure in biomimetic hydrophobicity*, **Cellulose**, 2010, 17 1103-1113

Conference Paper

5. **Hengrui Yang**, Haijin Zhu, Dujin Wang, John H. Xin, *Structure of The*

Thermo-responsive Poly(N-isopropylacrylamide) Grafted from Cotton Fabric

*Substrate. **European Polymer Congress.** Granada, Spain. Jun. 2011.*

Acknowledgements

At the beginning of this thesis, I would like to acknowledge many people who helped me in these three years in Hong Kong, Netherlands and Beijing. First of all, I would like express my sincerest gratitude to my chief supervisor professor John H Xin for providing the opportunity for this project to be taken. Without his expert advice, support and guidance, this project would not have been possible. I also would like to thank Prof. Xin for your fully support my visiting studying in Netherlands, which made my vision broader.

I would like to thank my co-supervisor Dr. A.C.C. Esteves(Catarina) in Eindhoven University of Technology. Thanks for guiding my study in TU/e, I really enjoyed the time we work together. Her warm encourage and good advice were invaluable on both an academic and a personal level, which I am extremely grateful.

My thanks also go to previous group leader professor Dujin Wang in Beijing. The solid-state NMR experiments were finished with his help. Thanks for always been my backup when I face the problem even though I was graduate.

Special thanks go to Prof. G. de With(Bert) for accepting me studying in his group in TU/e. Many thanks for M.M.R.M. Hendrix(Marco) and N.J.H.G.M. Lousberg(Nick) for helping me with experiments of OM, SEM and AFM.

Thanks my friends Haifeng Shi and Jing Li gave me many supports when I just

arrived in Hong Kong, their warm helps made me feel not alone in a new place.

Thanks my friend Baoquan Xie sharing the great experience when I applied the PhD position.

Thank my friends Yulan Chen, Feng Wang, Donglin Tang, Jianbin Lin, Mingyu Guo, Jing Wu, Xianwen Lou and Jiayi Cui who were also fighting in field of chemical synthesis. Thank for your kindness, friendly supports and useful discussions.

Thank my group mates in Hong Kong and Netherlands: Xianqiong Chen, Yi Wang, Bin Fei, Haifeng Lu, Li Li, Xiaowen Wang, Zongyue Yang, Yeeye Kong, Shijie Shao, Mark, Camille, Qinglin Guan, Lijing Xue, Maarten, Delei Chen. All of you are the treasure in my life.

Sincere thank my PhD financial support from the C.C. Lee Scholarship of the Lees Charitable Foundation Limited and the Hong Kong Polytechnic University Niche Areas Scheme.

感谢我的爸爸妈妈给了我整个世界，谢谢你们爱我的优点也爱我的缺点，谢谢你们认为我是世上最聪明漂亮的孩子，谢谢你们说“不怕，累了回来就好”，谢谢你们给我的不是财富，不是权力，是一颗会微笑的心。

最后谢谢我的先生朱海锦。都说人生就像是不知疲惫的旅行，而朋友就像是旅途中的驿站，每旅行到一个地方都会在驿站寻得休息和甘甜的泉水，然后又上路了，当你回头，座座驿站矗立身后就像人生的财富。而这次当我再次

启程，我很高兴我将不再独自前行，而是有你相伴。“愿得一心人，白首不相离”听你倾谈，倾谈给你听便是幸福。

TABLE OF CONTENTS

Chapter 1

Introduction	1
1.1 Research background	2
1.2 Significance of the study	3
1.3 Methodology	5
1.4 Framework of thesis	7

Chapter 2

Literature review	9
2.1 Stimuli-responsive polymer	10
2.1.1 Temperature-responsive polymer	11
2.1.2 pH-sensitive polymers	17
2.1.3 Electro- and light-sensitive polymers	19
2.2 Surface modification	21
2.2.1 Coating by physical force	21

2.2.2 Chemical modification to the substrates	22
2.2.2.1 Grafting-to method	22
2.2.2.2. Grafting-from method	24
2.3 The theory of wettability	30
2.3.1 Surface free energy	31
2.3.2 Surface micro structure	33
2.3.2.1 Wenzel model	34
2.3.2.2 Cassie model	36
2.4 The boundary between hydrophilic and hydrophobic	37
2.5 Wettability in natural world	39
2.6 Wettability of the biomimetic artificial surfaces	43
2.7 Reference	47
Chapter 3	
Grafting temperature responsive polymer onto cotton fiber	65
3.1. Introduction	66

3.2 Experimental	68
3.2.1 Materials	68
3.2.2 Instruments	68
3.2.3 Preparation of the cotton fabric initiator	69
3.2.4 Grafting of N-isopropylacrylamide from the initiator- functionalized cotton fabric	70
3.3 Result and discussion	72
3.3.1 Synthesis of Cotton-PNIPAAm-L polymer grafted surface via SI-ATRP	72
3.3.2 Characterization of Cotton-PNIPAAm-L grafted cotton surface	73
3.3.2.1 Fourier transform infrared spectroscopy (FTIR)	73
3.3.2.2 X-Ray photoelectron spectroscopy (XPS)	74
3.3.2.3 Scanning electron microscopy (SEM)	76
3.3.2.4 Static ¹ H wideline NMR spectra	78
3.3.2.5 The covalent bond between grafted polymer and substrate	84

3.4 Conclusions	87
3.5 References	89
Chapter 4	
Thermo-responsive behavior of the Cotton-PNIPAAm-L	95
4.1 Introduction	96
4.2 Experimental	97
4.3. Results and Discussion	97
4.3.1 ¹ H static spectroscopy	98
4.3.2 ¹ H MAS Spectroscopy	102
4.4 Conclusions	107
4.5 References	109
Chapter 5	
Improvement of the functionalization of a cotton fabric with a thermo-responsive polymer: Highly-grafted fabric (Cotton-PNIPAAm-H)	113
5.1 Introduction	114

5.2 Experiment	115
5.2.1 Materials	115
5.2.2 Instruments	115
5.2.3 Pre-treatments of the fabric	117
5.2.4 Immobilization of the polymerization initiator on the cotton fabric	118
5.2.4.1 Low temperature method	118
5.2.4.2 Room temperature method	119
5.2.4.3 High temperature method	119
5.2.5 Polymerization of N-Isopropylacrylamide (NIPAAm) from the initiator-immobilized cotton fabric	119
5.2.6 Cleavage of the grafted PNIPAAm	120
5.3 Result and discussion	121
5.3.1 Optimization of the pre-treatment of the cotton fabric	121
5.3.2 Optimization of the immobilization of the polymerization initiator on the cotton fabric: synthesis and characterization	126

5.3.2.1 Low temperature method	126
5.3.2.2 Room temperature method	126
5.3.2.3 High temperature method	128
5.3.3 Synthesis and characterization of the highly-grafted fabric (Cotton-PNIPAAm-H) via Surface-Initiated Atom Transfer Radical Polymerization (SI-ATRP)	130
5.3.3.1 FTIR spectroscopy	131
5.3.3.2 XPS	133
5.3.3.3 Grafting efficiency and the product compositions	134
5.3.3.3 NMR spectroscopy	136
5.3.3.4 TGA	138
5.3.3.5 GPC	140
5.3.3.6 SEM	141
5.3.3.7 OM	143
5.4 Conclusion	144
5.5 Reference	146

Chapter 6

The superamphiphilic switch behavior and humidity collecting ability of the highly grafted cotton fibers 151

6.1 Introduction 152

6.2 Experiment 153

6.2.1 Materials 153

6.2.2 Instruments 153

6.2.3 Synthesis of pure PNIPAAm 155

6.2.4 Humidity collection experiments 155

6.3 Results and Discussion 156

6.3.1 The superamphiphilic property of Cotton-PNIPAAm-H 156

6.3.1.1 Phase transition between superhydrophilicity and superhydrophobicity 156

6.3.1.2 Thermal responsive property 159

6.3.1.3 Swelling and deswelling triggered by temperature 161

6.3.2 Synthesis of pure PNIPAAm polymer 163

6.3.3 Humidity collecting ability of grafted cotton fiber	170
6.4 Conclusion	172
6.5 Reference	174
Chapter 7	
Conclusions and suggestion for future work	179
7.1 Conclusions	180
7.1.1 Low grafting efficiency sample	180
7.1.2 Improve the grafting efficiency	181
7.1.3 High grafting efficiency sample	181
7.2 Future work suggested	182

List of Figures

- Figure 2.1. A plot of typical polymer binary solution phase behavior including both an LCST a UCST.....12
- Figure 2.2. The transition of PNIPAAm molecule conformation in water at low (left) and high (right) temperature.....14
- Figure 2.3. Schematic illustration of photopolymerization on the glass plate: (a) immobilization of DATMS silane on to the surface of glass plate; (b) formation of cross-linked PNIPAAm layer on the surface; (c) reversible change of hydrophobic/hydrophilic surface properties....16
- Figure 2.4. Schematic illustration of the change of water meniscus height in capillary tube: (a) low temperature (20 °C); (b) high temperature (40 °C).....16
- Figure 2.5. Thermal responsive wettability for a (a) smooth and (b) PNIPAAm-modified rough surface.....17
- Figure 2.6. Schematic representation of the switching behavior of the mixed PE brushes upon the change of pH: low pH (a) and high pH (b).....18
- Figure 2.7. The water contact angle of the modified gold surface in different pH values: (a) The water droplet at pH=1, CA about 145°; (b) The water droplet at pH=13, CA near 0°.....19

Figure 2.8. Schematic diagram of the switch from straight (hydrophilic) to bent (hydrophobic) molecular conformations.....	20
Figure 2.9. Schematic illustration of the “Grafting-to” process at (a) low densities, (b) high densities.....	24
Figure 2.10. ATRP activation rate constants for various ligands with EtBriB in the presence of $\text{Cu}^{\text{I}}\text{Y}$ ($\text{Y}=\text{Br}$ or Cl) in MeCN at 35 °C: N2, red; N3, black; N4, blue; amine/imine, solid; pyridine, open. Mixed, left-half solid; linear, \square ; branched, \blacktriangle ; cyclic, \bullet	27
Figure 2.11. Synthesis of triblock copolymer brush, PS- <i>b</i> -PMA- <i>b</i> -PS by SI-ATRP.....	30
Figure 2.12. The critical surface tension of solid surface.....	32
Figure 2.13. The forces balance of a liquid drop on a solid surface demonstrated by Eq. 2.1.....	33
Figure 2.14. Wenzel model.....	35
Figure 2.15. Cassie model.....	37
Figure 2.16. (a), (b), (c) were SEM images of lotus leaf; (d) the fitted curve based on calculated data (contact angle, in degrees, against the mean outer diameter of protruding structures, in micrometers).....	40

Figure 2.17.(a)SEM images of duck feather and butterfly wing; (b) the models proposed for mechanism of distinct adhesion dependent on the direction along and against the RO direction.....	41
Figure 2.18. Images captured from a side view revealed the vortical footprints of the water strider.....	42
Figure 2.19. (a) side view of Gerridae’s leg in water; (b), (c) SEM images of mirco-, nano- structure on a leg.....	43
Figure 2.20. (a), (b), (c) SEM images of surface structure of lotus-like ACNT films; (d) sliding behavior of a water droplet on the films surface.....	44
Figure 2.21. Photoes of water drop on surface at different angles (a)0°, (b)45°, (c)90°, (d)180°.....	45
Figure 2.22. The contact angle results under various temperatures and pH values.....	46
Figure 3.1. FT-IR spectra of: a) bare cotton fabric and b) Cotton-PNIPAAm-L..	74
Figure 3.2. XPS overview spectra of: a) bare cotton surface and b) Cotton-PNIPAAm-Br surface.....	75

-
- Figure 3.3 SEM images: a) and b) bare cotton fabric; c) and d) Cotton-PNIPAAm-L. The rectangles in a) and c) represent typical areas selected for the magnifications of b) and d), respectively.....77
- Figure 3.4 ^1H static spectra of Cotton-A-Br and Cotton-PNIPAAm-L samples. Both spectra were recorded at room temperature and atmospheric humidity conditions.....80
- Figure 3.5 Line-fitting results of the wideline spectra. a) Cotton-ATMS-Br; b) Cotton-PNIPAAm.....81
- Figure 3.6 ^1H static spectra measured at room temperature (295 K) and 329 K: (a) Cotton-A-Br and (b) Cotton-PNIPAAm-L sample. For visualization purposes the spectra of Cotton-PNIPAAm-L measured at 329 K was horizontally shifted.....84
- Figure 3.7 MAS ^1H NMR spectra of Cotton-ATMS-Br and Cotton-PNIPAAm samples at room temperature and atmospheric humidity. The spectra were recorded at (a) room temperature (295 K) and (b) 329 K. The MAS rate was 8 kHz.....85
- Figure 4.1 ^1H NMR static spectra of Cotton-A-Br and Cotton-PNIPAAm-L soaked in D_2O . (a) Spectra of Cotton-A-Br measured at the temperatures of 295 K-330 K; (b) and (c) are the spectra of Cotton-PNIPAAm-L sample measured at 295 K-312 K and 312

K-330 K, respectively. The narrow lines of the spectra (square region) were expanded and shown as insets. Arrows indicate the direction of intensity change upon increasing temperature.....99

Figure 4.2 ¹H MAS NMR spectra of Cotton-A-Br and Cotton-PNIPAAm-L soaked in D₂O. (a) Spectra of Cotton-A-Br measured at the temperatures ranging from 295-322 K; (b) and (c) are the spectra of Cotton-PNIPAAm-L sample measured at temperatures ranging from 295-313 K and 313-322 K, respectively. The arrows indicate the direction of intensity change upon increasing temperature.....104

Figure 4.3 The temperature dependence of peak intensities at the resonances of 1.05 ppm in figure 9. The solid lines are included as guide for the eyes.....106

Figure 5.1. FTIR-ATR spectra of (a) untreated sample, (b) UV pretreated for 10min, (c) UV pretreated for 1hour.....122

Figure 5.2. FTIR spectra of (a) bare cotton sample, (b) Cotton-A-Br without UV pretreatment, (c) Cotton-A-Br with UV pretreatment.....124

Figure 5.3. FTIR spectra of (a) untreated cotton fabric sample, (b) Cotton-R-Br without UV pretreatment, (c) Cotton-R-Br with UV pretreatment.....127

Figure 5.4. FTIR spectra of (a) bare cotton sample, (b) Cotton-F-Br without UV pre-treatment, (c) Cotton-F-Br with UV pre-treatment, (d) Cotton-A-F-Br with UV pre-treatment.....	129
Figure 5.5. FTIR spectra of (a) bare cotton, (b) Cotton-R-Br and (c) Cotton-PNIPAAm-H.....	133
Figure 5.6. XPS wide-scan and Br 3d spectra of (a) bare cotton, (b) Cotton-R-Br and (c) Cotton-PNIPAAm-H.....	134
Figure 5.7. NMR spectra of the extracted solution from the reactor. DMF is used as an internal reference for quantification of the monomer concentration.....	137
Figure 5.8. Monomer conversion versus time of reaction given by the monomer peak intensities (b and c in Figure 5.7) on samples taken at different reaction times.....	138
Figure 5.9. Thermogravimetric analysis (TGA) curves of (a) bare cotton, (b) Pure PNIPAAm, (c) Cotton-PNIPAAm-H.....	139
Figure 5.10. Cotton-g-PNIPAAm TGA (a) and DTGA (b) curves.....	139
Figure 5.11. Gel Permeation Chromatography of the cleaved PNIPAAm from the PNIPAAm-cotton sample.....	141

Figure 5.12. SEM images of (a) Cotton and (c) Cotton-PNIPAAm-H.(b) and (d) the magnified image of (a) and (c), respectively.....	142
Figure 5.13. Optical microscope images of (a) bare cotton fibers, (b) pre-wet bare cotton fibers, (c) Cotton-PNIPAAm-H fibers, (d) pre-wet Cotton-PNIPAAm-H fibers. The images were recorded at room temperature (20 °C).....	144
Figure 6.1. Water CAs at two different temperatures for a Cotton-PNIPAAm-H surface. Half cycles: T=23 °C, and integral cycles: T=40 °C. (a) 23 °C and (b) 40 °C.....	158
Figure 6.2. Water CAs at two different temperatures for a pure PNIPAAm film surface (a) 23°C, and (b) 40°C.....	158
Figure 6.3. Photo pictures of fibers in pure water, (a) 23°C (I) bare cotton fibers, (II) Cotton-PNIPAAm-H fibers; (b) 40°C (I) bare cotton fibers, (II) Cotton-PNIPAAm-H fibers.....	159
Figure 6.4. Recycling DSC curves of Cotton-PNIPAAm. (a) 1 st cycle, (b) 2 nd cycle, (c) 3 rd cycle, (d) 4 th cycle, (e) 5 th cycle.....	161
Figure 6.5. Optical microscope images of wetting Cotton-PNIPAAm-H under different temperatures: (a) and (b) at 22°C, (c) and (d) at 34°C, (e) and (f) at 40°C.....	163

Figure 6.6 GPC curves of (a)PNIPAAm 1#, (b)PNIPAAm 5#.....166

Figure 6.7. GPC curve of polymer obtained by (a) using PMDETA as ligand; (b)
using M_{e6} TERN as legand.....169

Figure 6.8. SEM images of Cotton-PNIPAAm synthesis by using M_{e6} TERN as
ligand.....170

Figure 6.9. Humidity collection ability: water uptake (%) given by the weight
increase in relation to the original weights of Cotton-PNIPAAm-H
fiber, pure PNIPAAm and bare cotton fiber samples, when exposed to
100% humidity atmosphere, at different temperatures.....171

List of Tables

Table 3.1 Moisture contents (A %) of Cotton-ATMS-Br and Cotton-PNIPAAm samples at 295K and 26% relative humidity.....	82
Table 3.2 Positions and assignments of the peaks in figure 3.6.....	85
Table 5.1. Grafting yield and weight uptake percentage of the Cotton-PNIPAAm-H sample obtained from weighting, NMR and TGA methods.....	135
Table 6.1. Different operating ways to do the ATRP grafting.....	167

List of Schemes

Scheme 2.1. Propylene subunit in a polypropylene polymer.....	10
Scheme 2.2. Temperature responsive polymers.(a)poly(N-isopropylacrylamide) (PNIPAAm);(b)poly(2-carboxyisopropylacrylamide)(PCIPAAm);(c))poly(N,N'-diethylacrylamide)(PDEAAm);(d)poly(N-acryloyl-N'-a lkylpiperazine);(e)poly(N-(L)-(1-hydroxymethyl)propylmethacrylam ide(P(L-HMPMAAm)).....	13
Scheme 2.3. Schematic representation of the synthesis of binary brushes. PS chains, gray; PVP chains, black.....	23
Scheme 2.4. Mechanism for the atom transfer radical polymerization.....	26
Scheme 3.1 Synthesis of Cotton-A-Br initiator.....	70
Scheme 3.2 Grafting NIPAAm from Cotton-A-Br initiator.....	71
Scheme 3.3 Schematic illustration of the synthesis of Cotton-PNIPAAm-L fabrics.....	72
Scheme 4.1 Schematic illustration of the hydrophilic-hydrophobic phase transition of PNIPAAm modified cotton surface. At temperature $T <$ LCST, the hydrogen bonds between water molecules and PNIPAAm molecules are preferentially established and PNIPAAm molecules	

adopt an extended configuration. When $T > LCST$, the PNIPAAm molecules preferentially form intra-molecular hydrogen bonds and the polymer chains undergo a coil configuration.....	102
Scheme 5.1. Immobilization of Cotton-ATMS-Br initiator at low temperature.....	124
Scheme 5.2. Immobilization of Cotton-R-Br initiator at room temperature.....	126
Scheme 5.3. Immobilization of Cotton-F-Br initiator at high temperature.....	128
Scheme 6.1 Small molecule initiated ATRP of NIPAAm monomer.....	164

List of Symbols and Abbreviations

Symbols and Abbreviations	Notes
ATRP	Atom Transfer Radical Polymerization
pH	Potential of Hydrogen
LCST	Lower Critical Solution Temperature
HCST	High Critical Solution Temperature
UCST	Upper Critical Solution Temperature
PNIPAAm	Poly(N-isopropylacrylamide)
HPC	Hydroxypropl Cellulose
CA	Contact Angles
AAO	Anodic Aluminum Oxide
ACNT	Aligned Carbon Nanotubes
AFM	Atomic Force Microscope
TiO ₂	Titanium Dioxide
ZnO	Zinc Oxide

List of symbols and abbreviations

UV	Ultraviolet Light
GPS	3-glycidoxypropyl trimethoxysilane
PS	Polystyrene
PVP	Polyvinyl Pyrrolidone
CRP	Controlled Radical Polymerization
Pn-X	Alkyl Halide Initiator
M_t^n/L	Metal Complex
Pn^*	Free Radical
$X-M_t^{n+1}/L$	Oxidized Metal Complex
k_{act}	Activation Rate
EtBriB	Ethyl-2-bromoisobutyrate
Me ₆ TREN	Tris[2-(dimethylamino)ethyl]amine
PMDETA	<i>N,N,N',N'',N'''</i> -Pentamethyldiethylenetriamine
PMMA	Polymethyl Methacrylate
PDI	Polydispersity Index

SI-ATRP	Surface Initiate Atom Transfer Radical Polymerization
DMF	Dimethyl Formamide
γ_{sv}	Surface Tension
θ	Intrinsic Contact Angle
γ_c	Critical Surface Tension
PTEF	Polytetrafluoroethylene
θ_r	Apparent Contact Angle
SEM	Scanning Electron Microscopy
GPC	Gel Permeation Chromatography
NMR	Nuclear Magnetic Resonance
SS-NMR	Solid State Nuclear Magnetic Resonance
FTIR	Fourrier Transform Infrared
XPS	X-ray Photoelectron
SIP	Surface Initiated Polymerization

List of symbols and abbreviations

THF	Tetrahydrofuran
NaCO ₃	Sodium Carbonate
ATMS	Aminopropyl Trimethoxysilane
CuBr	Cuprous Bromide
M _w	Molecular weight
MAS	Magic Angle Spinning
FWHM	Full Width at Half Maximum
T	Temperature
D ₂ O	Deuterium Oxide
DSC	Differential Scanning Calorimeter
KBr	Potassium Bromide
DMAP	4-(Dimethylamine) Pyridine
TEA	Triethylamine
BiB	2-Bromisobutyryl Bromide
MeOH	Methanol

TMS	Tetramethylsilane
OM	Optical Microscopy
SEC	Size Exclusion Chromatography
BE	Band Energy
TGA	Thermogravimetric Analysis
EBP	Ethyl-2-Bromopropionate
DLS	Dynamic Light Scatter

Chapter 1

Introduction

1.1 Research background

In the past thousands of years, textiles have been widely used for human clothing instead of animal fur to protect our body. Having experienced the periods of keeping warm, making comfortable and pursuing elegant appearance, a brand-new technical revolution named “smart” appeared recently. In current time, people are no longer content with the soft surfaces and beautiful styles. Researchers sustain large efforts to create our clothing materials with high level that can sense and react to thermal, chemical, light, electrical, stress, magnetic or other environmental stimuli. We call them “smart textiles”. Generally, they can be classified as three different species according to their manners of response to stimuli: passive smart, active smart and very smart. Passive smart materials can only sense the environmental conditions or stimuli; active smart materials will sense and react to the conditions or stimuli; very smart materials can sense, react and adapt themselves accordingly. The conception of “smart textiles” comes from biomimetic, which aims to develop a “living” surface with various organism functions. Therefore, three components may present in the smart materials: sensors, actuators and controlling units. The sensors provide a nerve system to detect signals, thus in a passive smart material, the existence of sensors is essential. The actuators act upon the detected signal either directly or from a central control unit; together with the sensors, they are the essential element for active smart materials. At even higher levels, like very smart or intelligent materials, another kind of unit is essential, which works like the brain, with

cognition, reasoning and activating capacities. Active smart and very smart material, since their capable of responding and activated to perform a function, fascinated researchers in textile field.

Here are many ways to achieve the goal of “smart”. In the last few decades, a lot of interest in both industry and academic circle has been directed towards the modification of the chemical and physical properties of cellulose-based nature fibers, with the aim of obtaining new functional materials or preparing high-performance composites based on renewable resources. For this purpose, great efforts have been devoted to control properties such as wettability, hydrophobicity, and adhesion of the cellulose fibers by surface modification.

With most of the existing surface modification methods, however, it is rather difficult to control the molecular architecture, molecular weight and its distribution, and thickness of the grafted polymer mono layer. In this study, atom transfer radical polymerization (ATRP) technique was used to introduce a stimuli-responsive polymer chain with precisely controlled length and polydispersity onto the fabric surface. With this method, it may be possible to develop new intelligent fabrics with a wide range of covalently anchored polymer bristles.

1.2 Significance of the study

Poly(N-isopropylacrylamide) (PNIPAAm) is a well-known

thermo-responsive polymer and has been extensively studied by spectroscopic, chromatographic and thermoanalytical techniques. However, vast majority of the researches focused on the solution or gel systems as the polymer structures and thermo-responsive properties can be easily characterized in such systems by routine analytical techniques, e.g. thermal analysis, GPC, NMR, etc. More recently, some papers have been published applying this smart polymer onto solid substrates to obtain functional material surface. It is practically very difficult to study the structure and molecular dynamics of the grafted polymer without ripping it from the solid substrates. Therefore, the mechanism for the thermo-responsive behavior at molecular level is yet to be further investigated or confirmed.

The traditional surface modification techniques such as crosslinking, radiation grafting, and photografting have the problem of controlling the thickness of the graft polymers or the gel. Surface reconstruction of bulk polymers often results in long response times, which could vary from minutes to tens of hours depending on the composition of polymers.

In this study, we grafted PNIPAAm onto cotton fabric surface by atom transfer radical polymerization method to develop a new intelligent cotton fabric with thermo-responsive surface. From this grafting method the synthesis process could be controlled easily. Cotton fabrics were prepared with both low and high grafting efficiency. Solid-state NMR techniques under both static and

magic-angle spinning conditions has been applied to raw and cotton fabric samples with low grafting efficiency of polymer to study the physical properties and molecular dynamics of the chemically bonded PNIPAAm molecules. This work offers a possibility to further understanding of the structure and molecular dynamics of a stimulus-responsive polymer which is grafted on a solid substrate. The highly grafted smart cotton fabric surface realizes the smart transition between superhydrophilic and superhydrophobic at different temperatures. This fabric surface is able to capture moisture from atmosphere at lower temperature and release water at higher temperature. The process can be repeated many times in a short cycling time. This cotton fabric can be well applied in textile industry for a functional clothing material. Moreover, it may also provide a new insight into solutions for fresh water conversion and purification.

1.3 Methodology

The general methodologies were presented below and the details will be described in chapters 3, 4, 5 and 6.

Prepare the Cotton-PNIPAAm samples

The cotton fabric was washed and dried at 40 °C for 24 hours under vacuum. The cotton surface was first immobilized with aminopropyl trimethoxysilane (ATMS) molecules and then grafted the initiator (bromide) groups in present of triethylamine and 2-bromoisobutyryl bromide. The initiator

modified-cotton fabric (Cotton-A-Br) was inserted in a Schlenk flask, and degassed by three cycles of vacuum-nitrogen filling. A mixture of Methanol/H₂O, NIPAAm and Pentamethyldiethylenetriamine were then added into the Schlenk flask. The reaction proceeded with magnetic stirring at room temperature. After the reaction, the Schlenk flask was opened to let the air in and terminate the polymerization reaction. The PNIPAAm modified fabric (Cotton-PNIPAAm) was thoroughly washed and dried at 40 °C overnight.

Characterization of Cotton-PNIPAAm

The success of the polymer grafting was confirmed by the combined results from FTIR, XPS, SEM, OM and Solid-State NMR experiments

The grafting yield was evaluated by three different methods: NMR, TGA, and gravimetry.

¹H solid-state NMR techniques were used to characterize the molecular structure and dynamics of the PNIPAAm molecules grafted on a cotton fabric. This technique is a non-destructive method which allows to quantitatively characterize the molecular structure and dynamics of the grafted polymer without cleaving it from the substrate. The structure and dynamics of the PNIPAAm brushes were investigated by both static and MAS ¹H NMR techniques.

The surface wettability of grafted smart cotton fabric was studied by CA, and the completely reversible conversion between superhydrophobicity and

superhydrophilicity was characterized by DSC.

1.4 Framework of thesis

This thesis stated a PNIPAAm grafted cotton fabric switch between hydrophilic and hydrophobic by temperature trigger. It comprised seven chapters.

Chapter 1 introduced the research background of investigation, existing problems, the significance and aim of this thesis.

Chapter 2 summarized the literatures on structures and properties of smart polymers (temperature, pH, electron and light sensitive polymers), the various grafting techniques to immobilize such polymers onto a solid surface (physical adsorption and chemical bonding), and the effects that determine the wettability of the surfaces.

In Chapter 3, Poly(N-isopropylacrylamide) (PNIPAAm) brushes were polymerized directly from a cotton fabric by ATRP method. FTIR, XPS, SEM and solid state NMR (SS-NMR) were used to verify the presence of PNIPAAm. The covalent bond between the cotton surface and grafted polymer was confirmed by SS-NMR.

In Chapter 4, ^1H solid-state NMR techniques were used to characterize the molecular structure and dynamics of the PNIPAAm molecules grafted on a cotton fabric. The results demonstrate that the motion of the grafted PNIPAAm

brushes is restricted as the temperature rises above the low critical solution temperature (LCST), which was estimated to be ~ 34 °C. The ^1H solid-state NMR techniques proved to be an extremely sensitive and precise way to probe in-situ the LCST transition of the PNIPAAm while still grafted on the cotton fabric.

In Chapter 5, the grafting efficiency of the polymer on the cotton surface has been greatly improved in this chapter. The modified cotton fabric was characterized by FTIR, XPS, NMR, TGA, SEM and OM. It was shown that the cotton fibers were covered with PNIPAAm brushes with a high grafting efficiency. The PNIPAAm molecular brushes were cleaved from the cotton substrate and characterized by GPC to determine the molecular weight (M_n), molecular weight distribution (PDI) and grafting efficiency.

The surface wettability of a highly grafted smart cotton fabric was studied in Chapter 6. It exhibits superhydrophobicity with a water contact angle (CA) up to 140° at 40 °C, and superhydrophilicity with a water CA of 0° at room temperature. This special fabric surface was also used to capture moisture from atmosphere at lower temperature and release water at higher temperature. The reversible conversion between superhydrophobicity and superhydrophilicity can be achieved by DSC.

Chapter 7 summarized the whole work of the thesis, and some future studies and potential applications also be presented here.

Chapter 2

Literature review

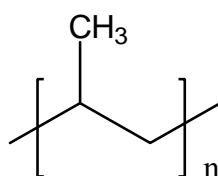
Abstract

Fabrication of a smart interface material using a chemical modification method has attracted a great attention in the recent years, due to the property of responding and adapting to various stimuli. Surface is the outmost layer of materials. Sometimes it can be considered more important than bulk because the surface properties generally determine the application of materials. Wettability between solid and liquid phase is an important interface property of the material surface.

In this chapter, the structures and properties of the most popular smart polymers including temperature, pH, electron and light sensitive polymers and the various grafting techniques to immobilize such polymers onto a solid surface will be summarized, including both physical adsorption and chemical bonding methods. The two effects: surface free energy and micro-structure which are generally considered to be the main factors that determine the wettability of the surfaces will be discussed in details. Some interesting study in literature about the wettability phenomena in nature will be shown, and moreover, some recent work of mimicking smart nature surfaces will also be presented.

2.1 Stimuli-responsive polymer

Life is polymeric in its essence. The most important components of living cells, proteins, carbohydrates and nucleic acids are polymers. And the components of synthetic rubber, fiber, plastic, dope and pastern are also polymers^{1,2}. Polymers are defined as a macromolecule composed of many smaller repeating structural subunits that are typically connected by covalent chemical bonds³. A typical example is *polypropylene* which contains repeating units of monomer *propylene* (Scheme 2.1). The repeating number n presents the degree of polymerization.



Scheme 2.1. Propylene subunit in a polypropylene polymer.

In general, polymers have been divided into two major classes: *natural* and *synthetic*. Since Henri Braconnot did the pioneering work in derivative cellulose compounds in 1811, polymer science have been developing for over 200 years⁴. Synthetic polymer materials such as nylon, polyethylene, teflon and silicone have formed the basis for a burgeoning polymer industry. The traditional synthetic polymers have been devoted to the supply of materials with low density, strong mechanical property, and environmental stability⁵. In recent years, an advanced group of polymers has emerged with their own unique chemical properties and

applications in various areas⁶. These polymers are coined with various names, ground on their physical or chemical properties such as “stimuli-responsive polymers”, “intelligent polymers”, “smart polymers”⁷⁻¹⁰ et al.

Smart polymers could respond with a dramatic property change to very slight changes in their environment. Nowadays, the properties of the smart polymers can be specifically tailored by changing their molecular structures. These very useful artificial polymers have great potential in the biotechnology and biomedicine applications. Smart polymers are becoming increasingly prevalent as scientists learn more about the chemistry and mechanisms that induce conformational changes in polymer structures. Based on this knowledge, it is possible to devise ways to take advantage of, and control them.

2.1.1 Temperature-responsive polymer

To trigger the environmentally responsive polymers, temperature is the most widely used stimulus, for the reason that can be easily controlled and widely applied^{8,9,11}. Lower Critical Solution Temperature (LCST) is an important property of temperature-responsive polymers. As the Figure 2.1 shows, Critical Solution Temperature can be considered as the temperature at which the phase of polymer and solution is inconsecutive altered according to their composition. For the polymers which have the Lower Critical Solution Temperature (LCST), they usually exhibit a homogeneous phase in the solution below LCST, and a phase separation above that temperature. On the contrary, if the polymers display a

homogeneous phase above a certain temperature point and a phase separation below that temperature, it is named High Critical Solution Temperature (HCST) or Upper Critical Solution Temperature (UCST)¹²⁻¹⁵.

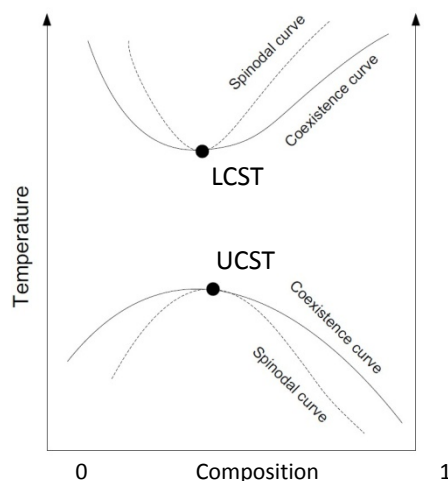
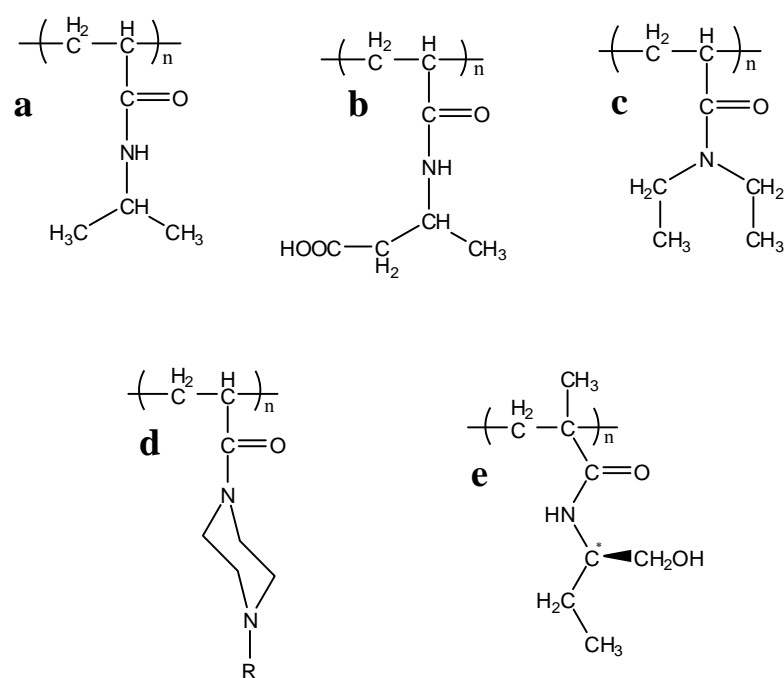


Figure 2.1 A plot of typical polymer binary solution phase behavior including both an LCST a UCST.

The polymers which have a LCST may contain of poly(N-substituted acrylamide), such as the molecules showed in Scheme 2.2^{11,16-19}. Among them, poly(N-isopropylacrylamide) (PNIPAAm) attracted most attentions and has been extensively studied because this polymer is soluble in water below 32 °C, and precipitated above 32 °C¹⁶. The reason for PNIPAAm appealed more attention is not only because it has a sharp transition at 32°C, but also because that temperature is very close to our human body temperature and can be well applied in the area of medicine and functional materials. The special property of PNIPAAm was first reported by Scarpa et al. in 1967²⁰. However, till now, over thousands of papers have been published related to its thermal sensitive property.

The mechanism of transition was clearly shown in Figure 2.2. At a low temperature, PNIPAAm is hydrophilic and can be well dissolved in water due to hydrogen bonds were formed between amide groups and water; however, the at a high temperature, it turns hydrophobic and phase separation can be observed immediately after the temperatures increased to above LCST because the molecules prefer to coil up and the amide groups formed intramolecular hydrogen bonds.



Scheme 2.2. Temperature responsive polymers. (a) poly(N-isopropylacrylamide)

(PNIPAAm); (b) poly(2-carboxyisopropylacrylamide) (PCIPAAm); (c)

poly(N,N'-diethylacrylamide) (PDEAAm); (d) poly(N-acryloyl-N'-alkylpiperazine); (e)

poly(N-(L)-(1-hydroxymethyl) propylmethacrylamide (P_L-HMPMAAm))

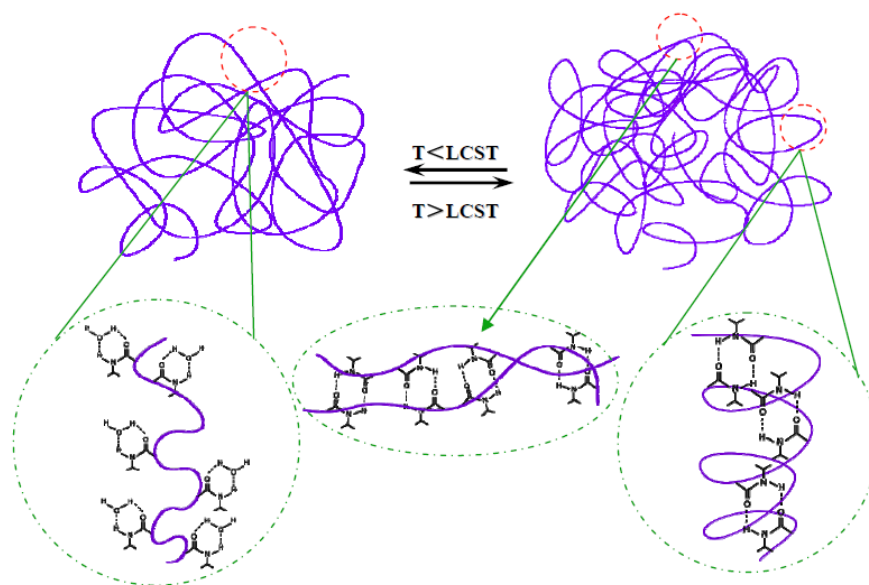


Figure 2.2. The transition of PNIPAAm molecule conformation in water at low (left) and high (right) temperatures²¹.

The present study about the PNIPAAm materials and its derivatives can be divided into two major classes: hydrogels and surface modification.

PNIPAAm hydrogel has great potential in the application of drug delivery systems. However, the application of the conventional hydrogel is kinetically restricted by its long response time. This problem was solved by the emergence of a new concept of micropore-structure²²⁻²⁴. This work was first carried out by Wu et al²³. By crosslinking PNIPAAm with hydroxypropyl cellulose (HPC), they successfully get a large pore volume, homogeneous pore size distribution and faster velocity of permeability. Another study to solve the problem of response lag was to synthesis the mircogels²⁵. Pelton et al prepared aqueous lattices with PNIPAAm, and studied the morphology and thermal response ability²⁶. Since the

pioneering work of Pelton et al, microgels have been studied extensively, and this system have been well applied in many different areas including environment protection (the absorbed and release of heavy metal ions), drug delivering and photoelectric switch, et al.^{25,27,28}.

Besides the hydrogel, PNIPAAm molecule is also extensively applied on surface modification of various substrates including polymer, silicon, metal, etc. L. Liang et al modified the capillary tube surface with PNIPAAm by photo-grafting method in the presence of the crosslinker *N,N'*-methylenebisacrylamide (BisAAm). The with photosensitizer *N,N'*-diethylaminodithiocarbamoylpropyl(trimethoxy)-silane (DATMS) was immobilized on glass surface, and then the PNIPAAm molecules was grafted, as shown in Figure 2.3. As a result of the LCST transition of the PNIPAAm, the polymer molecules become hydrophilic at lower temperature, and the surface tension of the capillary tube increases. The height of the water in capillary tube rose up to 7mm when temperature decreases from 40 °C to 20 °C (Figure 2.4)²⁹.

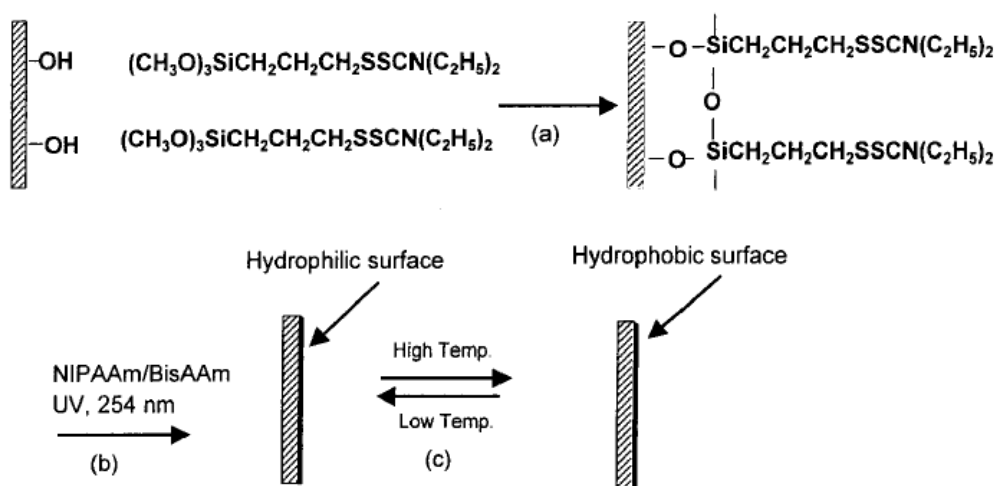


Figure 2.3. Schematic illustration of photopolymerization on the glass plate: (a) immobilization of DATMS silane on to the surface of glass plate; (b) formation of cross-linked PNIPAAm layer on the surface; (c) reversible change of hydrophobic/hydrophilic surface properties²⁹

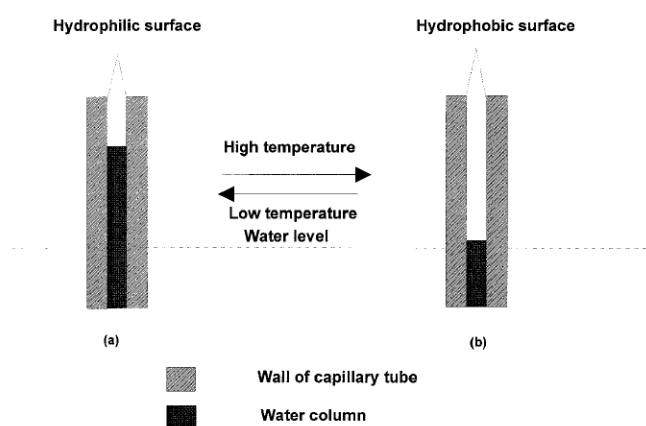


Figure 2.4. Schematic illustration of the change of water meniscus height in capillary tube: (a) low temperature (20 °C); (b) high temperature (40 °C)²⁹.

The PNIPAAm has also been grafted on the silica surface³⁰⁻³⁴. L. Jiang's group grafted PNIPAAm on both a flat and a rough silicon substrate, and significantly different contact angles (CAs) was obtained below and above LCST.

As shown in figure 2.5, this modified rough surface successfully realized a switch from superhydrophilic to superhydrophobic property, and this progress can be intelligently controlled by the temperature change³⁴.

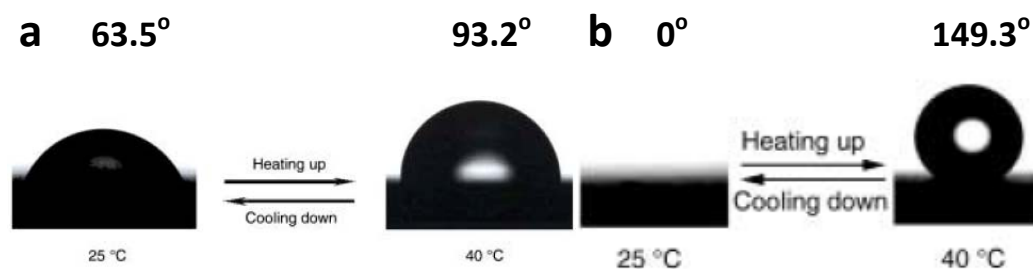


Figure 2.5. Thermal responsive wettability for a (a) smooth and (b) PNIPAAm-modified rough surface³⁴.

PNIPAAm was also grafted to commercial anodic aluminum oxide (AAO) membranes³⁵. It was found that with the increase of the pore size of AAO, the CA measured increases constantly at temperature above LCST, and decreases below LCST.

PNIPAAm was also grafted to aligned carbon nanotubes (ACNT)³⁶ in order to fabricate a functional carbon nanotube surface. Sun et al. used AFM to study diameter of PNIPAAm grafted nanotubes. They found a distinct reduction of the diameter of the carbon nanotubes when temperature was raised above the LCST.

2.1.2 pH-sensitive polymers

It is well known that a pH-responsive polymer may have two types of

functional groups: weak polyacids and weak polybases. These functional groups contain ionizable pendants which can accept and donate protons in response to the pH change in the environment³⁷. When the degree of ionic concentration changed, the hydrogen bond inside polymer gels will be broken. This behavior will induce a rearrangement of the polymer network structure and therefore the hydrogel swells.

The previous studies on the pH-sensitive polymers were mainly focused on the drug release³⁸⁻⁴⁰ and gene delivery⁴¹⁻⁴⁴ materials. However, in recent years, this type of polymer was also applied on solid substrate in order to achieve a stimuli-responsive surface. Their surface wettability attracted more and more attentions recently. Leonid et al. modified silicon wafer surface with two different types of polyelectrolytes with opposite charges by surface-grafted method. This gradient composition causes a gradient density of charge, and results in a gradient wettability behavior (Figure 2.6)⁴⁵.

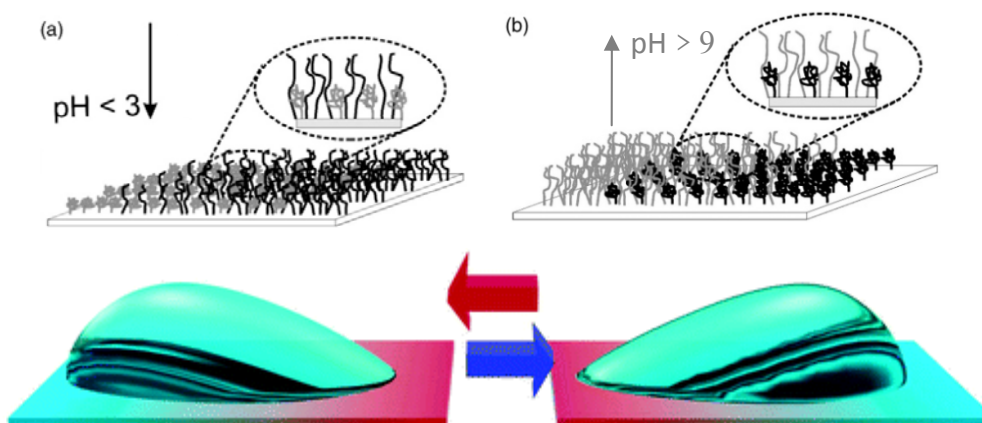


Figure 2.6. Schematic representation of the switching behavior of the mixed PE brushes upon the change of pH: low pH (a) and high pH (b)⁴⁵.

Zhang's group modified the rough gold surface with pH-responsive polymer by an electrodeposition method. This functional surface can switch from superhydrophobic in acid and neutral conditions to superhydrophilic in base condition. This switch process is fully reversible for many times, and it was also proved to exhibit good stability and mechanical properties^{46,47}.

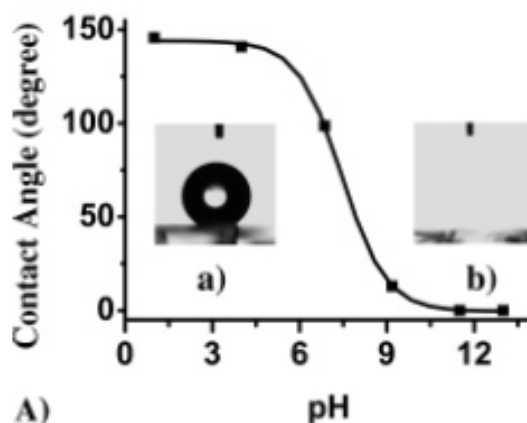


Figure 2.7. The water contact angle of the modified gold surface at different pH values: (a)

The water droplet on the surface at pH=1, CA about 145°; (b) The water droplet on the surface at pH=13, CA near 0°⁴⁶.

2.1.3 Electro- and light-sensitive polymers

The electro responsive polymer was less eye-catching comparing to the previous-mentioned PH- and temperature-responsive polymer. This kind of polymers usually consists of polyelectrolyte. The directional movement of the free ions under DC voltage in solution will induce the deformation of the polymer^{48,49}. Langer's group did a remarkable work on this topic. (16-Mercapto)

hexadecanoic acid (MHA) was used to modify the gold surface for the reason that (I) it could self-assemble on Au (111) into a monolayer; and (II) it has a hydrophilic end group of carboxylate but with a hydrophobic hydrocarbon main chain. As Figure 2.8 shows, when the substrate is applied with negative electrical potential, the negative charged carboxylate groups will locate on the surface layer because of the electric repulsive force between the negatively charged end group and the gold substrate. Therefore the surface shows hydrophilic property. However, when the gold substrate is applied with positive potential, the negative end groups will feel an attractive force to the substrate, thus the molecular chain bended and reveal the carbon chain, and exhibited hydrophobic property⁵⁰.

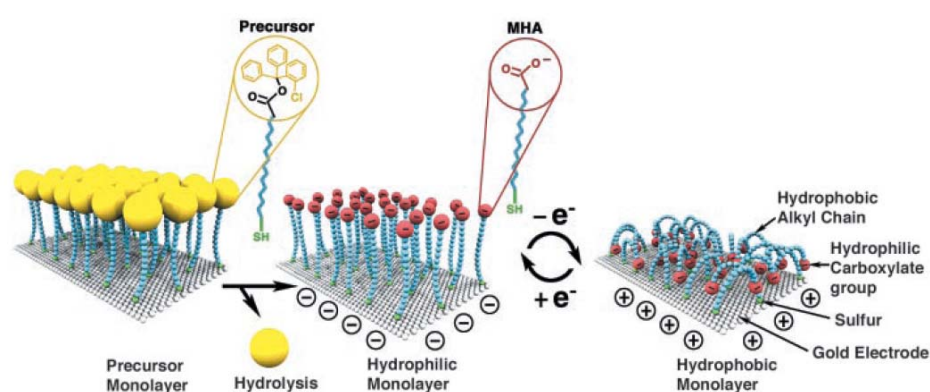


Figure 2.8. Schematic diagram of the switch from straight (hydrophilic) to bent (hydrophobic) molecular conformations⁵⁰.

Most of the studies related to light-sensitive polymer were conducted on inorganic substrates such as TiO₂ and ZnO. Since 1997 Fujishima's group published a paper on Nature⁵¹, reporting the amphiphilic property induced by UV light, this material has attracted a lot of attention and is also widely applied in

industry⁵²⁻⁶⁰. The recent study on the light responsive polymer could be summarized into different types. For one type, these polymers structure will change upon absorbing a certain wavelength of light^{61,62}. Another type is of some thermal sensitive polymer chains, and these functional groups could respond to the temperature increase caused by converting light energy into enthalpy. Suzuki et al. made gels contain PNIPAAm and chlorophyllin. Chlorophyllin is such a type of photon absorption that can absorb the visible light and transfer the energy into enthalpy. When the temperature of the polymer gel increases to 32°C and higher, it will deswell⁶³.

2.2 Surface modification

Material surface is a interface between the bulk and the outer environment⁶⁴. It is the outmost layer of the material, and the physical and chemical properties are generally considered to be very different from that of the bulk. Because the surface usually experiences adhesion, compatibility, stabilization, coloring and painting problems, sometimes surface property be considered more important than bulk's⁶⁵. For this reason, surface modification aroused interest to many researchers, and it was widely applied in different industries including medicine and textiles, et al.

2.2.1 Coating by physical force

A numerous of coating techniques based on physical interactions between

polymer and substrate can be classified as follows:

- Droplet evaporation
- Spray coating
- Spin coating
- Dip coating
- Doctor blading

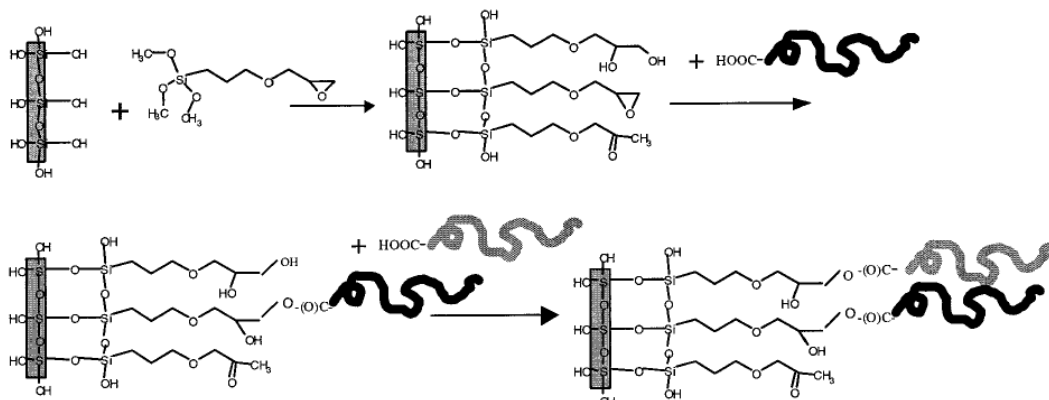
Despite of differences in these techniques, a common point shared by all these methods is that the coating is formed by solvent evaporating progress from a solution. These techniques are simple, and typically no complicated setups are required to prepare the coating. However, the physical interactions between polymer and substrate are rather weak forces. Therefore, the coatings prepared by these methods often have problems of desorption, dewetting and delamination, et al. To solve all the problems, and get a long-term stability of coating, the polymers have to be chemical bonded to the substrates.

2.2.2 Chemical modification to the substrates

2.2.2.1 Grafting-to method

The fictionalization process of the substrate surface by “Grafting-to” method can be performed using several techniques such as anionic, cationic,

living free radical, and ring-opening metathesis polymerization⁶⁶⁻⁶⁹. The surface properties can be also an important factor of the success of the synthesis. Silica and gold surface can immobilize polymers that containing hydroxyl, thiol and carboxyl functional chains. Minko et al. have grafted a polymer brushes on to a silicon surface using the “grafting to” technique (Scheme 2.3). Firstly, the 3-glycidoxypropyl trimethoxysilane (GPS) was grafted to silicon wafer by condensation reaction between alkoxy silane group and hydroxyl on the surface. Then, the carboxyl-terminated polystyrene and carboxyl-terminated poly(2-vinylpyridine) were grafted via a spin-coating/thermal annealing methods. Finally, a binary polymer brush layer was obtained by using the “grafting to” method⁷⁰.



Scheme 2.3 Schematic representation of the synthesis of binary brushes. PS chains, gray;
PVP chains, black⁷⁰.

Although it is easy to perform the “grafting to” reaction, there are limitations of this technique which can hinder its applications. First, the end group of polymer chain should be functioned with a high active anchor, such as

chlorosilyl group. However, if this group has been chosen, the polymer chain cannot contain amine, hydroxyl and carboxylic acid groups. Otherwise, these groups will deactivate the selected end group. Second, the “grafting to” process strictly limited the thickness of the grafted polymer layer, typically 1 to 5nm. This is attributes to the kinetic and thermodynamic characteristic of this technique. As showed in Figure 2.9, the polymer chains can easily attach to surface at low grafting densities. As soon as polymers covered the surface, the already-attached chains would form a kinetic barrier, and it will barrier against the coming chains to reach the surface⁷¹.

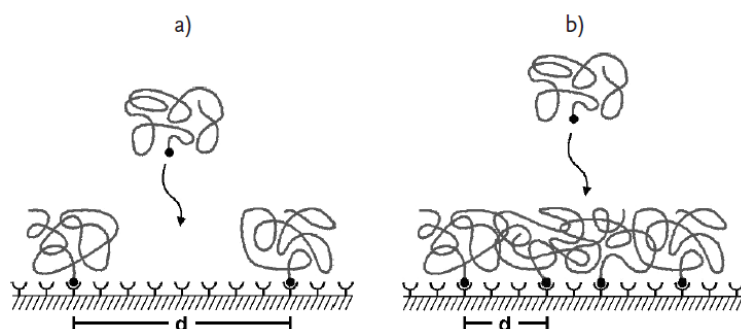


Figure 2.9. Schematic illustration of the “Grafting-to” process at (a) low densities, (b) high densities⁷¹.

2.2.2.2 Grafting-from method

Different with the “grafting-to” method, the “grafting-from” technique can avoid the problems listed above. “Grafting-from” technique involves the immobilization of a functional initiator in the first step which is suitable for polymer brush growing. The monomer can be grafted by free radical, ionic,

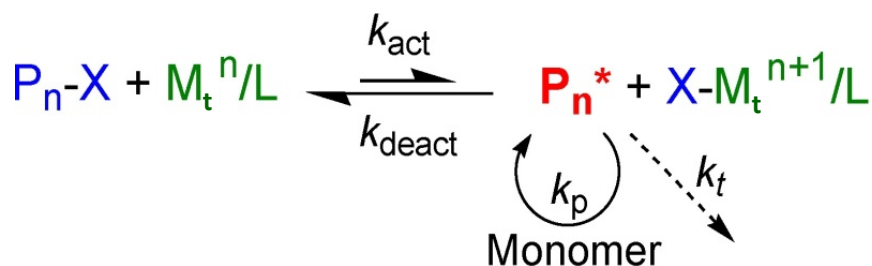
ring-opening metathesis and controlled radical polymerization⁷²⁻⁷⁷. Among these techniques, the controlled radical polymerization is considered to be superior to other techniques in the sense that it can provide uniform brush layer, tunable brush thicknesses, homopolymer layer or diblock copolymer layer. Atom transfer radical polymerization (ATRP) is one of the most popular techniques for controlled synthesis, and has been extensively used for surface modifications. This technique will be discussed in detail in the following sections.

The theory of ATRP

Atom Transfer Radical Polymerization (ATRP) is the most widely applied Controlled Radical Polymerization (CRP) technique due to its controllability in the synthesis of well-defined polymers and copolymers from vinyl monomers such as styrene^{78,79}, N-isopropylacrylamide⁸⁰ and meth/acrylates^{81,82}. This technique was first reported by Sawamoto and Matyjaszewski in 1995^{83,84}.

ATRP polymerization process is a dynamic equilibrium of activation and deactivation steps as shown in Scheme 2.4. The carbon-halogen bond of alkyl halide initiators (Pn-X) is homolytically cleaved by metal complexes (M_t^n /Ligand) oxidation, yielding free radical (Pn*) and oxidized metal complexes ($X-M_t^{n+1}$ /Ligand). The produced radical (Pn*) will break vinyl bond of monomer and grow the polymer chains (Pn-M*), and after a short time, the radical (Pn-M*) will transfer into a dormant condition because it substitutes the halogen atom from ($X-M_t^{n+1}$ /Ligand) and becomes (Pn-M-X). And then the second activation

loop starts⁸⁵.



Scheme 2.4. Mechanism for the atom transfer radical polymerization. Pn-X: alkyl halide

initiator; M_t^n/L : metal complexes; P_n^* : free radical; $\text{X-M}_t^{n+1}/\text{L}$: oxidized metal complexes⁸⁵.

In ATRP, ligand is an important factor to stabilize the metal salt. Figure 2.10 shows the activation rate constants (k_{act}) of different ligands with Ethyl 2-bromoisobutyrate (EtBriB)⁸⁶. The measured (directly or extrapolated) results were arranged in a logarithmic scale for a better comparison of activities of Cu/Ligands complexes. It should be noted that the catalyst will become more active when Cu^{II} state is better stabilized by the ligand according to electrochemical studies. Therefore, the extrapolated values may underestimate the values of k_{act} for active complexes⁸⁷⁻⁸⁹. Normally, tetradentate ligands form the most active complexes, in particular Cyclam-B, in which the ethylene linkage further stabilizes the Cu^{II} complex. Complexes with branched tetradentate ligands produce the most active catalysts *e.g.* $\text{Cu}^{\text{I}}\text{Br}/\text{Me}_6\text{TREN}$, $\text{Cu}^{\text{I}}\text{Br}/\text{Me}_6\text{TPMA}$ and also $\text{Cu}^{\text{I}}\text{Br}/\text{Cyclam-B}$ are the three most active complexes in Figure 2.10. This may be associated with a small entropic penalty in ligand

rearrangement from Cu^{I} to Cu^{II} state⁹⁰. Cyclic ligands are located in the middle of the scale, indicating normal activities when forming a Cu complex. Most of the linear tetradentate ligands are placed at the left side of the scale, except BPED. Tridentate ligands, *e.g.* PMDETA and BPMPA, form fairly active complex. All bidentate ligands are located at the left side of the scale, forming the least active ATRP complexes.

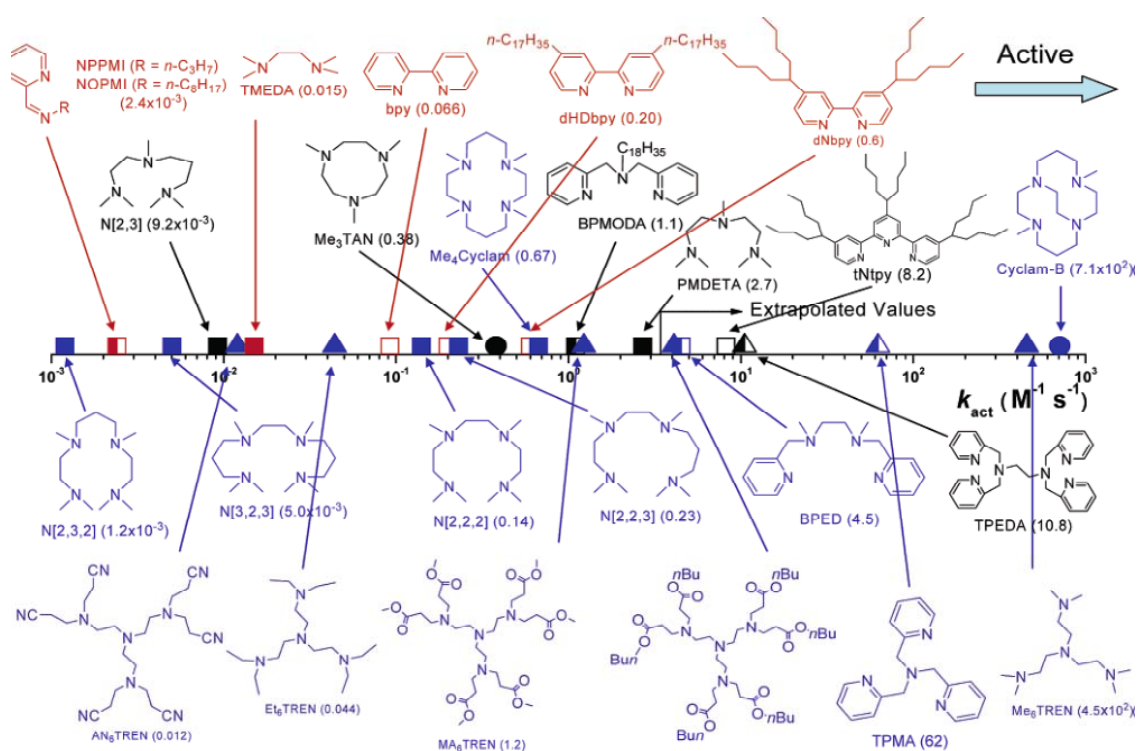


Figure 2.10. ATRP activation rate constants for various ligands with EtBriB in the presence of $\text{Cu}^{\text{I}}\text{Y}$ (Y=Br or Cl) in MeCN at 35 °C: N2, red; N3, black; N4, blue; amine/imine, solid; pyridine, open. Mixed, left-half solid; linear, □; branched, ▲; cyclic, ●⁸⁶.

The differences in activity for the resulting complexes exceed seven orders of magnitudes. The general order of activities of Cu complexes is related to their molecular structure and can be summarized into the following order: tetradentate

(cyclic-brdged) > tetridentate (branched) > tetradentate (cyclic) > tridentate > tetradentate (linear) > bidentate ligands. The nature of the N atoms is also important and it generally follows the order pyridine \geq aliphatic amine > imine. Ethylene is a better linkage compare to propylene for N atoms in the ligand. The activities of the Cu complexes strongly depend on the ligand structures, and even slightly difference in the molecular structure may lead to large differences in their activity.

Surface initiated Atom Transfer Radical Polymerization (SI-ATRP)

Growth of polymer at the interface by ATRP is a robust technology to precisely control the thickness, density and PDI of the tethered polymer brush. Beside this, the surface morphology and property of the interface could also be tuned by changing the composition and molecular structure of polymer segments.

Ohno et al. grafted PMMA brushes from gold nanoparticles by SI-ATRP, producing a shell composed of well-defined, high-density polymer brushes⁹¹. Balamurugan et al. grafted poly (N-isopropylacrylamide) brush on gold surface in DMF solution using SI-ATRP method. The reaction was carried out at room temperature and the polymer brushes reach a thickness of ~51 nm. Thermal responsive behavior and lower critical solution temperature transition was characterized by contact angle and surface Plasmon resonance⁹². Jonnes et al. deposited a grafting initiator on a gold surface by the microcontact printing technique. The monomers MMA, glycidyl methacrylate, n-butylacrylate and

HEMA were polymerized under aqueous conditions⁹³. This grafting technique perform in aqueous solution was later used in the synthesis of different brushes such as poly (N-isopropylacrylamide)⁹⁴ and poly (N, N-dimethylacrylamide)⁹⁵. Triblock copolymers brushes were grafted from a silicon surface. The initiator of bromoisobutyrate was bounded to the silicon wafer in the first step, and PS-*b*-PMA-*b*-PS block copolymer brushes were then grafted from the initiator by SI-ATRP, as showed in the Figure 2.11. The grafting brushes were characterized by ATR-FTIR and the thickness of brushes was measured using ellipometry⁹⁶.

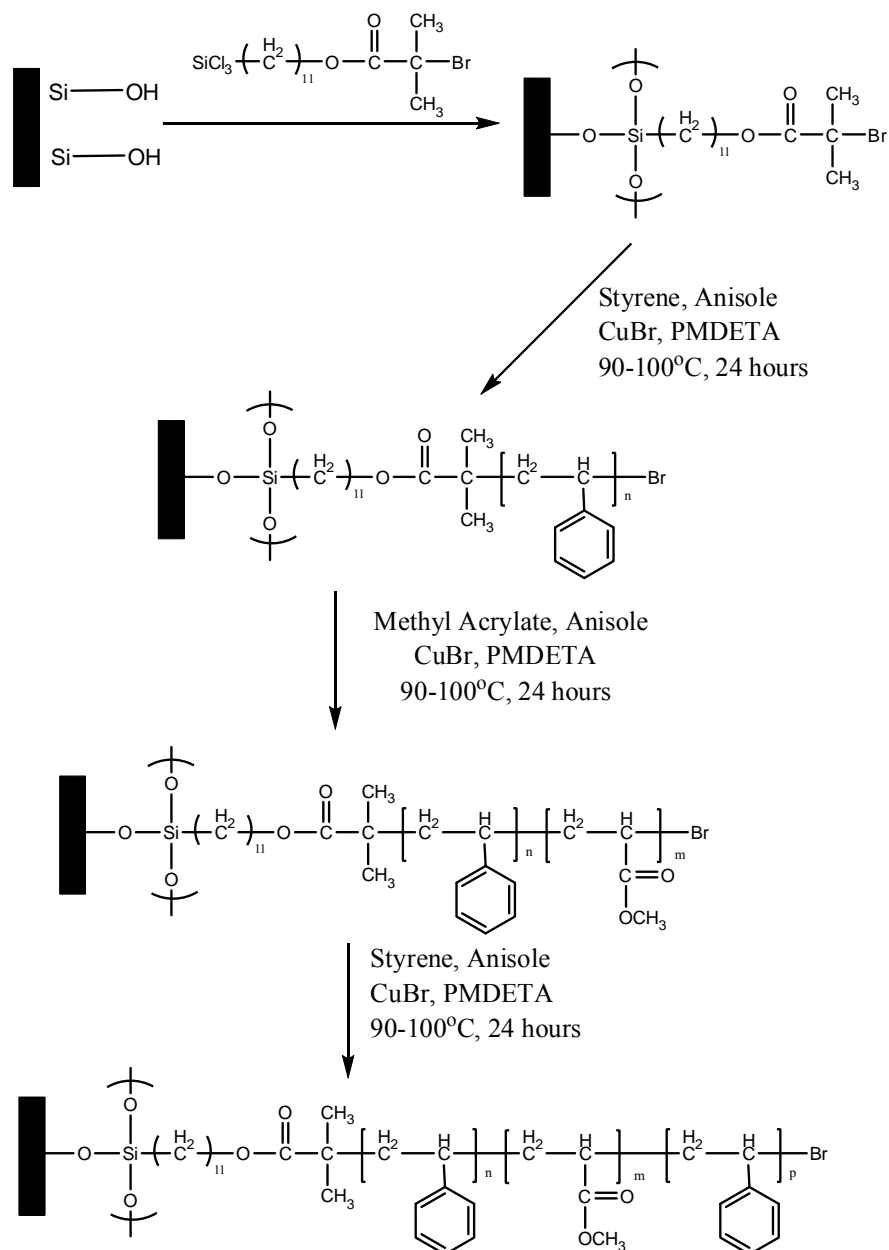


Figure 2.11. Synthesis of triblock copolymer brush, PS-*b*-PMA-*b*-PS by SI-ATRP⁹⁶.

2.3 The theory of wettability

Wettability is an important property of the solid surface both in industry and daily life⁹⁷⁻¹⁰⁴. An interesting phenomenon in nature is that the material of lotus is hydrophobic, however, the water drops on lotus are spherical and easily

roll off, and the lotus surface is considered to be “non-wettable”. Nowadays, people know that it is due to the micro-scale structure of the surface make the hydrophilic material to be non-wettable. It is well accepted that two factors will influence the surface wettability of a material: surface free energy and the micro-structure.

2.3.1 Surface free energy

Both the surface free energy and the surface tension (γ_{sv}) can be used to describe the surface property of a material. Generally speaking, a large value of γ_{sv} means a hydrophilic property, e.g., metal, metallic oxide and inorganic salt surfaces, et al., whereas a small γ_{sv} value corresponds to a hydrophobic property, such as polymer and organic surfaces.

Zisman et al. measured the contact angles (θ) of different liquid droplets on a given polymer surface. The result shows that when $\cos \theta$ is plotted against the surface tension, a straight line can be obtained. The intersection point of straight line and $\cos \theta=1$ was the critical surface tension (γ_c) which indicates the lowest surface tension to spread the droplets (showed in Figure 2.12). Therefore, the higher the value of γ_c , the easier the liquid can spread (with smaller contact angle), and vice versa¹⁰⁵.

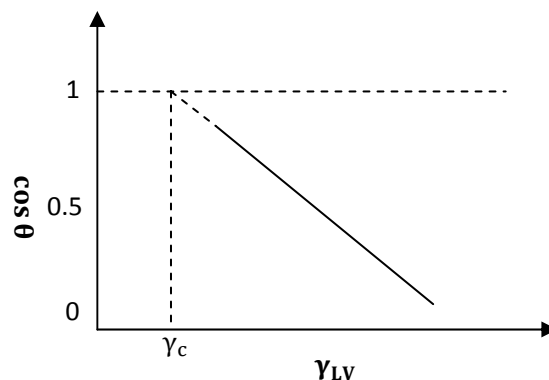


Figure 2.12. The critical surface tension of solid surface.

The surface wettability is highly dependent on the chemical composition of the surface materials. For example, if the hydrogen atoms are replaced by halogen element fluorine, γ_c will decrease, and the degree of replacement determines to which extent the γ_c will decrease. However, if the hydrogen atom is replaced by other atoms such as oxygen and nitrogen, the value of γ_c would increase and surface becomes more hydrophilic. The sequence of normal elements which increase γ_c is as follows:



For some special solid surfaces, e.g., polytetrafluoroethylene (PTFE), their critical surface tension is lower than most of liquids. Therefore, the liquids (including organic solvent and water) cannot spread on their surface. People refer to this kind of substrate as amphiphobic. This type of materials can be well applied in oil transmission pipe line because it can lower the flow resistance and minimize the deposition of salts crystallization from crude oil¹⁰⁶.

2.3.2 Surface micro structure

The angle that a liquid/vapor interface meets a solid surface is named contact angle. If a liquid drop cannot completely spread out on the solid surface, it has a non-zero contact angle (see the Figure 2.13). The contact angle is determined by the balance of surface tension among the interfaces of solid, liquid and vapor. Their relationships can be described by Young equation (Eq. 2.1):

$$\gamma_{SV} = \gamma_{SL} + \gamma \cos \theta \quad . \quad (\text{Eq. 2.1})$$

In this equation, γ_{SV} , γ_{SL} and γ are surface tensions between solid and vapor, solid and liquid, and liquid and vapor, respectively, and the θ is the contact angle of the droplet^{107,108}.

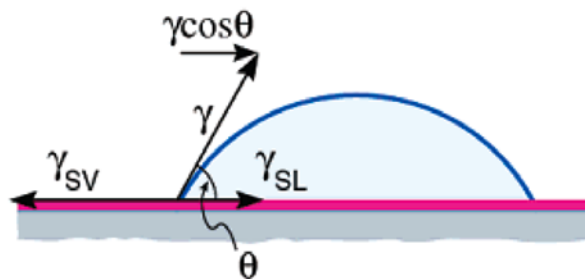


Figure 2.13. The forces balance of a liquid drop on a solid surface demonstrated by Eq.

$$2.1^{107}.$$

Young's equation is usually used to evaluate the wettability of a surface:

$\theta = 0$ completely wetting

$0 < \theta < 90^\circ$ wetting

$90^\circ < \theta < 180^\circ$ nonwetting

$\theta = 180^\circ$ completely nonwetting

However, it should be pointed out that Young's equation describes the contact angle of a droplet on an ideal surface which perfectly flat and homogeneous in composition. Zisman et al. reported that the functional group of $-\text{CF}_3$ gives the lowest surface free energy among all the tested materials¹⁰⁹. In 1999, Nakamae et al measured the contact angle of a flat surface which is composed of $-\text{CF}_3$ groups, and the contact angle was measured to be 119° ¹¹⁰. This value is still far away from that of a completely nonwetting surface which requires a contact angle of 180° . This result implied that a completely nonwetting surface can never be achieved by chemical modification on the surface. A surface roughness modification is also important to improve the contact angle.

2.3.2.1 Wenzel model

As discussed above, Young's equation assumed a perfectly flat solid surface. However, this ideal condition never exists in real life. Then the Wenzel model was Proposed in 1936 by Wenzel's group to describe of the relationship between the surface roughness and the wettability.¹¹¹. It was found that the surface roughness significantly increase the contact angle of a solid surface. The relationship between the contact angle and surface roughness (see Figure 2.14) can be quantified by

Wenzel:

$$\cos \theta_r = \gamma \cos \theta \quad (\text{Eq. 2.2})$$

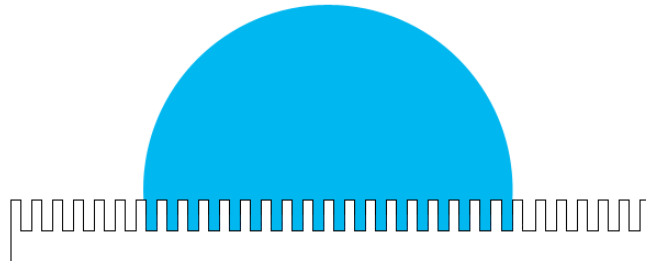


Figure 2.14. Wenzel model

Where γ is surface roughness ($\gamma \in (1, -\infty)$), θ_r and θ are the apparent and intrinsic contact angles on rough and smooth surfaces, respectively. Decreasing the value of γ will result in a larger apparent contact angle. It can be concluded from Wenzel equation that surface can be either more hydrophobic or more hydrophilic by increasing the surface roughness. When the intrinsic contact angle $\theta < 90^\circ$, the apparent contact angle θ_r decreases with the surface roughness; while $\theta > 90^\circ$, θ_r increases with the surface roughness. In other words, a hydrophilic surface will become more hydrophilic with increasing degree of roughness, while a hydrophobic surface will become more hydrophobic if the same type of roughness is introduced¹¹².

2.3.2.2 Cassie model

Wenzel equation reveals the relationship between apparent and intrinsic contact angles on a rough surface, but it is not applicable to the surface which contains different chemical components. Therefore, a more general model is needed to describe this phenomenon. Cassie model was on the basis of Wenzel model by using a linear combination of two Wenzel terms. In Cassie model¹¹³, surface was assumed to be composed by two different components, and each one is minimal and homogenous. The apparent contact angles of each component are θ_1 and θ_2 ; the total areas of each are f_1 and f_2 ; and the θ_r is the apparent contact angle of the solid surface. On the basis of the hypothesis above, Young's equation can be written as:

$$\cos \theta_r = f_1 \cos \theta_1 + f_2 \cos \theta_2 \quad (\text{Eq. 2.3})$$

According to Cassie and Baxter, if the surface has nonwetting property the recesses cannot be fully wetted. As Figure 2.15 shows, air can be trapped in the space between liquid and solid. Because the apparent contact angle between liquid and air is 180° , equation 2.3 can be modified to:

$$\cos \theta_r = f_1 \cos \theta_1 + f_2 \cos 180^\circ, \quad (\text{Eq. 2.4})$$

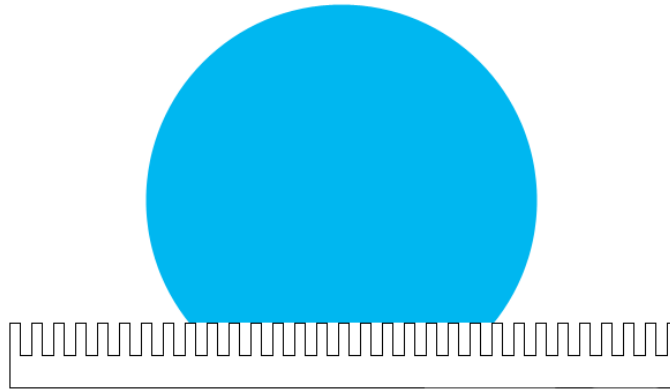


Figure 2.15. Cassie model

where f_1 is the total area of solid-liquid interface and f_2 is the total area of liquid-air interface.

2.4 The boundary between hydrophilic and hydrophobic

As discussed in the previous section, Young's equation gives a contact angle of 90° as the boundary between hydrophilic and hydrophobic. This means that when $\theta < 90^\circ$, the surface is hydrophilic, and when $\theta > 90^\circ$, the surface is hydrophobic by definition. However, more recently, researches have shown that boundary of a contact angle of 65° maybe more reasonable boundary to define the material to be hydrophilic and/or hydrophobic¹¹⁴.

In Young's equation, the contact angle θ is a balance of three forces among solid, liquid and vapor phases. The surface of liquid was treated to be the same as bulk phase. However, this assumption is not true in real case. The

structure and activity of water molecules on the surface are largely different from that in the bulk phase. The hydrophobicity of a solid surface can be studied by observing the water structure at the surface. When the contact angle $\theta < 65^\circ$ which indicates a hydrophilic surface with adhesion tension $> 30 \text{ dyn/cm}$, repulsive force can be detected between surfaces. In case of a hydrophobic surface with pure water contact angle $\theta > 65^\circ$ (adhesion tension $< 30 \text{ dyn/cm}$), a long-range attractive force can be detected. Therefore, it is reasonable to suggest that there are at least two distinct kinds of water structure and reactivity: a relatively less-dense water region with an open hydrogen-bonded network on the hydrophobic surfaces and a relatively more-dense water region with a collapsed hydrogen-bonded network on the hydrophilic surfaces. The study of Yoon¹¹⁵ and Berg¹¹⁶ also supported the discussion above which showing that the boundary between hydrophilic and hydrophobic is 65° .

As mentioned before, the functional group of $-\text{CF}_3$ gives the lowest surface free energy with the contact angle of 119° ^{109,110}. However, this value is still lower than the contact angle of a superhydrophobic surface which requires a minimum static contact angle of 150° ¹¹⁷. Therefore, in order to get a superhydrophobic property, either a certain level of roughness on the surface of a low free energy material, or a chemical modification with low surface free energy chemicals on a fixed roughness surface are required. The superhydrophilic surface is that the contact angle of which is lower than 10° , such as titanium dioxide under UV light⁵¹.

2.5 Wettability in natural world

Lotus leaf is a typical example in nature that displays superhydrophobic property. It attracted great interesting among scientist by the so-called “self-clean” effect which is due to the very special surface property¹¹⁸. Nearly 300 kinds of plant leaves were studied by Barthlott¹¹⁹ and Neihuis¹²⁰, and the results showed that the superhydrophobic property of the lotus leaf originates from both the miro-scale roughness and the hydrophobic wax crystals. Later, Jiang’s group found that the nonwetting property is not only from the above-indicated reasons, but also because of the nanoscale particles combined with the miro-scale papillae¹²¹. As showed in Figure 2.16, papillae with diameters ranging from 5 to 9 μm , were found on the lotus surface. The CA was measured to be $161.0^\circ \pm 2.7^\circ$. From the high-resolution SEM image, the branch-like nano-scale structures with the diameter of $124.3 \pm 3.2\text{nm}$ were observed. This micro-nano hierarchical structure was assumed to be the reason for its superhydrophobicity.

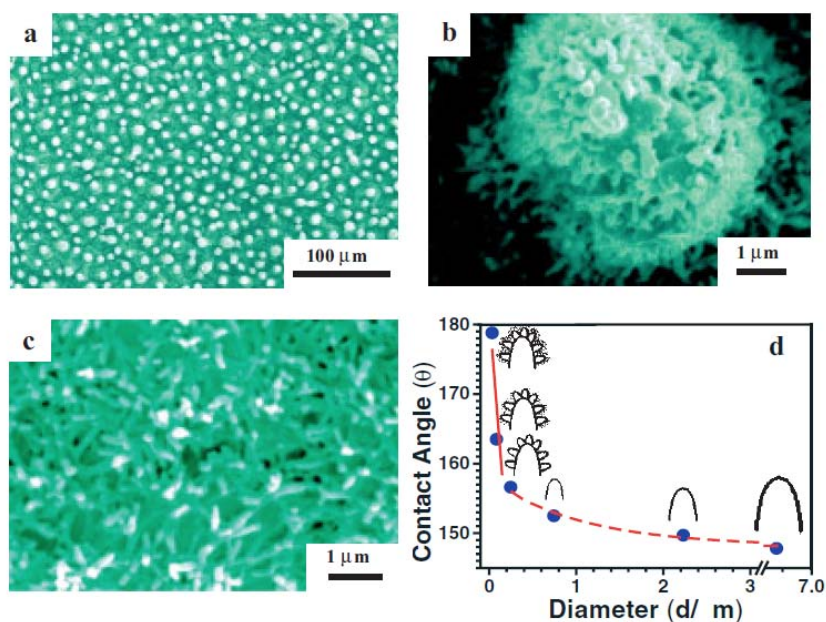


Figure 2.16. (a), (b), (c) are the SEM images of lotus leaf; (d) is the fitted curve based on the calculated data (contact angle, in degrees, against the mean outer diameter of protruding structures, in micrometers)¹²¹.

Both the feathers of duck¹²² and butterfly¹²³ were observed to be superhydrophobic. However, different with the lotus leaf on which water can roll in all directions, water on these feathers showed direction adhesion. A droplet can easily roll along the radial outward (RO) of the central axis of the body but is tightly pinned in the opposite direction. This is related to the special surface microstructures on the wings. From the SEM images in Figure 2.17a, the wing is composed of many quadrate scales, with a length of $\sim 150\mu\text{m}$ and a width of $\sim 70\mu\text{m}$. Every scale is also covered with $\sim 185\text{nm}$ in width and $\sim 585\text{nm}$ in length ridging stripes. These stripes are stacked stepwise along the RO direction, and the nano-tips emerge on the top of stripes are tilted slightly upward. When droplet rolling along the RO direction (Figure 2.17b I), it is a “dry” contact

process which with the air pocket trapped in the nano-grooves. As the water goes opposite direction, droplet presents the “wet” contact to the nano-strips (Figure 2.17b II) and be pinned on the surface¹²³.

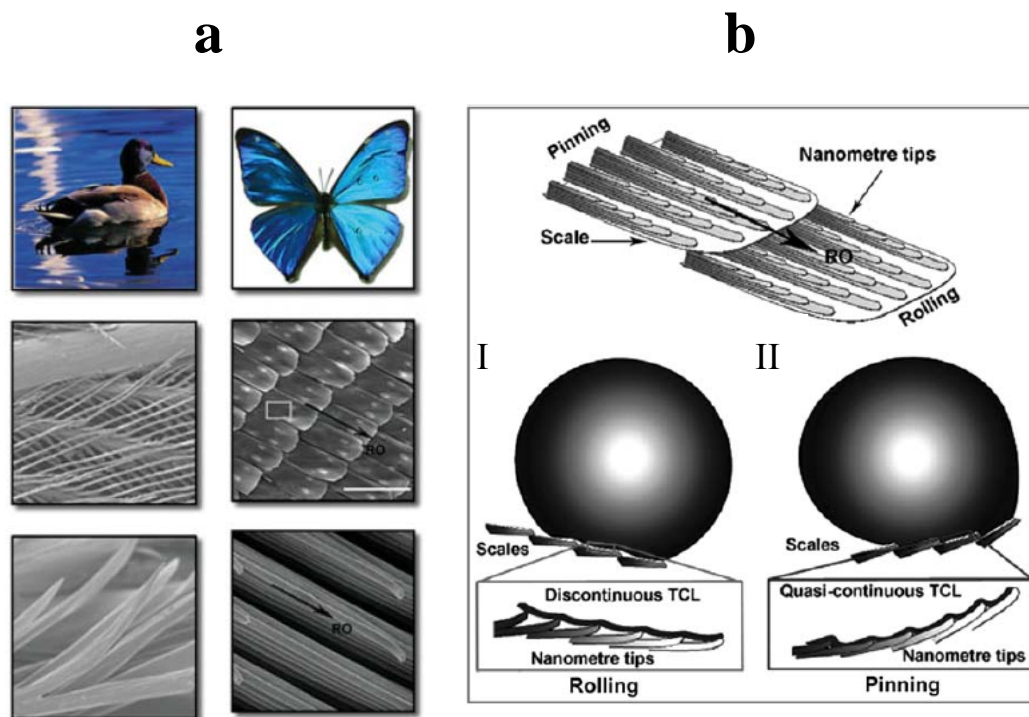


Figure 2.17. (a) SEM images of duck feather and butterfly wing; (b) the models proposed for mechanism of distinct adhesion dependent on the direction along and against the RO direction^{123,124}.

Water striders Gerridae is a common insect reside on the surface of rivers, ponds and ocean. Bush's et al. used a high-speed video and a particle-tracking method to capture the whole process of a Gerridae strider on the water surface. The images are showed in Figure 2.18. The strider transfers momentum through hemispherical vortices shed by its driving legs¹²⁵. The previous studies

considered the Gerridae supporting their weight by the surface tension force generated by the curvature of the free surface¹²⁶. However, recent study showed the physical features of the Gerridae legs are of numerous oriented setae (Figure 2.19)¹²⁷. These needle-shaped setae are found to be with diameters ranging from 3 micrometer at root to several nanometers at the top end. This structure is comparable to the heterogeneous surface of the lotus leaf and butterfly wings which is composed of solid and air phase. It is the heterogeneous surface with microstructures in different scales gives the leg's surface superhydrophobic property. The air that trapped in spaces in the microwetted and nanogrooves formed a cushion supporting their body on the water surface.

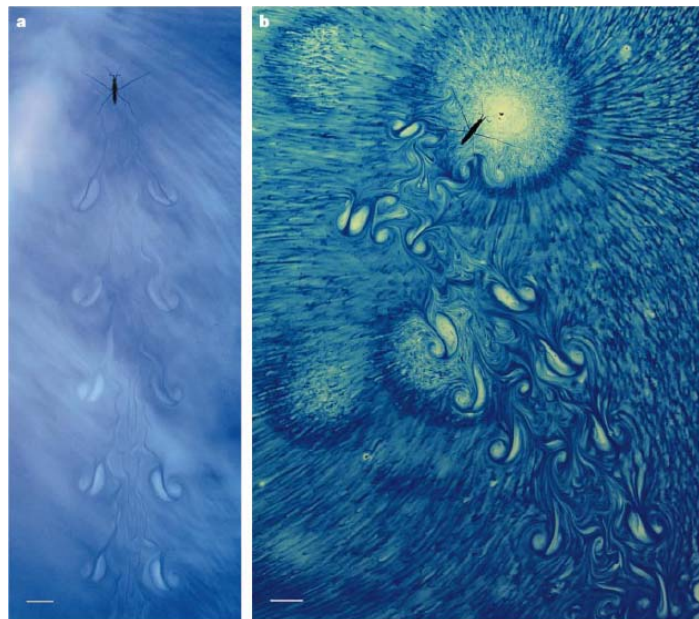


Figure 2.18. Images captured from a side view revealed the vortical footprints of the water strider¹²⁵.

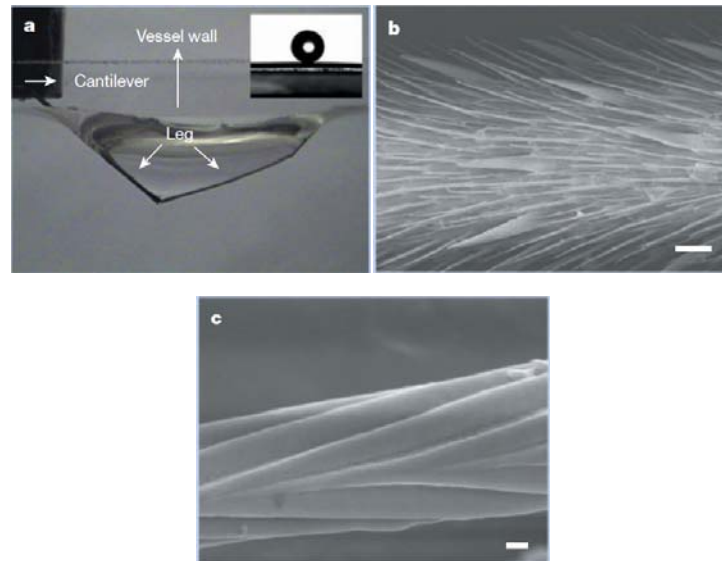


Figure 2.19. (a) side view of Gerridae's leg in water; (b), (c) SEM images of micro-, nano-structure on a leg¹²⁷.

2.6 Wettability of the biomimetic artificial surfaces

As discussed in Section 2.5, the “self-clean” property of the lotus leaf is originated from a combination of the micro/nano-scale structures. To mimic the surface of the lotus leaf, a nano-scale structure was fabricated on a aligned carbon nanotube (ACNT) to construct a superhydrophobic surface. As Figure 2.20 shows, the lotus-like film surface was composed of $2.89 \pm 0.32 \mu\text{m}$ papillae and 30-60nm carbon nanotube. CA on the ACNT was about 166° . Comparing with the densely packed ACNT surface, this micro-scale structure on the surface increases the CA and decreases the sliding angle. This multi-scale structure acts as an important role in constructing the superhydrophobic surface.

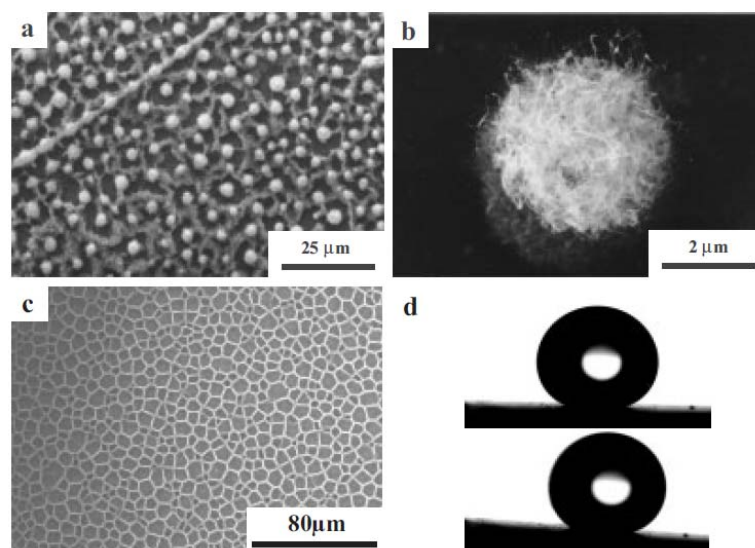


Figure 2.20. (a), (b), (c) SEM images of surface structure of the lotus-like ACNT films; (d) sliding behavior of a water droplet on the films surface¹²¹.

Using the same principle indicated in the above paragraph, a superhydrophobic surface was prepared by casting the poly (methyl methacrylate) (PMMA) and amphiphilic polyurethane (A-PU) dissolved in DMF solution¹²⁸. A roughness surface was formed during the solvent evaporation, and the contact angle reaches about 160° (Figure 2.21e). However, unlike the situation of water on lotus (Figure 2.21a,b,c,d), the droplet was pinned on the surface at any titled angles. This special wetting behavior is attributed to the surface composition with both hydrophobic and hydrophilic domain on nano-scale. The hydrophobic domains in combination with the porous structure lead to a very high contact angle; the hydrophilic domains contact with water at the interface and adhere the droplets.

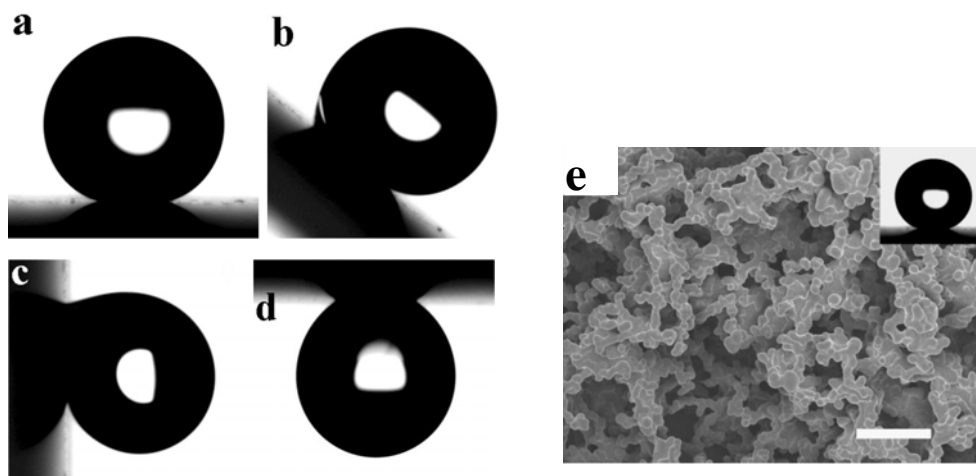


Figure 2.21. Photos of water drop on surface at different angles (a) 0° , (b) 45° , (c) 90° , (d)

180° ¹²⁸.

As has been mentioned in the previous section, Wenzel model reveals that a hydrophilic surface will become more hydrophilic with increasing degree of roughness; while a hydrophobic surface will become more hydrophobic if the same type of roughness is introduced. Based on this theory, a dual-stimuli-responsive surface with tunable wettability, reversible switching between superhydrophilicity and superhydrophobicity, and responsivity to both temperature and pH is reported¹²⁹. Such surfaces are obtained by simply fabricating a poly(*N*-isopropyl acrylamide-*co*-acrylic acid) [P(NIPAAm-*co*-AAc)] copolymer thin film on both a flat and a roughly etched silicon substrate. Reversible switching between superhydrophilicity and superhydrophobicity can be realized over both a narrow temperature range of about 10°C and over a relatively wide pH range of about 10. Figure 2.22a showed the contact angle results measured under different pH values and temperatures. When pH value is

stabled, the tendency of contact angles were showed in Figure 2.22b (black line: pH=2; red line: pH=4; green line: pH=7; blue line: pH=9). The hypothetical conformations of hydrogen bonding and repeating cycles were showed in Figure 2.22c and d, respectively. This dual-responsive property is a result of the combined effect of the chemical variation of the surface and the surface roughness.

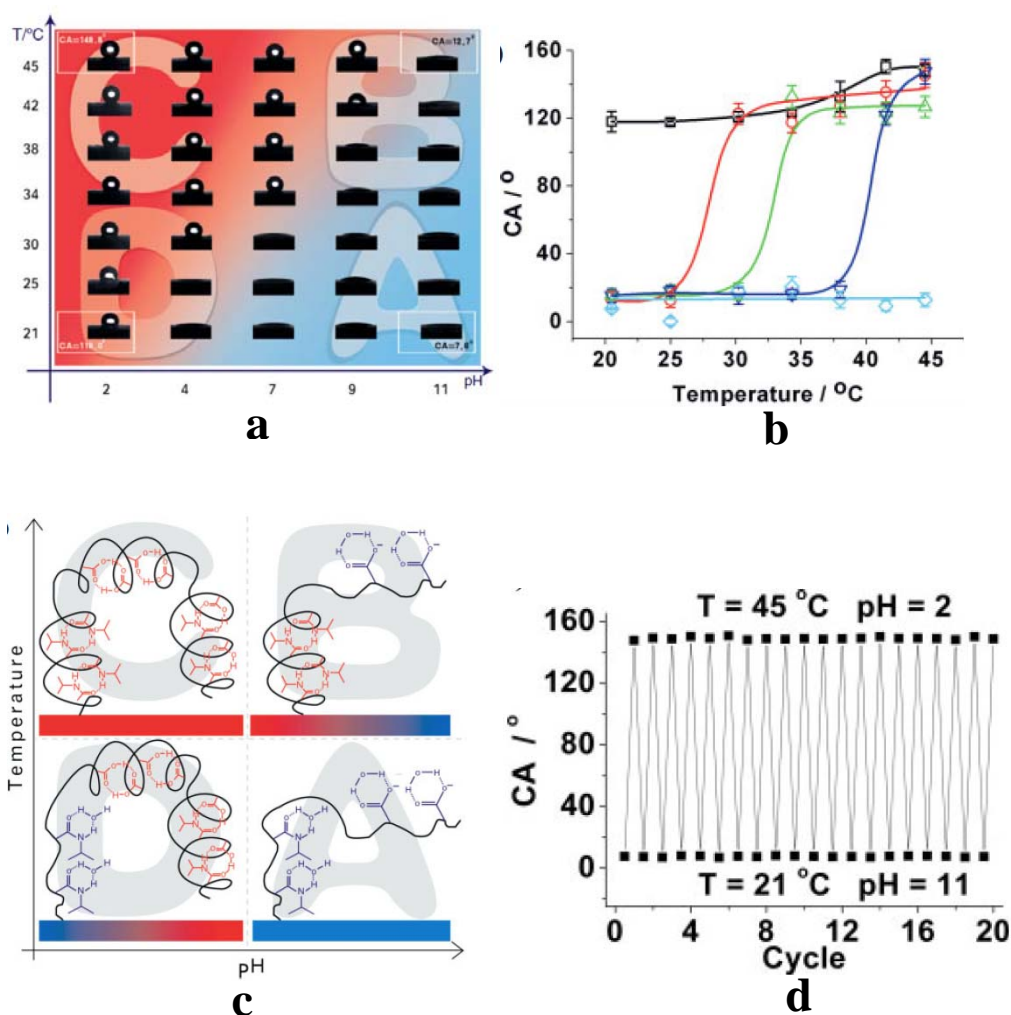


Figure 2.22. The contact angle results measured under various temperatures and pH

values¹²⁹.

2.7 References

- 1 Igor Yu Galaev, B. M. Smart Polymers for Bioseparation and Bioprocessing (2002).
- 2 TEXTBOOK OF POLYMER SCIENCE, 3RD EDITION - BILLMEYER,FW. *Plast. Eng.* 40, 76-76, (1984).
- 3 Pearce, E. M. Polymers: Chemistry and physics of modern materials. *Journal of Polymer Science Part A: Polymer Chemistry* 30, 1777-1777, (1992).
- 4 Appel, W. P. J., Nieuwenhuizen, M. M. L. & Meijer, E. W. in *Supramolecular Polymer Chemistry* 1-28 (Wiley-VCH Verlag GmbH & Co. KGaA, 2011).
- 5 Gordon, W., Too, C., Aleksandra, V., Igor Yu, G. & Mattiasson, B. in *Smart Materials* (CRC Press, 2008).
- 6 Kumar, A., Srivastava, A., Galaev, I. Y. & Mattiasson, B. Smart polymers: Physical forms and bioengineering applications. *Prog. Polym. Sci.* 32, 1205-1237, (2007).
- 7 Jeong, B. & Gutowska, A. Lessons from nature: stimuli-responsive polymers and their biomedical applications. *Trends in Biotechnology* 20, 305-311, (2002).
- 8 Hoffman, A. S. *et al.* Really smart bioconjugates of smart polymers and receptor proteins. *Journal of Biomedical Materials Research* 52, 577-586, (2000).
- 9 Galaev, I. Y. & Mattiasson, B. 'Smart' polymers and what they could do in biotechnology and medicine. *Trends in Biotechnology* 17, 335-340, (1999).

- 10 Kikuchi, A. & Okano, T. Intelligent thermoresponsive polymeric stationary phases for aqueous chromatography of biological compounds. *Prog. Polym. Sci.* 27, 1165-1193, (2002).
- 11 Ebara, M. *et al.* Copolymerization of 2-Carboxyisopropylacrylamide with N-Isopropylacrylamide Accelerates Cell Detachment from Grafted Surfaces by Reducing Temperature. *Biomacromolecules* 4, 344-349, (2003).
- 12 Toomey, R. & Tirrell, M. in *Annual Review of Physical Chemistry* Vol. 59 *Annual Review of Physical Chemistry* 493-517 (Annual Reviews, 2008).
- 13 Feng, Q. H., Chen, F. G. & Wu, H. R. PREPARATION AND CHARACTERIZATION OF A TEMPERATURE-SENSITIVE LIGNIN-BASED HYDROGEL. *BioResources* 6, 4942-4952, (2011).
- 14 Van Vlierberghe, S., Dubruel, P. & Schacht, E. Biopolymer-Based Hydrogels As Scaffolds for Tissue Engineering Applications: A Review. *Biomacromolecules* 12, 1387-1408, (2011).
- 15 Costa, R. O. R. & Freitas, R. F. S. Phase behavior of poly(N-isopropylacrylamide) in binary aqueous solutions. *Polymer* 43, 5879-5885, (2002).
- 16 Schild, H. G. POLY (N-ISOPROPYLACRYLAMIDE) - EXPERIMENT, THEORY AND APPLICATION. *Prog. Polym. Sci.* 17, 163-249, (1992).
- 17 Qiu, Y. & Park, K. Environment-sensitive hydrogels for drug delivery. *Adv. Drug*

- Deliv. Rev.* 53, 321-339, (2001).
- 18 Aoki, T., Muramatsu, M., Torii, T., Sanui, K. & Ogata, N. Thermosensitive Phase Transition of an Optically Active Polymer in Aqueous Milieu. *Macromolecules* 34, 3118-3119, (2001).
- 19 Gan, L. H., Gan, Y. Y. & Deen, G. R. Poly(N-acryloyl-N'-propylpiperazine): A New Stimuli-Responsive Polymer. *Macromolecules* 33, 7893-7897, (2000).
- 20 Scarpa, J. S., Mueller, D. D. & Klotz, I. M. Slow hydrogen-deuterium exchange in a non- α -helical polyamide. *Journal of the American Chemical Society* 89, 6024-6030, (1967).
- 21 Xia, F. 仿生多尺度智能界面材料的构筑及研究 Doctor thesis, (2008).
- 22 Kishi, R., Hirasa, O. & Ichijo, H. Fast responsive poly(N-isopropylacrylamide) hydrogels prepared by gamma-ray irradiation. *Polym. Gels Netw.* 5, 145-151, (1997).
- 23 Wu, X. S., Hoffman, A. S. & Yager, P. SYNTHESIS AND CHARACTERIZATION OF THERMALLY REVERSIBLE MACROPOROUS POLY(N-ISOPROPYLACRYLAMIDE) HYDROGELS. *J. Polym. Sci. Pol. Chem.* 30, 2121-2129, (1992).
- 24 Zhang, X.-Z. & Zhuo, R.-X. Preparation of fast responsive, thermally sensitive poly(N-isopropylacrylamide) gel. *European Polymer Journal* 36, 2301-2303,

- (2000).
- 25 Robert, P. Temperature-sensitive aqueous microgels. *Advances in Colloid and Interface Science* 85, 1-33, (2000).
- 26 Pelton, R. H. & Chibante, P. Preparation of aqueous latices with N-isopropylacrylamide. *Colloids and Surfaces* 20, 247-256, (1986).
- 27 Morris, G. E., Vincent, B. & Snowden, M. J. Adsorption of Lead Ions onto N-Isopropylacrylamide and Acrylic Acid Copolymer Microgels. *Journal of Colloid and Interface Science* 190, 198-205, (1997).
- 28 Saunders, B. R. & Vincent, B. Microgel particles as model colloids: theory, properties and applications. *Advances in Colloid and Interface Science* 80, 1-25, (1999).
- 29 Liang, Feng, X., Liu, J., Rieke, P. C. & Fryxell, G. E. Reversible Surface Properties of Glass Plate and Capillary Tube Grafted by Photopolymerization of N-Isopropylacrylamide. *Macromolecules* 31, 7845-7850, (1998).
- 30 Liang *et al.* Surfaces with Reversible Hydrophilic/Hydrophobic Characteristics on Cross-linked Poly(N-isopropylacrylamide) Hydrogels. *Langmuir* 16, 8016-8023, (2000).
- 31 Liang *et al.* Temperature-Sensitive Surfaces Prepared by UV Photografting Reaction of Photosensitizer and N-Isopropylacrylamide. *The Journal of Physical Chemistry B*

- 104, 11667-11673, (2000).
- 32 Kuckling, D., Harmon, M. E. & Frank, C. W. Photo-Cross-Linkable PNIPAAm Copolymers. 1. Synthesis and Characterization of Constrained Temperature-Responsive Hydrogel Layers. *Macromolecules* 35, 6377-6383, (2002).
- 33 Yakushiji, T. *et al.* Graft Architectural Effects on Thermoresponsive Wettability Changes of Poly(N-isopropylacrylamide)-Modified Surfaces. *Langmuir* 14, 4657-4662, (1998).
- 34 Sun, T. *et al.* Reversible Switching between Superhydrophilicity and Superhydrophobicity. *Angewandte Chemie International Edition* 43, 357-360, (2004).
- 35 Fu, Q. *et al.* Reversible Control of Free Energy and Topography of Nanostructured Surfaces. *Journal of the American Chemical Society* 126, 8904-8905, (2004).
- 36 Sun, T. *et al.* Responsive Aligned Carbon Nanotubes. *Angewandte Chemie International Edition* 43, 4663-4666, (2004).
- 37 Gil, E. S. & Hudson, S. A. Stimuli-responsive polymers and their bioconjugates. *Prog. Polym. Sci.* 29, 1173-1222, (2004).
- 38 Brannon-Peppas, L. & Peppas, N. A. Dynamic and equilibrium swelling behaviour of pH-sensitive hydrogels containing 2-hydroxyethyl methacrylate. *Biomaterials* 11, 635-644, (1990).

- 39 Khare, A. R. RELEASE BEHAVIOR OF BIOACTIVE AGENTS FROM PH-SENSITIVE HYDROGELS (VOL 4, PG 275, 1993). *J. Biomater. Sci.-Polym. Ed. 6*, U1-U1, (1994).
- 40 Khare, A. R. & Peppas, N. A. RELEASE BEHAVIOR OF BIOACTIVE AGENTS FROM PH-SENSITIVE HYDROGELS. *J. Biomater. Sci.-Polym. Ed. 4*, 275-289, (1993).
- 41 Godbey, W. T., Wu, K. K. & Mikos, A. G. Poly(ethylenimine) and its role in gene delivery. *Journal of Controlled Release* 60, 149-160, (1999).
- 42 Godbey, W. T. & Mikos, A. G. Recent progress in gene delivery using non-viral transfer complexes. *Journal of Controlled Release* 72, 115-125, (2001).
- 43 Urtti, A., Polansky, J., Lui, G. M. & Szoka, F. C. Gene delivery and expression in human retinal pigment epithelial cells: Effects of synthetic carriers, serum, extracellular matrix and viral promoters. *J. Drug Target.* 7, 413-421, (2000).
- 44 Tang, M. X., Redemann, C. T. & Szoka, F. C. In Vitro Gene Delivery by Degraded Polyamidoamine Dendrimers. *Bioconjugate Chemistry* 7, 703-714, (1996).
- 45 Ionov, L. *et al.* Inverse and Reversible Switching Gradient Surfaces from Mixed Polyelectrolyte Brushes. *Langmuir* 20, 9916-9919, (2004).
- 46 Jiang, Y. *et al.* Self-Assembled Monolayers of Dendron Thiols for Electrodeposition of Gold Nanostructures: Toward Fabrication of Superhydrophobic/Superhydrophilic

- Surfaces and pH-Responsive Surfaces. *Langmuir* 21, 1986-1990, (2005).
- 47 Yu, X., Wang, Z., Jiang, Y., Shi, F. & Zhang, X. Reversible pH-Responsive Surface: From Superhydrophobicity to Superhydrophilicity. *Advanced Materials* 17, 1289-1293, (2005).
- 48 Shiga, T., Hirose, Y., Okada, A. & Kurauchi, T. Bending of ionic polymer gel caused by swelling under sinusoidally varying electric fields. *Journal of Applied Polymer Science* 47, 113-119, (1993).
- 49 Gong, J. P., Nitta, T. & Osada, Y. Electrokinetic Modeling of the Contractile Phenomena of Polyelectrolyte Gels. One-Dimensional Capillary Model. *The Journal of Physical Chemistry* 98, 9583-9587, (1994).
- 50 Lahann, J. *et al.* A Reversibly Switching Surface. *Science* 299, 371-374, (2003).
- 51 Wang, R. *et al.* Light-induced amphiphilic surfaces. *Nature* 388, 431-432, (1997).
- 52 Wang, R., Sakai, N., Fujishima, A., Watanabe, T. & Hashimoto, K. Studies of Surface Wettability Conversion on TiO₂ Single-Crystal Surfaces. *The Journal of Physical Chemistry B* 103, 2188-2194, (1999).
- 53 Machida, M., Norimoto, K., Watanabe, T., Hashimoto, K. & Fujishima, A. The effect of SiO₂ addition in super-hydrophilic property of TiO₂ photocatalyst. *Journal of Materials Science* 34, 2569-2574, (1999).

- 54 Sakai, N., Wang, R., Fujishima, A., Watanabe, T. & Hashimoto, K. Effect of Ultrasonic Treatment on Highly Hydrophilic TiO₂ Surfaces. *Langmuir* 14, 5918-5920, (1998).
- 55 Miyauchi, M., Nakajima, A., Hashimoto, K. & Watanabe, T. A Highly Hydrophilic Thin Film Under 1 $\mu\text{W}/\text{cm}^2$ UV Illumination. *Advanced Materials* 12, 1923-1927, (2000).
- 56 Sakai, N., Fujishima, A., Watanabe, T. & Hashimoto, K. Enhancement of the Photoinduced Hydrophilic Conversion Rate of TiO₂ Film Electrode Surfaces by Anodic Polarization. *The Journal of Physical Chemistry B* 105, 3023-3026, (2001).
- 57 Nakajima, A., Koizumi, S.-i., Watanabe, T. & Hashimoto, K. Photoinduced Amphiphilic Surface on Polycrystalline Anatase TiO₂ Thin Films. *Langmuir* 16, 7048-7050, (2000).
- 58 Wang, R. *et al.* Photogeneration of Highly Amphiphilic TiO₂ Surfaces. *Advanced Materials* 10, 135-138, (1998).
- 59 Qi, K. H. & Xin, J. H. Room-Temperature Synthesis of Single-Phase Anatase TiO₂ by Aging and its Self-Cleaning Properties. *ACS Appl. Mater. Interfaces* 2, 3479-3485, (2010).
- 60 Wang, R. H., Wang, X. W. & Xin, J. H. Advanced Visible-Light-Driven Self-Cleaning Cotton by Au/TiO₂/SiO₂ Photocatalysts. *ACS Appl. Mater.*

- Interfaces* 2, 82-85, (2010).
- 61 Porcar, I., Perrin, P. & Tribet, C. UV-Visible Light: A Novel Route to Tune the Type of an Emulsion. *Langmuir* 17, 6905-6909, (2001).
- 62 Higashi, N., Shimizu, K. & Niwa, M. Surface Monolayers of Poly(l-glutamic Acid)-Functionalized Amphiphiles: Effect of Attachment of Spiropyran to the Polymer Segment. *Journal of Colloid and Interface Science* 185, 44-48, (1997).
- 63 Suzuki, A. & Tanaka, T. Phase transition in polymer gels induced by visible light. *Nature* 346, 345-347, (1990).
- 64 Brewis, D. M. Polymer surfaces and interfaces, Wiley, Chichester, 1987, 272 pages, £31.50/\$67.50, ISBN 0471 91214 X. W. J. Feast and H. S. Munro (Eds). *Surface and Interface Analysis* 11, 217-217, (1988).
- 65 Kato, K., Uchida, E., Kang, E.-T., Uyama, Y. & Ikada, Y. Polymer surface with graft chains. *Prog. Polym. Sci.* 28, 209-259, (2003).
- 66 Tsubokawa, N., Hosoya, M., Yanadori, K. & Sone, Y. Grafting Onto Carbon Black: Reaction of Functional Groups on Carbon Black with ACYL Chloride-Capped Polymers. *Journal of Macromolecular Science: Part A - Chemistry* 27, 445-457, (1990).
- 67 Benoit, D., Chaplinski, V., Braslau, R. & Hawker, C. J. Development of a universal alkoxyamine for "living" free radical polymerizations. *Journal of the American*

Chemical Society 121, 3904-3920, (1999).

- 68 Huang, N. P. *et al.* Poly(L-lysine)-g-poly(ethylene glycol) layers on metal oxide surfaces: Surface-analytical characterization and resistance to serum and fibrinogen adsorption. *Langmuir* 17, 489-498, (2001).
- 69 Sheiko, S. S., Sumerlin, B. S. & Matyjaszewski, K. Cylindrical molecular brushes: Synthesis, characterization, and properties. *Prog. Polym. Sci.* 33, 759-785, (2008).
- 70 Minko, S. *et al.* Synthesis of Adaptive Polymer Brushes via “Grafting To” Approach from Melt. *Langmuir* 18, 289-296, (2002).
- 71 R uhe, J. in *Polymer Brushes* 1-31 (Wiley-VCH Verlag GmbH & Co. KGaA, 2005).
- 72 Biesalski, M., Johannsmann, D. & Ruhe, J. Synthesis and swelling behavior of a weak polyacid brush. *The Journal of Chemical Physics* 117, 4988-4994, (2002).
- 73 Biesalski, M. & R uhe, J. Synthesis of a Poly(p-styrenesulfonate) Brush via Surface-Initiated Polymerization. *Macromolecules* 36, 1222-1227, (2003).
- 74 Fan, X. *et al.* Polymer Brushes Grafted from Clay Nanoparticles Adsorbed on a Planar Substrate by Free Radical Surface-Initiated Polymerization. *Langmuir* 19, 916-923, (2002).
- 75 Zhou, Q., Fan, X., Xia, C., Mays, J. & Advincula, R. Living Anionic Surface

- Initiated Polymerization (SIP) of Styrene from Clay Surfaces. *Chemistry of Materials* 13, 2465-2467, (2001).
- 76 Advincula, R. *et al.* Polymer Brushes by Living Anionic Surface Initiated Polymerization on Flat Silicon (SiO_x) and Gold Surfaces: Homopolymers and Block Copolymers. *Langmuir* 18, 8672-8684, (2002).
- 77 Quirk, R. P., Mathers, R. T., Cregger, T. & Foster, M. D. Anionic Synthesis of Block Copolymer Brushes Grafted from a 1,1-Diphenylethylene Monolayer. *Macromolecules* 35, 9964-9974, (2002).
- 78 Xia, J. & Matyjaszewski, K. Controlled/"Living" Radical Polymerization. Atom Transfer Radical Polymerization Using Multidentate Amine Ligands. *Macromolecules* 30, 7697-7700, (1997).
- 79 Jankova, K., Chen, X., Kops, J. & Batsberg, W. Synthesis of Amphiphilic PS-b-PEG-b-PS by Atom Transfer Radical Polymerization. *Macromolecules* 31, 538-541, (1998).
- 80 Masci, G., Giacomelli, L. & Crescenzi, V. Atom Transfer Radical Polymerization of N-Isopropylacrylamide. *Macromolecular Rapid Communications* 25, 559-564, (2004).
- 81 Street, G., Illsley, D. & Holder, S. J. Optimization of the synthesis of poly(octadecyl acrylate) by atom transfer radical polymerization and the preparation of all comblike

- amphiphilic diblock copolymers. *Journal of Polymer Science Part A: Polymer Chemistry* 43, 1129-1143, (2005).
- 82 Shipp, D. A., Wang, J.-L. & Matyjaszewski, K. Synthesis of Acrylate and Methacrylate Block Copolymers Using Atom Transfer Radical Polymerization. *Macromolecules* 31, 8005-8008, (1998).
- 83 Kato, M., Kamigaito, M., Sawamoto, M. & Higashimura, T. Polymerization of Methyl Methacrylate with the Carbon Tetrachloride/Dichlorotris-(triphenylphosphine)ruthenium(II)/Methylaluminum Bis(2,6-di-tert-butylphenoxide) Initiating System: Possibility of Living Radical Polymerization. *Macromolecules* 28, 1721-1723, (1995).
- 84 Wang, J.-S. & Matyjaszewski, K. Controlled/"living" radical polymerization. atom transfer radical polymerization in the presence of transition-metal complexes. *Journal of the American Chemical Society* 117, 5614-5615, (1995).
- 85 Matyjaszewski, K. & Xia, J. Atom Transfer Radical Polymerization. *Chemical Reviews* 101, 2921-2990, (2001).
- 86 Tang, W. & Matyjaszewski, K. Effect of Ligand Structure on Activation Rate Constants in ATRP. *Macromolecules* 39, 4953-4959, (2006).
- 87 Matyjaszewski, K., Paik, H.-j., Zhou, P. & Diamanti, S. J. Determination of Activation and Deactivation Rate Constants of Model Compounds in Atom Transfer

- Radical Polymerization I. *Macromolecules* 34, 5125-5131, (2001).
- 88 Rorabacher, D. B. Electron Transfer by Copper Centers. *Chemical Reviews* 104, 651-698, (2004).
- 89 Qiu, J., Matyjaszewski, K., Thouin, L. & Amatore, C. Cyclic voltammetric studies of copper complexes catalyzing atom transfer radical polymerization. *Macromolecular Chemistry and Physics* 201, 1625-1631, (2000).
- 90 Pintauer, T. & Matyjaszewski, K. Structural aspects of copper catalyzed atom transfer radical polymerization. *Coordination Chemistry Reviews* 249, 1155-1184, (2005).
- 91 Ohno, K., Koh, K.-m., Tsujii, Y. & Fukuda, T. Synthesis of Gold Nanoparticles Coated with Well-Defined, High-Density Polymer Brushes by Surface-Initiated Living Radical Polymerization. *Macromolecules* 35, 8989-8993, (2002).
- 92 Balamurugan, S., Mendez, S., Balamurugan, S. S., O'Brien, M. J. & López, G. P. Thermal Response of Poly(N-isopropylacrylamide) Brushes Probed by Surface Plasmon Resonance. *Langmuir* 19, 2545-2549, (2003).
- 93 Jones, D. M. & Huck, W. T. S. Controlled Surface-Initiated Polymerizations in Aqueous Media. *Advanced Materials* 13, 1256-1259, (2001).
- 94 Jones, D. M., Smith, J. R., Huck, W. T. S. & Alexander, C. Variable Adhesion of Micropatterned Thermoresponsive Polymer Brushes: AFM Investigations of

- Poly(N-isopropylacrylamide) Brushes Prepared by Surface-Initiated Polymerizations. *Advanced Materials* 14, 1130-1134, (2002).
- 95 Kizhakkedathu, J. N. & Brooks, D. E. Synthesis of Poly(N,N-dimethylacrylamide) Brushes from Charged Polymeric Surfaces by Aqueous ATRP: Effect of Surface Initiator Concentration. *Macromolecules* 36, 591-598, (2003).
- 96 Boyes, S. G., Brittain, W. J., Weng, X. & Cheng, S. Z. D. Synthesis, Characterization, and Properties of ABA Type Triblock Copolymer Brushes of Styrene and Methyl Acrylate Prepared by Atom Transfer Radical Polymerization. *Macromolecules* 35, 4960-4967, (2002).
- 97 Shull, K. R. & Karis, T. E. Dewetting dynamics for large equilibrium contact angles. *Langmuir* 10, 334-339, (1994).
- 98 Tretinnikov, O. N. & Ikada, Y. Hydrogen Bonding and Wettability of Surface-Grafted Organophosphate Polymer. *Macromolecules* 30, 1086-1090, (1997).
- 99 Crevoisier, G. d., Fabre, P., Corpart, J.-M. & Leibler, L. Switchable Tackiness and Wettability of a Liquid Crystalline Polymer. *Science* 285, 1246-1249, (1999).
- 100 Rieutord, F. & Salmeron, M. Wetting Properties at the Submicrometer Scale: A Scanning Polarization Force Microscopy Study. *The Journal of Physical Chemistry B* 102, 3941-3944, (1998).

- 101 Yoo, D., Shiratori, S. S. & Rubner, M. F. Controlling Bilayer Composition and Surface Wettability of Sequentially Adsorbed Multilayers of Weak Polyelectrolytes. *Macromolecules* 31, 4309-4318, (1998).
- 102 Thünemann, A. F., Schnöller, U., Nuyken, O. & Voit, B. Diazosulfonate Polymer Complexes: Structure and Wettability. *Macromolecules* 33, 5665-5671, (2000).
- 103 Thünemann, A. F. Complexes of Polyethyleneimine with Perfluorinated Carboxylic Acids: Wettability of Lamellar Structured Mesophases. *Langmuir* 16, 824-828, (1999).
- 104 Ichimura, K., Oh, S.-K. & Nakagawa, M. Light-Driven Motion of Liquids on a Photoresponsive Surface. *Science* 288, 1624-1626, (2000).
- 105 Ellison, A. H., Fox, H. W. & Zisman, W. A. Wetting of Fluorinated Solids by Hydrogen-Bonding Liquids. *The Journal of Physical Chemistry* 57, 622-627, (1953).
- 106 Liu, X., Liang, Y., Zhou, F. & Liu, W. Extreme wettability and tunable adhesion: biomimicking beyond nature? *Soft Matter* 8, 2070-2086, (2012).
- 107 Tadmor, R. Line Energy and the Relation between Advancing, Receding, and Young Contact Angles. *Langmuir* 20, 7659-7664, (2004).
- 108 Young, T. An Essay on the Cohesion of Fluids. *Philosophical Transactions of the Royal Society of London* 95, 65-87, (1805).

- 109 Hare, E. F., Shafrin, E. G. & Zisman, W. A. Properties of Films of Adsorbed Fluorinated Acids. *The Journal of Physical Chemistry* 58, 236-239, (1954).
- 110 Nishino, T., Meguro, M., Nakamae, K., Matsushita, M. & Ueda, Y. The Lowest Surface Free Energy Based on $-CF_3$ Alignment. *Langmuir* 15, 4321-4323, (1999).
- 111 Wenzel, R. N. RESISTANCE OF SOLID SURFACES TO WETTING BY WATER. *Industrial & Engineering Chemistry* 28, 988-994, (1936).
- 112 Dorrer, C. & Ruhe, J. Some thoughts on superhydrophobic wetting. *Soft Matter* 5, 51-61, (2009).
- 113 Cassie, A. B. D. & Baxter, S. Wettability of porous surfaces. *Transactions of the Faraday Society* 40, 546-551, (1944).
- 114 Vogler, E. A. Structure and reactivity of water at biomaterial surfaces. *Advances in Colloid and Interface Science* 74, 69-117, (1998).
- 115 Yoon, R.-H., Flinn, D. H. & Rabinovich, Y. I. Hydrophobic Interactions between Dissimilar Surfaces. *Journal of Colloid and Interface Science* 185, 363-370, (1997).
- 116 Berg, J. M., Eriksson, L. G. T., Claesson, P. M. & Borve, K. G. N. Three-Component Langmuir-Blodgett Films with a Controllable Degree of Polarity. *Langmuir* 10, 1225-1234, (1994).
- 117 Wang, S. & Jiang, L. Definition of Superhydrophobic States. *Advanced Materials*

- 19, 3423-3424, (2007).
- 118 Ball, P. Engineering Shark skin and other solutions. *Nature* 400, 507-509, (1999).
- 119 Barthlott, W. & Neinhuis, C. Purity of the sacred lotus, or escape from contamination in biological surfaces. *Planta* 202, 1-8, (1997).
- 120 NEINHUIS, C. & BARTHLOTT, W. Characterization and Distribution of Water-repellent, Self-cleaning Plant Surfaces. *Annals of Botany* 79, 667-677, (1997).
- 121 Feng, L. *et al.* Super-Hydrophobic Surfaces: From Natural to Artificial. *Advanced Materials* 14, 1857-1860, (2002).
- 122 Kennedy, R. J. Directional Water-shedding Properties of Feathers. *Nature* 227, 736-737, (1970).
- 123 Zheng, Y., Gao, X. & Jiang, L. Directional adhesion of superhydrophobic butterfly wings. *Soft Matter* 3, 178-182, (2007).
- 124 Fan Xia, L. J. Bio-Inspired, Smart, Multiscale Interfacial Materials. *Advanced Materials* 9999, NA, (2008).
- 125 Hu, D. L., Chan, B. & Bush, J. W. M. The hydrodynamics of water strider locomotion. *Nature* 424, 663-666, (2003).
- 126 Keller, J. B. Surface tension force on a partly submerged body. *Physics of Fluids* 10, 3009-3010, (1998).

- 127 Gao, X. & Jiang, L. Biophysics: Water-repellent legs of water striders. *Nature* 432, 36-36, (2004).
- 128 Zhao, N. *et al.* A novel ultra-hydrophobic surface: Statically non-wetting but dynamically non-sliding. *Advanced Functional Materials* 17, 2739-2745, (2007).
- 129 Xia, F. *et al.* Dual-responsive surfaces that switch superhydrophilicity and superhydrophobicity. *Advanced Materials* 18, 432-+, (2006).

Chapter 3

Grafting temperature responsive polymer onto cotton fabric

Abstract

Atom transfer radical polymerization (ATRP) is the most widely applied controlled “living” radical polymerization technique. In this chapter, an ATRP approach was used to polymerize Poly(N-isopropylacrylamide) (PNIPAAm) brushes, directly from a cotton fabric. The presence of PNIPAAm on the surface of the cotton fabric was verified by FTIR, XPS and solid state NMR (SS-NMR), and the surface morphology was investigated by scanning electronic microscope (SEM). The covalent bond between the cotton surface and grafted polymer was confirmed by SS-NMR. To the best of our knowledge, it is the first time PNIPAAm was grafted to a cotton fabric. This work provides a highly potential synthesis and analysis route towards stimuli-responsive cotton fibers, which may have exceptional applications as novel intelligent fabrics for the textile related industries.

3.1 Introduction

In the past decades, many research works have been dedicated towards the modification of the chemical and physical properties of cellulose-based natural fibers, both in industry and in academic circles, aiming at imparting new and high performance functions to the fibers¹⁻⁵. For this purpose, great efforts have been devoted to the surface modification of cellulose fibers in order to control its properties, such as wettability, hydrophobicity or adhesion^{6,7}. As the most consumed fiber, cotton is composed of nearly 99% of cellulose⁸. The functionalization of cotton fiber via surface modification has high potential to create high-tech and high added-value textiles. Once modified with polymers, the cotton fibers could be used on sports clothes with improved thermal or elastic properties, water repellent, self-cleaning or oil-water separating fabrics. A particular interesting strategy would be to graft *stimuli*-responsive polymers that would turn a natural fiber into a smart material that responds to changes in the environment, *e.g.* Temperature, pH or light. The emerging applications of *stimuli*-responsive polymers have a large potential and have attracted much interest, as recently reviewed by Minko *et al.*⁹.

Currently, one of the most attractive ways to modify surfaces with polymer brushes is to perform Surface-Initiated Polymerization (SIP) *via* a “grafting from” approach. In particular, Atom Transfer Radical Polymerization (ATRP) SIP is a robust and versatile technique that has been used to graft (co)polymer chains

with controlled polydispersity and degree of polymerization from a large variety of substrates, e.g. silicon¹⁰⁻¹², gold^{13,14}, silica¹⁵, porous substrates^{16,17} and cellulose fibers as well^{1,4,5,7}.

In this work, a “grafting from” ATRP approach was used to polymerize Poly(*N*-isopropylacrylamide) (PNIPAAm) brushes, directly from a cotton fabric. PNIPAAm is a well-known thermo-responsive polymer that shows an extended hydrophilic chain conformation below its lower critical solution temperature (LCST, ~ 32 °C) in aqueous solution and undergoes a phase transition to insoluble and hydrophobic aggregates when the temperature is above its LCST¹⁸. To the best of our knowledge, the attempt to directly modify a cotton fiber with a *stimuli*-responsive polymer has not been reported in the literature. This work may open the possibility of creating a new intelligent cotton fabric which may adapt its surface wettability properties, *i.e.* from hydrophilic to hydrophobic and vice versa to the temperature fluctuation in the environment.

In this work, an extensive study to characterize *in-situ* the structure and dynamics of the PNIPAAm brushes directly grown from the surface of a cotton fabric was performed, while still covalently bonded to the substrate. FTIR, XPS, SEM and proton NMR techniques, both under static and magic-angle spinning conditions, have been used to characterize the bare, ATRP-initiator modified and PNIPAAm modified cotton fabrics.

3.2 Experimental

3.2.1 Materials

Cotton fabric obtained from textile innovators division of SDL ATLAS. The following chemicals were used without further purification, unless stated otherwise: acetone (Unichem, 99.8% purity), tetrahydrofuran (THF, Unichem, 99.8% purity), sodium carbonate (Na_2CO_3 , Aldrich, 99.0% purity), aminopropyl trimethoxysilane (ATMS, Aldrich, 99.0% purity), toluene (Unichem, 99.8% purity), triethylamine (TEA, Aldrich, 99.0% purity), 2-bromoisobutryl bromide (BiB, Aldrich, 99.0% purity), n-hexane (Aldrich, 99.0% purity), CuBr (Aldrich, 99.0% purity), methanol (Unichem, 99.8% purity), pentamethyldiethylenetriamine (PMDETA, Aldrich, 99.0% purity), dichloromethane (Unichem, 99.8% purity).

3.2.2 Instruments

FT-IR spectra were collected with a Perkin-Elmer 2000 Spectrometer in transmission mode and using dry KBr Pellets. A background spectrum was collected before each measurement. 32 scans were averaged to get a better signal-to-noise ratio. The spectral resolution was 4 cm^{-1} for all the measurements.

XPS data were obtained with an ESCALab 220i-XL electron spectrometer from VG Scientific using 300W Al- $K\alpha$ radiation. The base pressure was about 3×10^{-9} Mbar. The binding energies were calibrated to the C1s line at 284.8 eV.

Scanning Electron Microscopy (SEM) images were recorded on a JEOL JSM-6700F field emission microscope with 10 kV operating voltage. The pressure inside chamber was below 10^{-5} mbar. A thin layer of gold was deposited over the cotton samples before moving them into the chamber.

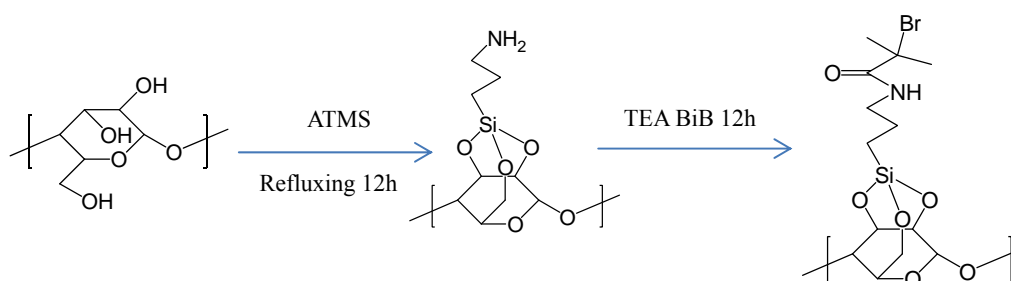
All the solid state NMR experiments were performed on a Bruker Avance III wide-bore solid-state NMR spectrometer operating at ^1H Larmor frequency of 400.13 MHz. A standard 4mm CP magic angle spinning (MAS) double resonance probe head was used for all the measurements. The MAS frequency of 8 kHz and 90° pulse duration of $4\mu\text{s}$ were used in ^1H MAS experiments. Typically 16 transients with a recycle delay of 10s were collected for each spectrum. The longest T_1 relaxation time of the sample is estimated to be shorter than 2s. Hence, a recycle delay of 10s was expected to be long enough for the full relaxation of the spectra.

3.2.3 Preparation of the cotton fabric initiator

The cotton fabric was rinsed with acetone, tetrahydrofuran (THF) and subsequently boiled in a sodium carbonate aqueous solution (10 wt %) for 4 hours. After the washing procedures, the fabric was dried at 40°C for 24 hours under vacuum. The immobilization of aminopropyl trimethoxysilane (ATMS) molecules on the cotton surface was conducted by adding 10.00 ml ATMS into a 200.00 ml toluene solution in which a small piece of cotton (0.8253 g) was immersed, and refluxing for 12 h. Next, the fabric was washed by acetone, THF

and water and dried at 40 °C for 24 hours

A small piece of the dried cotton-A fabric (0.2027 g) was then immersed in toluene (200.00 mL) to which 3.75 mmol of triethylamine were added. To this mixture 3.75 mmol of 2-bromoisobutyryl bromide were added drop-wise while keeping the temperature at 0 °C. The mixture was stirred for 1 hour at 0 °C and then heated to room temperature (ca. 25 °C). After reaching the desired temperature, the mixture was left stirring for 12 hours. The initiator modified-cotton fabric (Cotton-A-Br) was removed from the solution, washed with toluene and acetone and finally dried at room temperature under vacuum for 24 h (see Scheme 3.1).

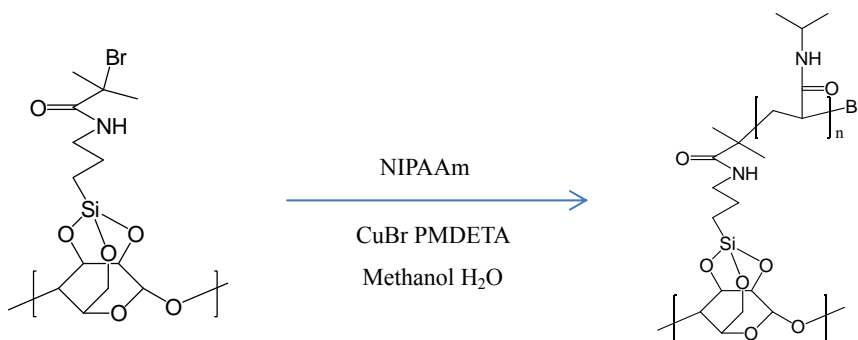


Scheme 3.1 Synthesis of Cotton-A-Br initiator.

3.2.4. Grafting of N-isopropylacrylamide from the initiator- functionalized cotton fabric

The *N*-Isopropylacrylamide (NIPAAm) (97.0 % purity) monomer was purchased from Aldrich, recrystallized twice in *n*-hexane and dried under vacuum before use. CuBr (10 mg, 0.069 mmol) and a small piece of initiator

modified-cotton fabric (27.3 mg, Cotton-ATMS-Br) were inserted in a Schlenk flask which was degassed by three cycles of vacuum-nitrogen filling, to remove any traces of oxygen. A mixture of Methanol/H₂O (1:1 v/v, total volume of 4.00 ml), NIPAAm (0.783 g, 6.9 mmol) and Pentamethyldiethylenetriamine (PMDETA, 14.00 μl) were degassed under argon flow for about 2 hours. This mixture was then added into the Schlenk flask filled with the solids, through a N₂ purged syringe needle. The reaction proceeded with magnetic stirring at room temperature for 2 hours. After the reaction, the Schlenk flask was open to let the air in and terminate the polymerization reaction. The PNIPAAm modified fabric (Cotton-PNIPAAm-L) was thoroughly washed in dichloromethane (CH₂Cl₂), acetone and H₂O to remove the residual monomer and catalyst complex. The Cotton-PNIPAAm-L fabric was finally dried at 40 °C overnight (see Scheme 3.2).

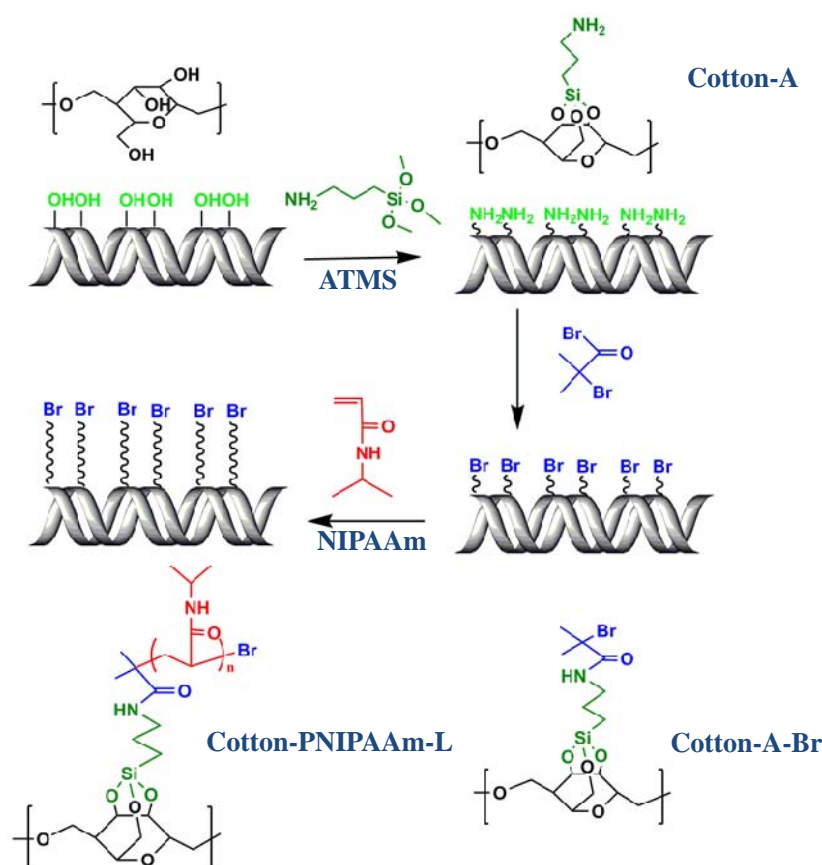


Scheme 3.2 Grafting NIPAAm from Cotton-A-Br initiator.

3.3 Result and discussion

3.3.1 Synthesis of Cotton-PNIPAAm-L polymer grafted surface via SI-ATRP

PNIPAAm brushes were grafted directly from a cotton fabric by a typical Surface-Initiated Atom Transfer Radical Polymerization (SI-ATRP) procedure in a methanol/water mixture. The synthetic procedure is schematically illustrated in Scheme 3.3.



Scheme 3.3 Schematic illustration of the synthesis of Cotton-PNIPAAm-L fabrics.

First, aminopropyl trimethoxysilane (ATMS) was immobilized on the

cotton surface (Cotton-A), to provide amine groups at the cotton surface for the further linking of the ATRP bromine initiator. Subsequently, 2-bromoisobutyryl bromide was reacted with the amino-terminated cotton surface to obtain the surface grafted initiator (Cotton-A-Br). Finally, the initiator immobilized cotton was immersed in a monomer solution to initiate the surface polymerization of PNIPAAm brushes (Cotton-PNIPAAm-L). The grafting reaction was conducted at room temperature for 2 hours.

3.3.2 Characterization of Cotton-PNIPAAm-L grafted cotton surface

3.3.2.1 Fourier transform infrared spectroscopy (FTIR)

In order to confirm the success of the grafting procedure, FTIR was used. Figure 3.1 shows the comparison of the FTIR spectra of the bare cotton fabric and the PNIPAAm modified samples (Cotton-PNIPAAm-L). The spectrum of Cotton-PNIPAAm-L shows two bands at 1650 cm^{-1} and 1540 cm^{-1} which are assigned to the typical amide I and II stretching vibrations of PNIPAAm^{19,20}. The amide band II is absent in spectrum of the bare cotton fiber. The vibration band at 1635 cm^{-1} observed for both spectra is attributed to the absorbed water²¹. In the spectrum of Cotton-PNIPAAm-L, this band overlaps with the amide band I at 1650 cm^{-1} which therefore exhibits higher intensity. Although the IR spectrum of the Cotton-A-Br sample was collected, it was not possible to identify the presence of the typical bands of the Br-initiator, most likely due to the large

difference of intensities between the cotton fiber and the Br-initiator vibration bands. Nevertheless, this characterization strongly suggests the presence of the PNIPAAm at the surface of the cotton fiber, since the main vibration bands of NIPAAm were identified for the modified cotton sample.

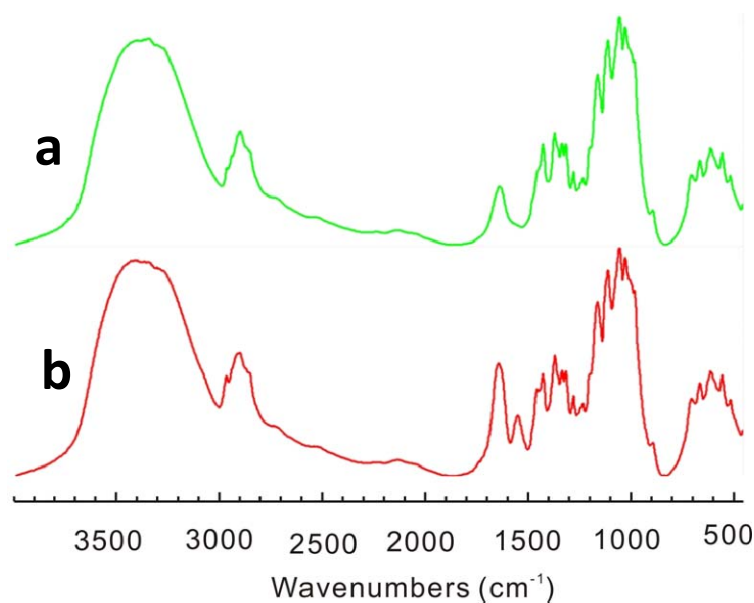


Figure 3.1 FT-IR spectra of: a) bare cotton fabric and b) Cotton-PNIPAAm-L.

3.3.2.2 X-Ray photoelectron spectroscopy (XPS)

In addition to the FTIR spectra, the presence of the polymer on the cotton fabric was verified by XPS as well. In the wide scan spectrum of bare cotton sample, only the C1s and O1s signals were identified (Figure 3.2 a). In the case of Cotton-PNIPAAm-L samples, however, the presence of distinctive N1s signal is a further indication that the cotton fibers are covered by PNIPAAm. Moreover, comparing the relative intensity of C1s/O1s in both spectra, it was found that the intensity of C1s increases significantly in the Cotton-PNIPAAm-L sample, which

is also an evidence of the presence of a polymer on the surface. Also in this case, it was not possible to detect the presence of Br atoms at the surface of the Cotton-A-Br sample.

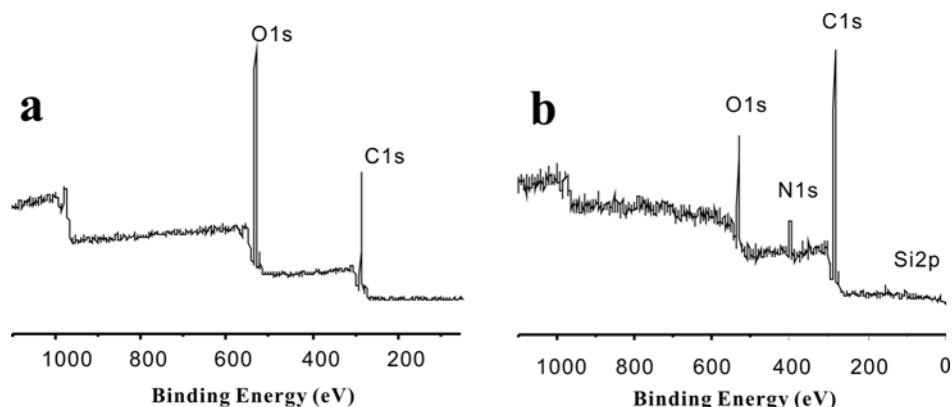


Figure 3.2 XPS overview spectra of: a) bare cotton surface and b) Cotton-PNIPAAm-Br surface

Both FTIR and XPS results suggest the presence of PNIPAAm molecules on the cotton fibers surface. The fact that presence of the Br-initiator can not be identified may indicate a low grafting efficiency of the ATRP-initiator and the low initiation efficiency may further lead to a low grafting efficiency of the PNIPAAm brushes. The low grafting efficiency of the initiator can be explained by the low density of the hydroxyl group available for the ATRP reaction. It is well known that the cellulose molecules in the cotton fiber are highly crystallizable due to its polarity. Most of the hydroxyl groups are densely packed in the crystalline lattice and therefore are not accessible to the initiator molecules. Based on this explanation, a possible method to improve grafting efficiency is to

treat the cotton surface by Plasma, UV irradiation methods, etc., in order to produce more polar groups on the cotton surface. It will be shown in Chapter 5 that this treatment is very efficient in improving the grafting efficiency of the ATRP-initiator.

3.3.2.3 Scanning electron microscopy (SEM)

In addition to the chemical structure analysis, SEM was used to investigate the surface morphology of the cotton fibers before and after modification. It can be observed in Figure 3.3 b that the surfaces of bare cotton fibers are clean and smooth. In contrast, the PNIPAAm modified-cotton fibers show a much different surface structure (Figure 3.3 d). PNIPAAm molecules seem to congregate in the form of granules, with diameters ranging from 100 to 200 nanometers at the surface of the cotton fibers. It should be noticed that these images were collected under normal vacuum and temperature conditions of SEM operation, meaning that the cotton is in the dry state. It was then expected that the PNIPAAm molecules at the surface of the cotton fabric would indeed adopt a coiled (aggregated) configuration, since there is no possibility to interact with water. Therefore, a rough surface with significant number of polymer aggregates was observed for the Cotton-PNIPAAm-L sample. This is a direct evidence of the surface grafting and in fact it shows qualitatively that the grafting efficiency is rather low. The preparation of highly grafted cotton fabrics (Cotton-PNIPAAm-H) and its thermal-responsive behavior will be discussed in chapters 5 and 6.

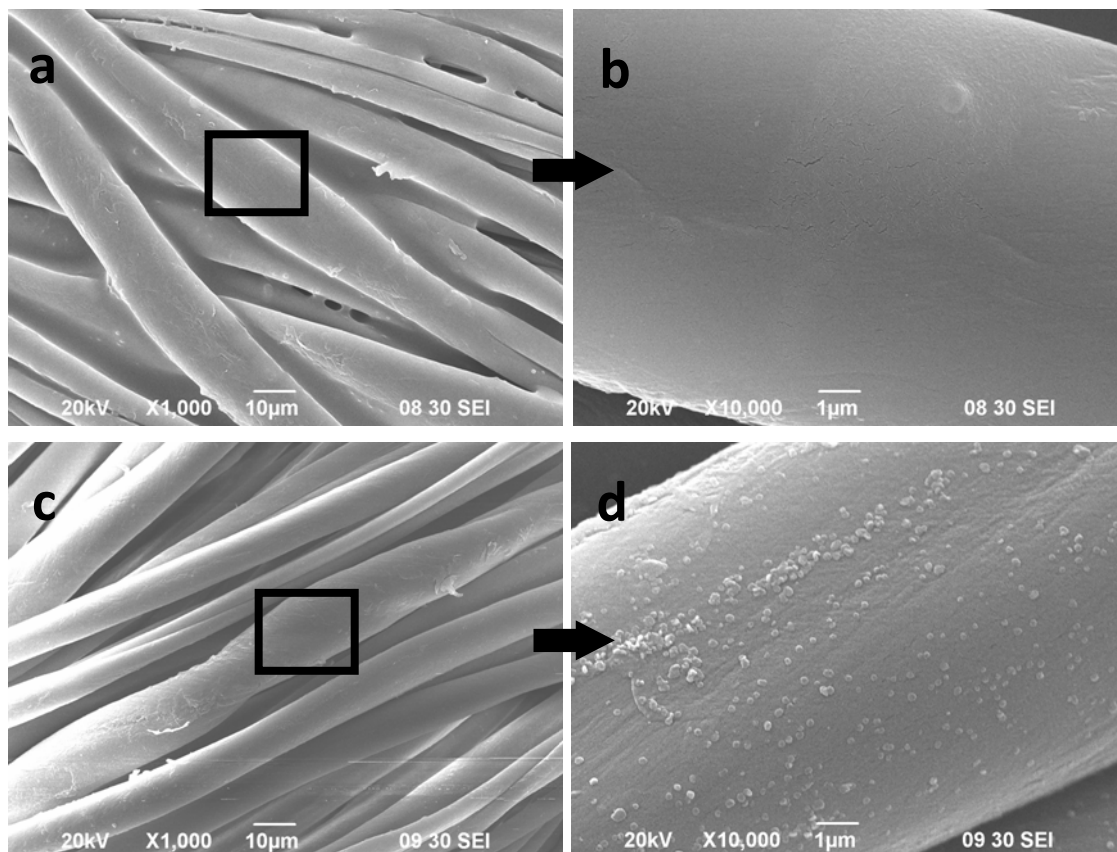


Figure 3.3 SEM images: a) and b) bare cotton fabric; c) and d) Cotton-PNIPAAm-L. The rectangles in a) and c) represent typical areas selected for the magnifications of b) and d), respectively.

Several attempts have been made to recover the grafted polymer for further characterization (M_w , PDI and grafting efficiency), but all turned out to be unsuccessfully. The residual amounts of solid collected were either too small for analyses or contaminated with cotton fibers residues which were degraded during the cleavage process. This is a long-standing difficulty faced by many other authors who tried to characterize the grafted polymer chains on various substrates^{22,23}, namely on cotton fibers, because the cellulose fibers are generally

fragile and easy to be damaged, and therefore it is practically impossible to cleave the polymer molecules from the substrate. In order to overcome this problem, some researchers proposed to added a sacrificial initiator parallel during the reaction.¹⁶ Another interesting method is to couple the target polymer molecules by a weak bond which can be easily cleaved from the substrate afterwards.¹⁷ However, the disadvantages of these methods are, first of all, the initiation efficiency of the sacrificial initiator has to be assumed to be the same as that of the initiator on the substrate; second, the coupling agent has to be selected according to the target polymers, and no versatile methods available for all different kinds of polymer chains.

In this study, a different route to characterize this PNIPAAm modified cotton fabrics was pursued by studying *in situ* the structure and dynamics of the polymer brushes at the surface of the cotton fibers, without performing a surface detachment. ¹H solid-state NMR techniques have been reported as being extremely sensitive and precise on probing the LCST transition of PNIPAAm^{24,25}. Herein, they were used to probe the transition behavior of the PNIPAAm brushes un-cleaved from the surface of the cotton fibers, and to prove the surface grafting of the polymer, in spite of the low grafting efficiency observed.

3.3.2.4 Static ¹H wideline NMR spectra

In order to investigate the structure and dynamic transitions of PNIPAAm brushes grafted on the cotton fabric, both Magic Angle Spinning (MAS) and

static ^1H solid-state NMR experiments were performed. For comparison, the Cotton-A-Br sample is used as a reference.

^1H static NMR spectra of solid samples are usually broad and featureless because of the strong dipolar-dipolar interactions. However, the linewidth of the static spectra retains resourceful information about the molecular motions, which may lead to a line-narrowing of the proton spectra²⁶. In a typical solid-state static ^1H NMR spectrum, differences in molecular mobility results in a two-component lineshape showing a narrow peak superimposed on a broad peak. In the time domain, alternatively, such a spectrum is characterized by an initial fast decay followed by a slower decay. In its application in polymer systems, this two-component relaxation behavior is often explained by a two-region model in which hard domains (crystalline) yield a fast decay and soft domains (mobile or amorphous) yield slow decay^{27,28}.

Figure 3.4 presents the static ^1H wideline NMR spectra of Cotton-A-Br and Cotton-PNIPAAm-L samples. In the spectra of both samples, two components, a mobile component as represented by the narrow line and a rigid component represented by the broad line, can be identified.

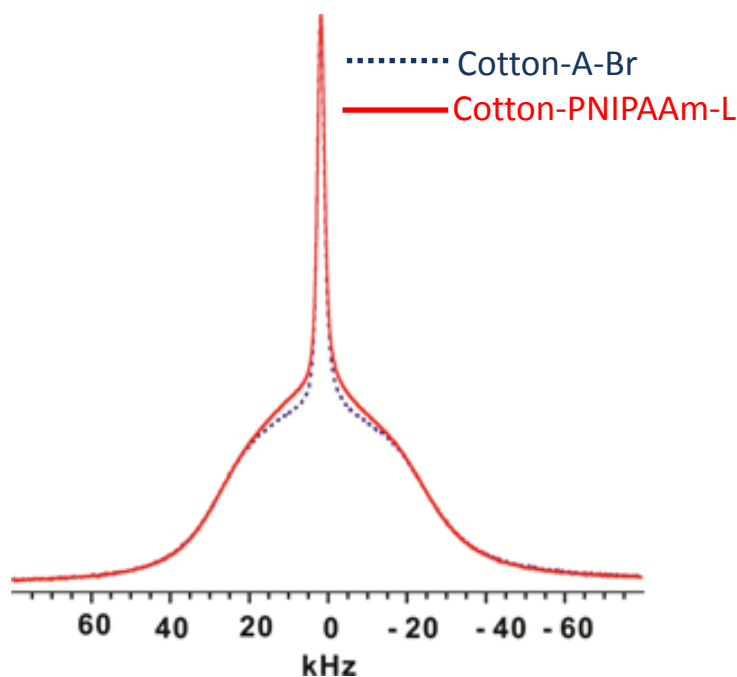


Figure 3.4 ^1H static spectra of Cotton-A-Br and Cotton-PNIPAAm-L samples. Both spectra were recorded at room temperature and atmospheric humidity conditions.

The narrow peak observed in the ^1H wideline spectra is assigned to the moisture absorbed by the cotton fabric²⁹. This was confirmed by the disappearance of the narrow peak from the proton spectra after blowing dry compressed air to the cotton samples, while the narrow peak was observed again in the spectra after re-exposing the samples to the atmospheric humidity.

In the Cotton-PNIPAAm-L spectrum, however, in addition to the broad and narrow line, a third intermediate component was identified. It is narrower than the broad line, yet still broader than the narrow line associated with the adsorbed moisture (Figure 3.5). This intermediate component is assigned to the PNIPAAm molecules grafted from the cotton surface. The amount of the mobile component

in both samples can be quantified by the deconvolution of the static ^1H spectra in Figure 3.4. The weight percentage of the grafted PNIPAAm in the Cotton-PNIPAAm-L sample is estimated from the area of the intermediate line (figure 3.5b) to be 3.2 %.

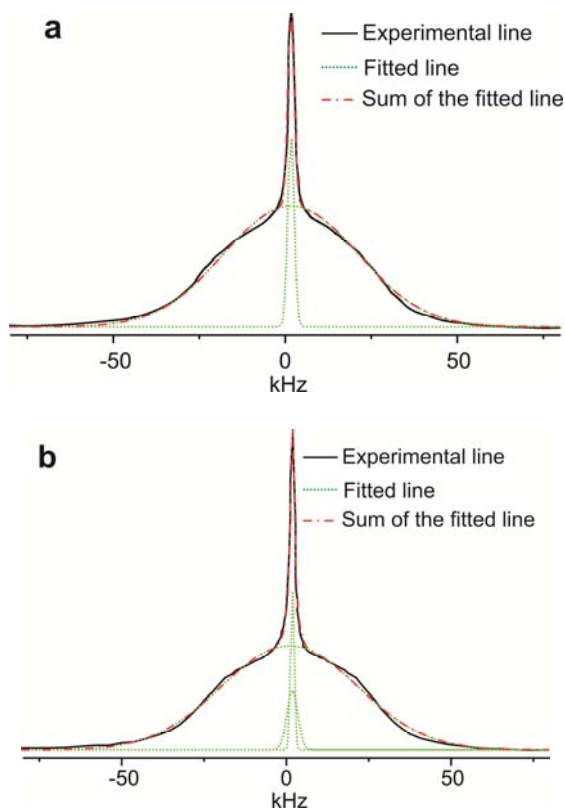


Figure 3.5 Line-fitting results of the wideline spectra. a) Cotton-ATMS-Br; b)

Cotton-PNIPAAm-L.

These NMR estimated results are compared with the moisture content $A\%$, which is defined by

$$A\% = \frac{m - m_{od}}{m_{od}} \times 100\% \quad (\text{Equation 3.1})$$

where m is the mass of the samples (exposed to atmospheric moisture) and

m_{od} is the oven-dried mass of the samples. Table I shows the comparison of the moisture contents of both samples, calculated by NMR and weighting methods. For the Cotton-A-Br sample, the moisture contents obtained by these two methods fit very well to each other. This result further confirms that the narrow component in figure 3.4 is purely attributed to moisture, and it completely rules out the possibility that it corresponds to a higher mobility of the cotton fabric induced by the absorption of water, which would also result in a narrow line.

Table 3.1 Moisture contents (A %) of Cotton-ATMS-Br and Cotton-PNIPAAm-L samples at 295K and 26% relative humidity.

Methods \ Sample	Cotton-ATMS-Br	Cotton-PNIPAAm-L
NMR ^a	4.3 %	2.4 % ^c
Weighting ^b	4.5 %	3.9 %

^a Calculated from the line-fitting of the static spectra in Figure 3.4. ^b The samples mass was averaged from 10 measurements. ^c Calculated from the area of the narrow line only.

The moisture content of Cotton-PNIPAAm-L is lower than the Cotton-A-Br sample. The value obtained from NMR is 2.4 %, which is also significantly lower than the value obtained from the weighting method. It should be pointed that the value obtained by NMR is probably underestimated since PNIPAAm-immobilized water may be of faster T_2 relaxation nature, compared to

the water adsorbed by cotton, and therefore contributes to the medium linewidth.

In order to study the temperature effects on both of the cotton initiator and cotton grafted PNIPAAm samples, ^1H static spectra were measured at low and high temperatures. Figure 3.5 shows the comparison of the ^1H static spectra measured at room temperature and at 329 K. The lineshape of the Cotton-A-Br does not change with temperature in the measured temperature range (Figure 3.5 a). In the case of Cotton-PNIPAAm-L (Figure 3.5 b), however, the spectra exhibits an increase of the relative intensity of the narrow peak with increasing temperature, while the linewidth of the broad component keeps almost invariable with temperature. The increase in the narrow component can be explained by the increase of the mobility of the water molecules which are bonded to PNIPAAm. It is also noted that the third component with medium linewidth still exists at higher temperature. This means that the mobility of PNIPAAm molecules itself remains the same at this temperature (329 K, 56 °C), which is far above the expected LCST.

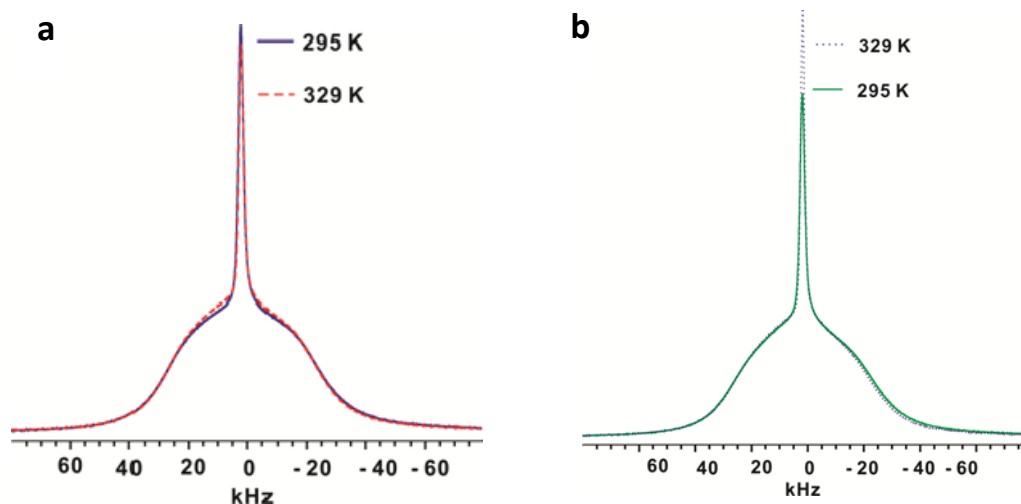


Figure 3.6 ^1H static spectra measured at room temperature (295 K) and 329 K: (a) Cotton-A-Br and (b) Cotton-PNIPAAm-L sample. For visualization purposes the spectra of Cotton-PNIPAAm-L measured at 329 K was horizontally shifted.

3.3.2.5 The covalent bond between grafted polymer and substrate

Magic angle spinning (MAS) solid-state ^1H NMR has long been recognized as a necessary complement for the static ^1H wideline experiments. Figure 3.6 shows the comparison of the MAS ^1H NMR spectra of the Cotton-A-Br and Cotton-PNIPAAm-L samples at different temperatures. The positions and assignments of the peaks are summarized in Table 3.2.

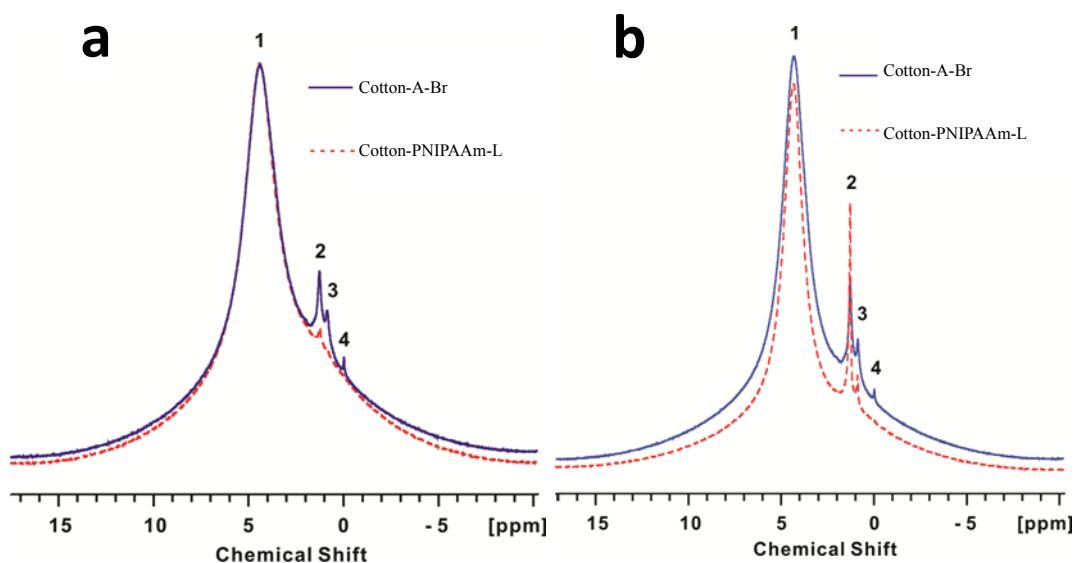


Figure 3.7 MAS ^1H NMR spectra of Cotton-ATMS-Br and Cotton-PNIPAAm-L samples at room temperature and atmospheric humidity. The spectra were recorded at (a) room temperature (295 K) and (b) 329 K. The MAS rate was 8 kHz.

Table 3.2 Positions and assignments of the peaks in figure 3.6.

	Peak 1	Peak 2	Peak 3	Peak 4
Chemical shift (ppm)	4.4	1.2	0.8	0
Assignment	Moisture	ATMS-Br	ATMS-Br	ATMS-Br

The chemical shift of Peak 1 is about 4.4 ppm, which is typically assigned to neutron water. In the present spectra, therefore, it can be assigned to the moisture adsorbed by cellulose molecules, but the linewidth of the peak is

reduced upon the MAS conditions to a FWHM (Full Width at Half Maximum) of less than 1 kHz. The peaks 2, 3 and 4 in the spectrum of Cotton-A-Br (figure 3.6 a) are assigned to the ATMS-Br macroinitiator which was immobilized on the cotton surface. This assignment is supported by the result of ^1H MAS spectra of pristine cotton fabric with the same spinning rate, which shows no peak at these positions. At room temperature the proton signals of the PNIPAAm molecules are not visible due to their macromolecular nature and low mobility. The signal corresponding to the PNIPAAm is therefore broad and embedded in the baseline.

The linewidth of the peaks 2, 3 and 4 in the Cotton-A-Br spectrum are quite narrow due to the high mobility of the ATMS molecules. By grafting with PNIPAAm, however, the peak 3 and 4 vanished and the intensity of peak 2 decreases dramatically as well. One possible interpretation for this observation is that the ATMS-Br macroinitiator is highly mobile before grafting with PNIPAAm since only one end is chemically bonded to the cotton surface. Once they chemically bond to PNIPAAm, the mobility of ATMS-Br macroinitiator decreases dramatically, because both ends are pinned up to the solid phases with low mobility. Therefore, peak 2, 3, 4 become broadened and embedded in the broad main peak, due to their restricted molecular mobility. These results strongly indicate that the PNIPAAm brushes are covalently bonded to the cotton-surface rather than being physically adsorbed. This is further supported by the SEM analyses which show the PNIPAAm aggregates covering the cotton surfaces.

Figure 3.6b shows the ^1H MAS spectra of Cotton-A-Br and Cotton-PNIPAAm-L measured at 329 K (56 °C). The lineshape of narrow moisture component in Cotton-A-Br remains nearly unchanged as compared with the spectra at room temperature, whereas the lineshape of moisture in Cotton-PNIPAAm-L is apparently narrower at 329 K. Generally, the linewidth of a ^1H MAS spectrum is dominated by the residual homonuclear dipolar-dipolar (D-D) interactions³⁰ which are not fully averaged by magic-angle spinning. Fast molecular motion can reduce the D-D interactions, and therefore leads to a narrow lineshape. This means that the mobility of water molecules in PNIPAAm increased at higher temperature, while in the cotton the water mobility remains almost the same. These results are consistent with the previous conclusion from the static proton experiments.

3.4 Conclusions

Cotton fabric surfaces were modified with thermo-responsive PNIPAAm brushes using a surface-initiated ATRP method. The success of the polymer grafting was confirmed by the combined results from FTIR, XPS, SEM and Solid-State NMR experiments. The grafting efficiency is rather low because of the low density of hydroxyl group available to the ATRP reaction. The structure and dynamics of the PNIPAAm brushes were investigated by both static and MAS ^1H NMR techniques. It has been shown that PNIPAAm molecules are immobilized by the covalent bond with cotton surface. The mobility of

PNIPAAm molecules is significantly restricted even at higher temperature (329 K).

3.5 References

- 1 Carlmark, A. & Malmstrom, E. E. ATRP grafting from cellulose fibers to create block-copolymer grafts. *Biomacromolecules* 4, 1740-1745, (2003).
- 2 Kono, H., Yunoki, S., Shikano, T., Fujiwara, M., Erata, T. & Takai, M. CP/MAS ¹³C NMR Study of Cellulose and Cellulose Derivatives. 1. Complete Assignment of the CP/MAS ¹³C NMR Spectrum of the Native Cellulose. *Journal of the American Chemical Society* 124, 7506-7511, (2002).
- 3 Kono, H., Erata, T. & Takai, M. CP/MAS ¹³C NMR Study of Cellulose and Cellulose Derivatives. 2. Complete Assignment of the ¹³C Resonance for the Ring Carbons of Cellulose Triacetate Polymorphs. *Journal of the American Chemical Society* 124, 7512-7518, (2002).
- 4 Carlmark, A. & Malmstrom, E. Atom transfer radical polymerization from cellulose fibers at ambient temperature. *J. Am. Chem. Soc.* 124, 900-901, (2002).
- 5 Fujita, M., Shoda, S. & Kobayashi, S. Xylanase-catalyzed synthesis of a novel polysaccharide having a glucose-xylose repeating unit, a cellulose-xylan hybrid polymer. *J. Am. Chem. Soc.* 120, 6411-6412, (1998).
- 6 Singh, B., Gupta, M., Verma, A. & Tyagi, O. S. FT-IR microscopic studies on coupling agents: treated natural fibres. *Polym. Int.* 49, 1444-1451, (2000).
- 7 Botaro, V. R., Gandini, A. & Belgacem, M. N. Heterogeneous chemical

- modification of cellulose for composite materials. *J. Thermoplast. Compos.* 18, 107-117, (2005).
- 8 Lewin, M. in *International Fiber Science and Technology Series* (ed Menachem Lewin) (CRC Press;, New York, 2006).
- 9 Stuart, M. A. C., Huck, W. T. S., Genzer, J., Muller, M., Ober, C., Stamm, M., Sukhorukov, G. B., Szleifer, I., Tsukruk, V. V., Urban, M., Winnik, F., Zauscher, S., Luzinov, I. & Minko, S. Emerging applications of stimuli-responsive polymer materials. *Nat Mater* 9, 101-113, (2010).
- 10 Zhao, B. & Brittain, W. J. Synthesis of tethered polystyrene-block-poly(methyl methacrylate) monolayer on a silicate substrate by sequential carbocationic polymerization and atom transfer radical polymerization. *J. Am. Chem. Soc.* 121, 3557-3558, (1999).
- 11 Ejaz, M., Yamamoto, S., Ohno, K., Tsujii, Y. & Fukuda, T. Controlled graft polymerization of methyl methacrylate on silicon substrate by the combined use of the Langmuir-Blodgett and atom transfer radical polymerization techniques. *Macromolecules* 31, 5934-5936, (1998).
- 12 Kong, X. X., Kawai, T., Abe, J. & Iyoda, T. Amphiphilic polymer brushes grown from the silicon surface by atom transfer radical polymerization. *Macromolecules* 34, 1837-1844, (2001).
- 13 Shah, R. R., Merreceyes, D., Husemann, M., Rees, I., Abbott, N. L., Hawker, C. J.

- & Hedrick, J. L. Using atom transfer radical polymerization to amplify monolayers of initiators patterned by microcontact printing into polymer brushes for pattern transfer. *Macromolecules* 33, 597-605, (2000).
- 14 Kim, J. B., Bruening, M. L. & Baker, G. L. Surface-initiated atom transfer radical polymerization on gold at ambient temperature. *J. Am. Chem. Soc.* 122, 7616-7617, (2000).
- 15 von Werne, T. & Patten, T. E. Preparation of structurally well-defined polymer-nanoparticle hybrids with controlled/living radical polymerizations. *J. Am. Chem. Soc.* 121, 7409-7410, (1999).
- 16 He, H. T., Jing, W. H., Xing, W. H. & Fan, Y. Q. Improving protein resistance of alpha-Al₂O₃ membranes by modification with POEGMA brushes. *Appl. Surf. Sci.* 258, 1038-1044, (2011).
- 17 Vasani, R. B., McInnes, S. J. P., Cole, M. A., Jani, A. M. M., Ellis, A. V. & Voelcker, N. H. Stimulus-Responsiveness and Drug Release from Porous Silicon Films ATRP-Grafted with Poly(N-isopropylacrylamide). *Langmuir* 27, 7843-7853, (2011).
- 18 Schild, H. G. POLY (N-ISOPROPYLACRYLAMIDE) - EXPERIMENT, THEORY AND APPLICATION. *Prog. Polym. Sci.* 17, 163-249, (1992).
- 19 Lindqvist, J., Nyström, D., Östmark, E., Antoni, P., Carlmark, A., Johansson, M., Hult, A. & Malmström, E. Intelligent Dual-Responsive Cellulose Surfaces via Surface-Initiated ATRP. *Biomacromolecules* 9, 2139-2145, (2008).

- 20 Kim, D. J., Kang, S. M., Kong, B., Kim, W.-J., Paik, H.-j., Choi, H. & Choi, I. S. Formation of Thermoresponsive Gold Nanoparticle/PNIPAAm Hybrids by Surface-Initiated, Atom Transfer Radical Polymerization in Aqueous Media. *Macromolecular Chemistry and Physics* 206, 1941-1946, (2005).
- 21 Schmidt-Rohr, K. & Spiess, H. W. *Multidimensional Solid State NMR and Polymers*. 55 (Academic Press, 1994).
- 22 Schönhoff, M., Larsson, A., Welzel, P. B. & Kuckling, D. Thermoreversible Polymers Adsorbed to Colloidal Silica: A ¹H NMR and DSC Study of the Phase Transition in Confined Geometry. *The Journal of Physical Chemistry B* 106, 7800-7808, (2002).
- 23 Garnweitner, G., Smarsly, B., Assink, R., Ruland, W., Bond, E. & Brinker, C. J. Self-Assembly of an Environmentally Responsive Polymer/Silica Nanocomposite. *Journal of the American Chemical Society* 125, 5626-5627, (2003).
- 24 Diez-Pena, E., Quijada-Garrido, I., Barrales-Rienda, J. M., Schnell, I. & Spiess, H. W. Advanced ¹H Solid-State NMR Spectroscopy on Hydrogels, 1. The Effect of Hydrogen Bonding in the Collapse of Poly(methacrylic acid) (PMAA) Hydrogels. *Macromol. Chem. Phys.* 205, 430-437, (2004).
- 25 Diez-Pena, E., Quijada-Garrido, I., Barrales-Rienda, J. M., Schnell, I. & Spiess, H. W. Advanced ¹H Solid-State NMR Spectroscopy on Hydrogels, 2. *Macromol. Chem. Phys.* 205, 438-447, (2004).

- 26 Fyfe, C. A. *Solid State NMR for Chemists*. (C. F. C. Press, 1983).
- 27 Assink, R. A. *Macromolecules* 11, 1233-1237, (1978).
- 28 Resing, H. A. *Adv. Mol. Relax. Process.* 3, 199-226, (1972).
- 29 Taylor, R. E., French, A. D., Gamble, G. R., Himmelsbach, D. S., Stipanovic, R. D., Thibodeaux, D. P., Wakelyn, P. J. & Dybowski, C. ^1H and ^{13}C solid-state NMR of *Gossypium barbadense* (Pima) cotton. *J. Mol. Struct.*, 177-184, (2008).
- 30 Levitt, M. H. *Spin Dynamics: Basics of Nuclear Magnetic Resonance*. (2008).

Chapter 4

Thermo-responsive Behavior of the Cotton-PNIPAAm-L

Abstract

¹H solid-state NMR techniques were used to characterize the molecular structure and dynamics of the PNIPAAm molecules grafted on a cotton fabric. This technique is a non-destructive method which allows to quantitatively characterize the molecular structure and dynamics of the grafted polymer without cleaving it from the substrate. The results demonstrate that the motion of the grafted PNIPAAm brushes is restricted as the temperature rises above the low critical solution temperature (LCST), which was estimated to be ~ 34 °C. A broad transition temperature region was found, in contrast with the typical sharp transition of PNIPAAm reported in the literature. Variable temperature (VT) experiments were used to investigate the nature of the hydrophilic-hydrophobic transitions of the grafted polymer. The ¹H solid-state NMR techniques proved to be an extremely sensitive and precise way to probe in-situ the LCST transition of the PNIPAAm while still grafted on the cotton fabric.

4.1 Introduction

The structure and morphology of PNIPAAm has been extensively studied by spectroscopic, chromatographic, thermoanalytical and surface-specific characterization techniques^{1,2}. In most cases, the grafted polymer brushes have to be cleaved and recovered from the solid substrates for further characterizations. This is an extremely time and energy consuming process³. Moreover, the polymer structure and composition may change during the cleavage and purification procedures leading to irreproducible and unreliable results. Only a few scattered studies can be found in the literature concerning the characterization of polymer brushes still anchored on solid surfaces by using the solid-state NMR techniques⁴⁻⁶.

In this work, an extensive study to characterize *in-situ* the structure and dynamics of the PNIPAAm brushes directly grafted from the surface of a cotton fabric was performed, while still connected to the substrate. Proton NMR techniques, both under static and magic-angle spinning conditions, have been used to characterize the bare, ATRP-initiator modified and PNIPAAm modified cotton fabrics. The interaction between water and the PNIPAAm grafted brushes is the primary concern of the study due to the fact that hydrogen bonding plays a major role in the *stimuli*-responsive behavior of PNIPAAm.

4.2 Experimental

For this study, the Cotton-PNIPAAm-L samples with low grafting of PNIPAAm was used which reported in the previous chapter. All the solid state NMR experiments were performed on a Bruker Avance III wide-bore solid-state NMR spectrometer operating at ^1H Larmor frequency of 400.13 MHz. A standard 4 mm CP magic angle spinning (MAS) double resonance probe head was used for all the measurements. The MAS frequency of 8 kHz and 90° pulse duration of 4 μs were used in ^1H MAS experiments. Typically 16 transients with recycle delay of 10 s were collected for each spectrum. The longest T_1 relaxation time of the sample is estimated to be shorter than 2 s. Hence, a recycle delay of 10 s was expected to be long enough for the full relaxation of the spectra. Before performing the variable temperature (VT) experiments, the sample temperature was deliberately calibrated under static and MAS condition, respectively, using lead nitrate as reference sample⁷. For the VT experiments a N_2 flow was used instead of the air.

4.3 Results and Discussion

In order to investigate the structure and dynamic transitions of PNIPAAm brushes grafted on the cotton fibers surface, both static ^1H solid-state NMR and Magic Angle Spinning (MAS) experiments were performed. For comparison, the Cotton-A-Br sample is used as a reference.

4.3.1 ^1H static spectroscopy

It is well known that the broadening of proton lines in solids is dominated by homonuclear dipolar coupling interactions⁸. Motions with rates exceeding the dipolar couplings of protons, typically 50 kHz, can be detected through the reduction of the static dipolar linewidth. This phenomenon has been exploited in ^1H wide-line spectroscopy to reveal information about the molecular dynamics of the different components in polymer blends or copolymers^{9,10}. In some cases, this simple experiment can provide valuable information from the difference in the widths of their proton resonances. ^1H NMR spectroscopy has been used by many researchers to study the thermo-reversible transition of PNIPAAm. Generally, it has been reported that a broadening of the proton linewidth can be observed above the LCST¹¹⁻¹⁵.

In this study, the ^1H wide-line spectra of the Cotton-A-Br and Cotton-PNIPAAm-L samples were measured in the water saturated state. The samples were saturated in D_2O (1:1, Polymer/ D_2O , w/w) overnight to equilibrate. In figure 4.1, the temperature dependency of the proton NMR resonances of the Cotton-A-Br and Cotton-PNIPAAm-L samples are shown, with a temperature range from 295 K (22 °C) to 330 K (57 °C).

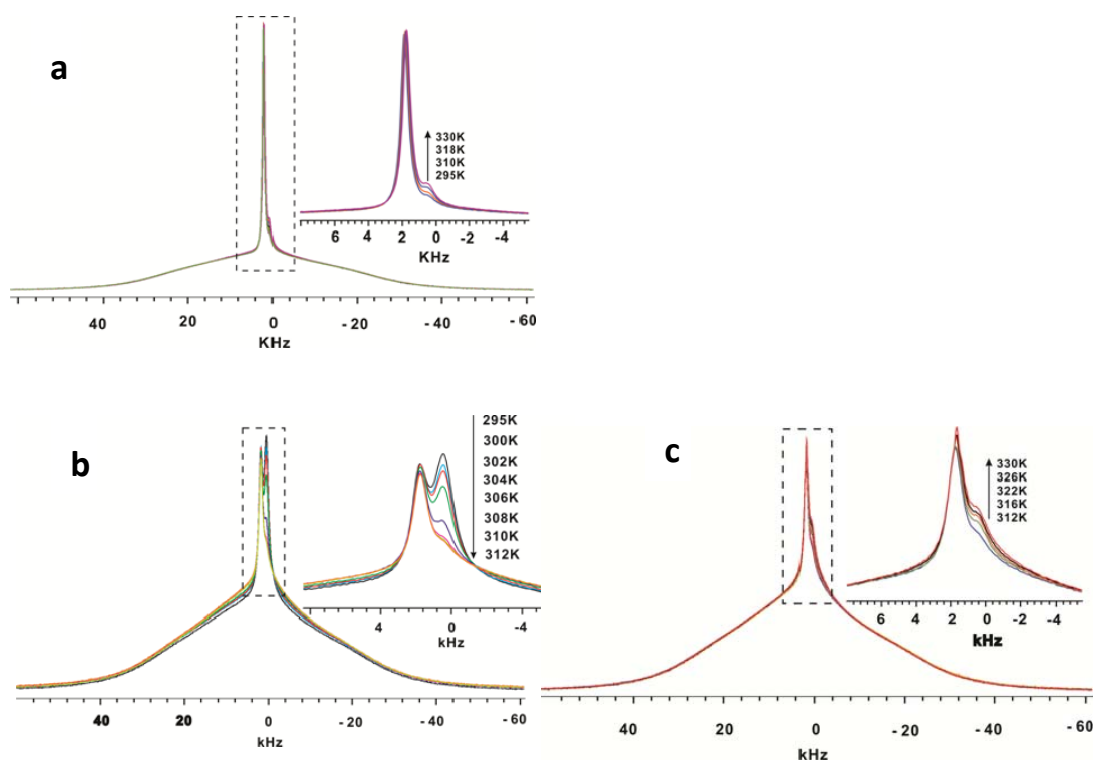


Figure 4.1 ^1H NMR static spectra of Cotton-A-Br and Cotton-PNIPAAm-L soaked in D_2O .

(a) Spectra of Cotton-A-Br measured at the temperatures of 295 K-330 K; (b) and (c) are the spectra of Cotton-PNIPAAm-L sample measured at 295 K-312 K and 312 K-330 K, respectively. The narrow lines of the spectra (square region) were expanded and shown as insets. Arrows indicate the direction of intensity change upon increasing temperature.

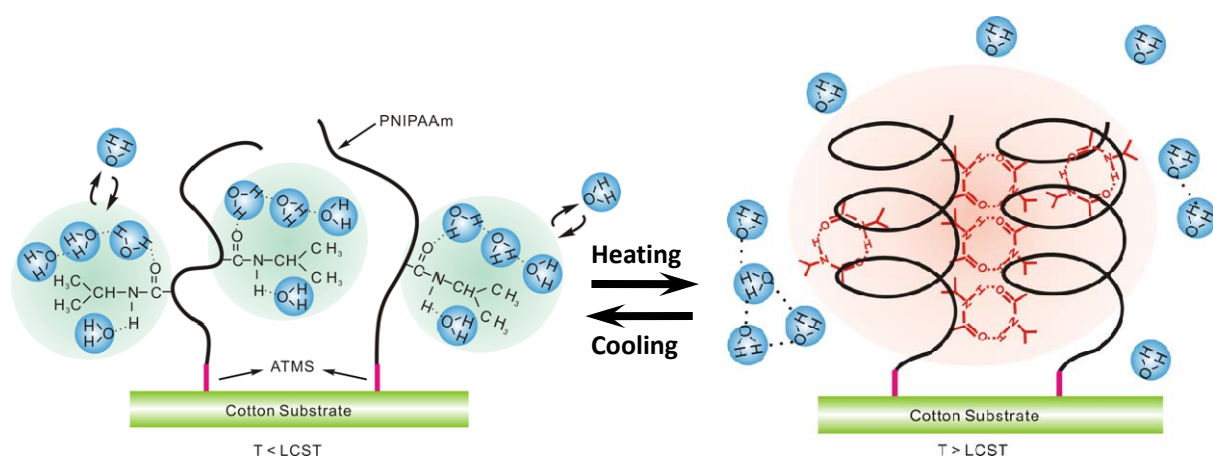
Two resonance peaks can be identified in the spectra of both samples. The units of the horizontal axis can be translated into chemical shifts (ppm) by dividing the center frequency of the spins, which is 400.13 MHz in the present experiments. The chemical shift of the low-field peak (left hand) and high-field peak (right hand) are about 4.5 ppm and 0.9 ppm, respectively. Therefore, according to the chemical shift, the high-field peak was attributed to water

molecules from the solvent (D-OH) used to wet the fabrics. The low-field peak which presents as a shoulder in the spectra of Cotton-A-Br (figure 4.1a) and a well-resolved peak in the spectra of Cotton-PNIPAAm-L at low temperatures (figure 4.1b), was assigned to the aliphatic resonance region of the cotton and PNIPAAm molecules, respectively. Notice that these high-field peaks are not observed in the static spectra of the unsoaked samples (see figure 3.5). This indicates that the presence of a larger amount of water molecules, upon soaking with D₂O, increases the mobility of both cotton and PNIPAAm molecules.

The temperature dependence of hydrogen bonding and the mobility of water molecules can be monitored by the chemical shift of the D-OH peak and its broadening. The water peaks for both samples shifts constantly to higher field as the temperature increases. This effect has been studied previously and attributed to the temperature dependence of the water hydrogen bonding^{11,16}.

In Figure 4.1a, the temperature dependency of the ¹H NMR resonance of Cotton-A-Br in the temperature range from 295 K to 330 K is shown. The lines become gradually narrower with the increasing temperature, and therefore resulting in a better resolution. This line-narrowing of Cotton-A-Br can be readily understood in terms of higher molecular mobility at elevated temperatures, as also discussed from the results of the MAS spectra shown in Figure 3.6, with non-soaked samples. The temperature dependency of Cotton-PNIPAAm-L is, however, completely different. As shown in figure 4.1b,

within the temperature range from 295 to 312 K, the intensity of the aliphatic resonance peak at lower field (4.5 ppm) decreases continuously with the increasing temperature. However, when the temperature increases further from 312 to 330 K (Figure 4.1c), the reverse effect is observed and the intensity increases, similarly to what was observed in the Cotton-A-Br. It is also very interesting to notice that in the temperature range from 295 to 312 K the broad component of Cotton-PNIPAAm-L in Figure 4.1b becomes broader at higher temperature, unlike the signal of broad component in Cotton-A-Br. On the other hand, in the range of 312 to 330 K (Figure 4.1c), the linewidth keeps constant. This behavior, combined with the previously mentioned decrease of the intensity of aliphatic resonance peak with the increasing temperature, can be explained by the thermo-responsive behavior of PNIPAAm molecules. At low temperatures, the PNIPAAm molecules preferentially bond to D₂O through hydrogen bonds. So, it is mobile enough to give rise to sharp peak in the aliphatic region. With the increasing temperature, PNIPAAm molecules gradually turn into a more hydrophobic state and form hydrogen bonds amongst themselves (See Scheme 4.1). The mobility of each molecule is therefore seriously restricted by the hydrogen-bonded polymer networks. At the higher temperature region, ranging from 312 to 330 K, the hydrophilic-hydrophobic transition has finished, and the slow increase of aliphatic resonance intensity is attributed to the increased molecular mobility at elevated temperature.



Scheme 4.1 Schematic illustration of the hydrophilic-hydrophobic phase transition of PNIPAAm modified cotton surface. At temperature $T < LCST$, the hydrogen bonds between water molecules and PNIPAAm molecules are preferentially established and PNIPAAm molecules adopt an extended configuration. When $T > LCST$, the PNIPAAm molecules preferentially form intra-molecular hydrogen bonds and the polymer chains undergo a coil configuration.

4.3.2 ^1H MAS Spectroscopy

The results obtained show that static ^1H NMR experiments provide a new possibility to probe qualitatively the LCST transition of PNIPAAm-grafted on solid substrates, namely on cotton fabrics. Comparing to the traditionally DSC and swelling experiments used for this purpose, the method described in this study is much more sensitive, precise and more importantly, it has the versatility regardless of the PNIPAAm molecules being in liquid, gel or solid state, or even grafted on a solid substrate, like the present study. However, the main drawback

of the static ^1H NMR experiments is the resolution. What has been observed through the static experiments is the temperature dependence of the overall aliphatic signal from all the components. Therefore, in order to further study the molecular dynamics of each component in more details and gain better resolution, ^1H MAS spectroscopy was used.

Figure 4.2 shows the aliphatic resonance region of the Cotton-A-Br and Cotton-PNIPAAm-L in the temperature range from 295 K (22 °C) to 322 K (49 °C). The resonance lines at 1.18 ppm and 0.77 ppm, which have the same chemical shift as the peak 2 and peak 3 in Figure 6, are assigned to the ATMS-Br molecules. The resonance line at 1.05 ppm in Figure 9b and 9c is attributed to the PNIPAAm molecules, whose signal is not observable in the ^1H MAS spectra of un-soaked sample (Figure 3.6).

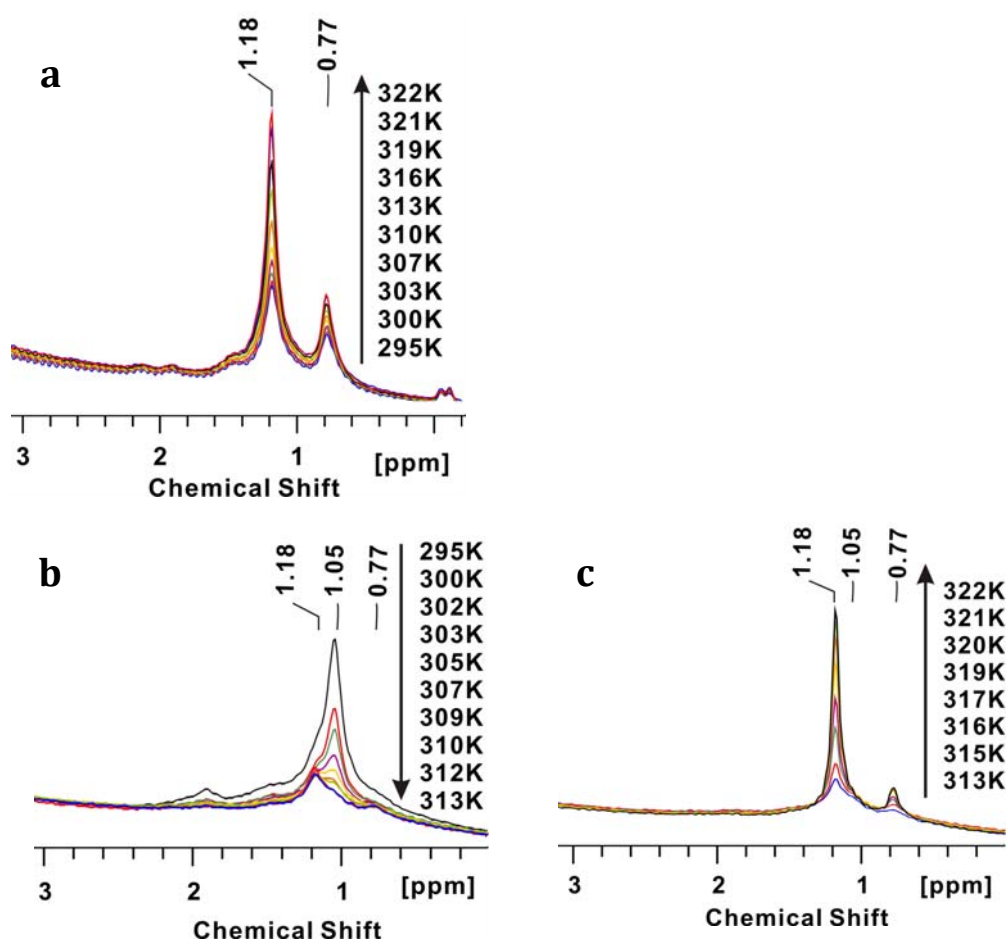


Figure 4.2 ^1H MAS NMR spectra of Cotton-A-Br and Cotton-PNIPAAm-L soaked in D_2O .

(a) Spectra of Cotton-A-Br measured at the temperatures ranging from 295-322 K; (b) and (c) are the spectra of Cotton-PNIPAAm-L sample measured at temperatures ranging from 295-313 K and 313-322 K, respectively. The arrows indicate the direction of intensity change upon increasing temperature.

Figure 4.2a shows the temperature dependency of ATMS-Br resonance of the Cotton-A-Br sample. The intensity of 1.18 ppm peak increases continuously with increasing temperature. The same behavior is observed for the Cotton-PNIPAAm-L sample between 313 and 322 K. One possible explanation for this behavior is constraint on the ATMS-Br molecules from PNIPAAm

grafted brushes. In the Cotton-A-Br sample, only one end of ATMS-Br molecule is chemically bonded, therefore the mobility of ATMS molecules is relatively high and it increases with increasing temperature. As for the Cotton-PNIPAAm-L sample, both ends of ATMS-Br molecules are chemically bonded, but since at this temperature range, which is above LCST, the PNIPAAm brushes preferentially hydrogen bond within themselves, there is almost no interaction with the solvent, hence the ATMS-Br molecules behave the same.

In the temperature region between 295 and 313 K, however a completely different behavior is observed. In this temperature range, which is below LCST, PNIPAAm interacts preferentially with solvent molecules and adopts an extended configuration (Scheme 4.1). Hence it becomes much more mobile as the temperature increases in this range and goes over the phase transition, which explains the intensity decrease in the peak at 1.05 ppm in figure 9b. Accordingly, the resonance of the ATMS-Br molecules becomes less significant and remains fairly constant within this temperature range.

The hydration and dynamic behavior of pure PNIPAAm in aqueous solution has been studied by several authors^{17,18}. Most of the studies, however, focused on free PNIPAAm chains. In this study, the intensities of the resonance peak attributed to surface-grafted PNIPAAm were plotted against the range of temperature studied and are shown in Figure 4.3.

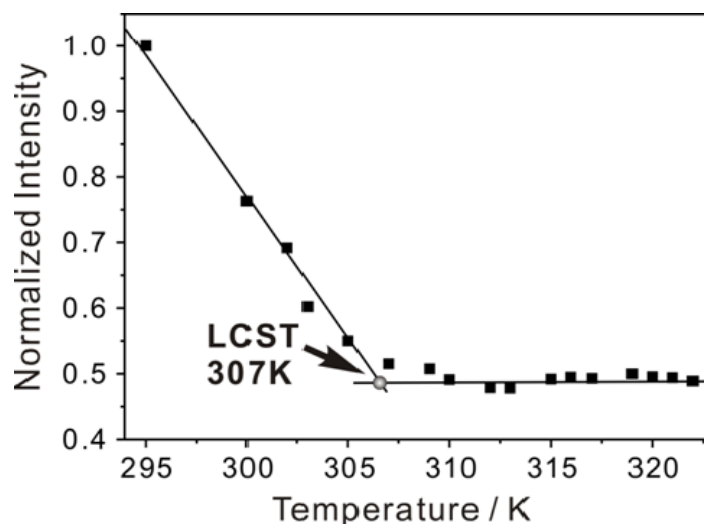


Figure 4.3 The temperature dependence of peak intensities at the resonances of 1.05 ppm in figure 9. The solid lines are included as guide for the eyes.

In the lower temperature range (from 295 K to 307 K), the resonance intensity decreases continuously with increasing temperature. This phenomenon can be readily understood in terms of thermo-responsive hydrophilic-hydrophobic phase transition of the PNIPAAm molecules (as schematically illustrated in Scheme 4.1).

The continuous decrease of intensity with increasing temperature implies a continuous phase transition in the temperature range below 307 K. Above this temperature, the phase transition finished and the intensity is almost constant with temperature. At temperature below LCST, the PNIPAAm molecules grafted on the Cotton are expected to preferentially form hydrogen bonds with water. The PNIPAAm molecules are in an extended configuration and exhibit high mobility, therefore it can give rise to sharp peak (higher intensity) in the aliphatic

region. With the temperature increase, the PNIPAAm molecules gradually turn into a more hydrophobic state and prefer to form inter- and intra-molecular hydrogen bonding with themselves. The mobility of each molecule is therefore seriously restricted by the hydrogen-bonded polymer networks, and the resonance of PNIPAAm vanishes as a result of broadening of the linewidth.

In conclusion, in contrast to the LCST transition of pure PNIPAAm which shows a sharp transition around 305 K (32 °C)^{19,20}. It can be reported that cotton-grafted PNIPAAm exhibits a much wider transition temperature range. The onset point of the LCST transition of PNIPAAm molecules is observed at the temperature of 307 K (34 °C) (figure 4.3). This temperature value is in good agreement with other LCST values of surface-grafted PNIPAAm reported in the literature, which were obtained by DSC²¹ and swelling experiments²².

4.4 Conclusions

A cotton fabric was modified with thermo-responsive PNIPAAm using a surface-initiated ATRP method. In spite of the low-grafting efficiency obtained for the first samples (Cotton-PNIPAAm-L), the structure and dynamics of the PNIPAAm brushes were investigated by both static and MAS ¹H NMR techniques, while still grafted on the cotton fabric. NMR results from D₂O saturated samples showed that while the temperature is below the LCST of PNIPAAm, the resonance peak of PNIPAAm molecules increases in intensity with the increasing temperature. This was attributed to the

hydrophilic-hydrophobic phase transition of PNIPAAm. In contrast to the typical sharp transition of pure PNIPAAm reported in previous NMR studies in the literature²³, the surface-grafted PNIPAAm displays a broad transition temperature region below its LCST, which may be due to the anchoring of the polymer branches to the fabric surfaces. The LCST of the PNIPAAm brushes grafted on the cotton fabric was estimated by VT-¹H MAS spectra to be 307 K (34 °C), which is in agreement those reported in the literature^{21,22} for PNIPAAm grafted on different solid substrates.

This work shows that ¹H solid-state NMR techniques are extremely sensitive and resourceful on probing the LCST transition of thermo-sensitive polymer brushes grafted on a complex substrate, *i.e.* cotton fabric, even at low grafting efficiency, a non-destructive probing of the polymer responsive behavior was possible. Hence, harsh cleavage procedures which typically promote substrate degradation and non-reliable or irreproducible analyses of the cleaved polymer molecules can be avoided.

The work carried out to improve the polymer grafting efficiency on the cotton fabric is described in the following chapter. This work, on the other hand, clearly paves the way to prepare *stimuli*-responsive cotton fabrics, even with a slight modification of the cellulose-based surfaces of cotton. This technology has high potential for advanced applications on the textile industry envisioning numerous possibilities for fabricating novel intelligent fabrics.

4.5 References

- 1 Carlmark, A. & Malmstrom, E. E. ATRP grafting from cellulose fibers to create block-copolymer grafts. *Biomacromolecules* **4**, 1740-1745, (2003).
- 2 Matyjaszewski, K. *et al.* Polymers at interfaces: Using atom transfer radical polymerization in the controlled growth of homopolymers and block copolymers from silicon surfaces in the absence of untethered sacrificial initiator. *Macromolecules* **32**, 8716-8724, (1999).
- 3 Princi, E. *et al.* Synthesis and mechanical characterisation of cellulose based textiles grafted with acrylic monomers. *Eur. Polym. J.* **42**, 51-60, (2006).
- 4 Chung, P.-W., Kumar, R., Pruski, M. & Lin, V. S. Y. Temperature Responsive Solution Partition of Organic-Inorganic Hybrid Poly(N-isopropylacrylamide)-Coated Mesoporous Silica Nanospheres. *Advanced Functional Materials* **18**, 1390-1398, (2008).
- 5 Schönhoff, M., Larsson, A., Welzel, P. B. & Kuckling, D. Thermoreversible Polymers Adsorbed to Colloidal Silica: A ¹H NMR and DSC Study of the Phase Transition in Confined Geometry. *The Journal of Physical Chemistry B* **106**, 7800-7808, (2002).
- 6 Castelvetro, V., Geppi, M., Giaiacopi, S. & Mollica, G. Cotton fibers encapsulated with homo- and block copolymers: Synthesis by the atom transfer radical

- polymerization grafting-from technique and solid-state NMR dynamic investigations. *Biomacromolecules* **8**, 498-508, (2007).
- 7 Bielecki, A. & Burum, D. P. Temperature Dependence of ^{207}Pb MAS Spectra of Solid Lead Nitrate. An Accurate, Sensitive Thermometer for Variable-Temperature MAS. *J. Magn. Reson. A* **116**, 215-220, (1995).
- 8 Spiess, H. W. in *Encyclopedia of Magnetic Resonance* (John Wiley & Sons, Ltd, 2007).
- 9 Schmidt-Rohr, K. & Spiess, H. W. *Multidimensional Solid State NMR and Polymers*. 55 (Academic Press, 1994).
- 10 Brierty, V. J. M. & Packer, K. J. *Nuclear Magnetic Resonance in Solid Polymers*. 29-30 (Cambridge University Press, 1993).
- 11 Deshmukh, M. V., Vaidya, A. A., Kulkarni, M. G., Rajamohanan, P. R. & Ganapathy, S. LCST in poly(N-isopropylacrylamide) copolymers: high resolution proton NMR investigations. *Polymer* **41**, 7951-7960, (2000).
- 12 Ganapathy, S., Rajamohanan, P. R., Badiger, M. V., Mandhare, A. B. & Mashelkar, R. A. Proton magnetic resonance imaging in hydrogels: volume phase transition in poly(N-isopropylacrylamide). *Polymer* **41**, 4543-4547, (2000).
- 13 Zeng, F., Tong, Z. & Feng, H. N.m.r. investigation of phase separation in poly(N-isopropyl acrylamide)/water solutions. *Polymer* **38**, 5539-5544, (1997).

- 14 Tanaka, N., Matsukawa, S., Kurosu, H. & Ando, I. A study on dynamics of water in crosslinked poly (N-isopropylacrylamide) gel by n.m.r. spectroscopy. *Polymer* **39**, 4703-4706, (1998).
- 15 Tokuhito, T., Amiya, T., Mamada, A. & Tanaka, T. NMR study of poly(N-isopropylacrylamide) gels near phase transition. *Macromolecules* **24**, 2936-2943, (1991).
- 16 Gottlieb, H. E., Kotlyar, V. & Nudelman, A. NMR Chemical Shifts of Common Laboratory Solvents as Trace Impurities. *The Journal of Organic Chemistry* **62**, 7512-7515, (1997).
- 17 Zhang, Q. L. *et al.* Wettability switching between high hydrophilicity at low pH and high hydrophobicity at high pH on surface based on pH-responsive polymer. *Chem. Commun.*, 1199-1201, (2008).
- 18 Ono, Y. & Shikata, T. Hydration and Dynamic Behavior of Poly(N-isopropylacrylamide)s in Aqueous Solution: A Sharp Phase Transition at the Lower Critical Solution Temperature. *J. Am. Chem. Soc.* **128**, 10030-10031, (2006).
- 19 Schild, H. G. POLY (N-ISOPROPYLACRYLAMIDE) - EXPERIMENT, THEORY AND APPLICATION. *Prog. Polym. Sci.* **17**, 163-249, (1992).
- 20 Gil, E. S. & Hudson, S. M. Stimuli-responsive polymers and their bioconjugates. *Progress in Polymer Science* **29**, 1173-1222, (2004).

- 21 Diez-Pena, E., Quijada-Garrido, I., Frutos, P. & Barrales-Rienda, J. M. Analysis of the Swelling Dynamics of Cross-Linked P(N-iPAAm-co-MAA) Copolymers and Their Homopolymers under Acidic Medium. A Kinetics Interpretation of the Overshooting Effect. *Macromolecules* **36**, 2475-2483, (2003).
- 22 Diez-Pena, E., Quijada-Garrido, I. & Barrales-Rienda, J. M. On the Water Swelling Behaviour of Poly(N-Isopropylacrylamide) [P(N-iPAAm)], Poly(methacrylic acid) [P(MAA)], Their Random Copolymers and Sequential Interpenetrating Polymer Networks (IPNs). *Polymer* **43**, 4341-4348, (2002).
- 23 Díez-Peña, E., Quijada-Garrido, I., Barrales-Rienda, J. M., Schnell, I. & Spiess, H. W. Advanced ¹H Solid-State NMR Spectroscopy on Hydrogels, 2. *Macromolecular Chemistry and Physics* **205**, 438-447, (2004).

Chapter 5

Improvement of the functionalization of a Cotton fabric with a thermo-responsive polymer: Highly-grafted fabric (Cotton-PNIPAAm-H)

Abstract

The grafting efficiency of the polymer on the cotton surface has been greatly improved as described in this chapter. A short-time UV pretreatment coupled with a room temperature immobilization method proved to be the best method to increase the grafting efficiency of the ATRP-initiator. The modified cotton fabric was characterized by FTIR, XPS, NMR, TGA, SEM and OM. It was shown that the cotton fibers were covered with PNIPAAm brushes with a high grafting efficiency. The PNIPAAm molecular brushes were cleaved from the cotton substrate and characterized by GPC to determine the molecular weight (M_n), molecular weight distribution (PDI) and grafting efficiency.,

5.1 Introduction

The application of a Atom Transfer Radical Polymerization (ATRP) grafting method in textile finishing can impart some unique properties, and in some cases, is superior to the conventional textile finishing treatments^{1,2}. In this study, the smart polymer was proposed to introduce on fabric surface by ATRP grafting method. In the previous chapters, a thermo-responsive polymer PNIPAAm was grafted onto the cotton fabric surface using a Surface Initiated (SI)-ATRP method. The success of grafting was confirmed by FTIR, XPS and SEM techniques. The structure and dynamics of the molecules was investigated by solid state NMR methods. Although the SS-NMR technique proved to be an extremely sensitive method which could detect the phase transition of the grafted PNIPAAm with low grafting efficiency, the grafting efficiency of the thermal-responsive polymer is a very important issue from material point of view. Industry application requires sufficiently high grafting efficiency to endow the material with high performance. Therefore, in this chapter, efforts have been made to improve the grafting efficiency of the PNIPAAm on the cotton fabric. Three different aspects were investigated to improve the grafting efficiency: *promoting the reactivity of fabric, changing the immobilization method of the Cotton-initiator and optimizing the parameters and conditions of the polymerization from the surface.*

5.2 Experiment

5.2.1 Materials

The cotton fabric was obtained from Textile Innovators Division of SDL ATLAS. The following chemicals were used without further purification, unless stated otherwise: 4-(Dimethylamino) pyridine (DMAP, Aldrich 99%), triethylamine (TEA, Aldrich 99%), 2-bromisobutyryl bromide (BiB, Aldrich, 98%), aminopropyl trimethoxysilane (ATMS, Aldrich, 99.0% purity), pentamethyldiethylenetriamine (PMDETA, Aldrich 99%), copper (I) bromide (CuBr, Aldrich, 99%), tetrahydrofuran (THF, WRT, 99.8%), methanol (MeOH, WRT, 99.8%). N-isopropylacrylamide (NIPAA, Aldrich 97% purity) was recrystallized three times in *n*-hexane for the purpose of purification, and then dried under vacuum for 24 hours at room temperature.

5.2.2 Instruments

Infrared measurements were carried on with a Varian FT-IR3100 by using dry KBr pellets. Before each measurement, a background spectrum (averaged from 100 scans co-added) was collected. All the spectra were collected between 4000 and 600 cm^{-1} , with a resolution of 2 cm^{-1} . Each spectrum was obtained from the average of 200 scans to get a better signal-to-noise ratio.

X-Ray Photoelectron Spectroscopy (XPS) was performed using a Thermo Scientific K-Alpha instrument equipped with a monochromatic Al $\text{K}\alpha$ X-ray

source operating at 200 W. The base pressure was about 1.6×10^{-8} Mbar. Wide energy survey scans were collected over the range of 0-1350 eV binding energy (BE). The binding energies were calibrated to the C1s line at 284.8 eV.

Scanning Electron Microscopy (SEM) images were recorded with XL30ESEM-FEG, with a voltage of 5 kV and spot of 2. The pressure inside the chamber was below 10^{-5} mbar and the working distance was 11 mm. A thin layer of gold was deposited over the cotton samples before inserting them into the chamber.

^1H NMR experiments were performed on a Varian Gemini 400 MHz spectrometer. The proton chemical shifts were recorded in ppm downfield using Tetramethylsilane (TMS) as a reference. Each spectrum was obtained from the average of 32 scans to achieve a better signal to noise ratio. To determine the monomer conversion in time, Deuterated Methanol and water were used as solvents. *N,N*-Dimethylformamide (DMF, Aldrich 99.9% purity) was used as an internal reference (10.00 μl). To follow the monomer conversion a sample was taken from the reaction mixture at different times: 0, 5, 10, 60, 120, 240, 1080 and 1440 minutes. Each sample was injected into a sealed NMR tube for ^1H NMR measurements containing the internal reference.

The thermal stability of the unmodified and modified fiber was determined with TGA using a TGA Q500 apparatus from TA Instruments. The samples were heated from 30°C to 700°C at a heating rate of 10°C/min under a nitrogen flow

of 60 mL/min.

Optical microscopy (OM) analyses were performed with a Polyvar Optical Microscope (Reichert Hung). The cotton samples were sandwiched between two glass slides and placed inside a temperature controlled Linkam-cell. The fibers diameters were calculated using the Polyvar software and averaged from 5 measurements.

The molecular weight and molecular weight distribution (polydispersity index, PDI) of the copolymers were measured on a size exclusion chromatography (SEC) instrument (Equipped with Waters 2414 refractive index detector and Waters 1525 Binary HPLC Pump, using Waters Styragel HT2, HT3, HT4 THF 7.8 × 300 mm² columns.). THF was used as an eluent at a flow rate of 1 mL/min and polystyrene (PS) samples were used to calibration standards

The UV pretreatment was performed on PSD benchtop UVT/Ozone Systems (NOVASCAN). Working conditions: 200-240 VAC, 0.5 AMP, temperature 20 °C.

5.2.3 Pre-treatments of the fabric

The cotton fabric was immersed in a water solution with detergent and left in the boiling solution for 1 hour. After this period, the cotton fabric was sequentially rinsed with acetone and ethanol finally left in water inside a sonication bath for 3 min. This procedure was repeated for 3 times. The fabric

dried in an oven at 60 °C under vacuum and finally pretreated on each side with UV light for 10 minutes or 1 hour, using a PSD-UVT benchtop UV-cube. These two irradiation times were chosen according to previous work on cellulose-based surfaces described in the literature³⁻⁵.

5.2.4 Immobilization of the polymerization initiator on the cotton fabric

5.2.4.1 Low temperature method

The cotton fabric was washed as described above and irradiated with UV for 10 min on each side. After this pre-treatment, the fabric was immersed in a toluene solution (200.00 mL) containing 10.00 mL of Aminopropyltrimethoxysilane (ATMS) and left under reflux overnight.

After this period, the cotton fabric was dried and immersed in a toluene solution (200.00 mL) containing Triethylamine (TEA, 2.1mL). Next, 2-Bromoisobutyl Bromide (BiB, 1.86mL) was added dropwise into the solution kept at 0 °C with an ice bath. The mixture was stirred at 0 °C for 1 hour and then heated to room temperature (ca. 25 °C), after reaching this temperature, the reaction proceeded for 12 hours. The cotton fabric with the immobilized initiator (cotton-initiator) was cleaned sequentially with toluene, acetone and water, and finally dried under vacuum at 40 °C for 24 hours.

5.2.4.2 Room temperature method

The cotton fabric was washed as described above and irradiated with UV for 10 min on each side. The pre-treated fabric was immersed in a solution of dry THF (15.00 mL) containing a catalytic amount of 4-(Dimethylamino)pyridine (DMAP) and TEA. The initiator BiB was finally added into the solution. The reaction was kept at room temperature for 12 hours under a flow of Argon, bubbling into the solution. The product was thereafter thoroughly rinsed sequentially with THF, acetone and water for 3 times, and finally dried in an oven at 40°C for 24 hours under vacuum.

5.2.4.3 High temperature method

The cotton fabric was washed, pretreated by UV irradiation and grafted with using the same method described in Section 5.2.4.1. The dried fabric was immersed in a solution of dry THF (100.00 mL) containing a catalytic amount of Py (pyridine) and BiB (0.6 mL) and left under reflux and an Argon flow bubbling in the solution for 15min. After this period, the fabric was washed sequentially by THF, acetone and water for 3 times in a sonication bath. The fabric was finally dried in an oven at 40°C for 24 hours under vacuum.

5.2.5 Polymerization of *N*-Isopropylacrylamide (NIPAAm) from the initiator-immobilized cotton fabric

The Cotton fabric (0.0314g), CuBr (14.5mg, 0.101mmol),

N-Isopropylacrylamide (NIPAAm 1.141g, 10.1mmol) and pentamethyldiethylenetriamine (PMDETA, 21 μ l, 0.101mmol) were added into a MeOH/H₂O (3:1 v/v, 4 mL) solution previously degassed by an Argon flow. The solution was frozen by liquid nitrogen and degassed by three vacuum-argon cycles, to remove the oxygen. The Schlenk flask was then kept at room temperature under magnetic stirring for 24h. After reaction, the product was sequentially washed with methanol, ethanol and H₂O to remove the residual monomer and the catalyst complex. The modified fabric (Cotton-PNIPAAm-H) was finally dried in an oven at 40 °C under vacuum, overnight.

Extended purification procedure: The Cotton-PNIPAAm-H fabric was Soxhlet extracted with 200.00 mL of Methanol for 1 hour to remove the non-reacted monomer, the polymer absorbed at the surface (not covalently bonded) and the remaining catalyst complex. After the extraction the fabric was dried under vacuum at 40 °C for 24 hours. The extraction solutions and washing solvents fractions were collected and evaporated in a rotary evaporator, to collect the solid fractions for further characterization.

5.2.6 Cleavage of the grafted PNIPAAm

Cotton-PNIPAAm-H was put into 50.00 mL of NaOH solution (2 wt %) and left under magnetic stirring for 48 hours at room temperature. The solution was filtrated through a glass filter, and dialyzed (membrane M_w CO =1000, from Union Carbide) against water for 48 hours to remove residual NaOH. Finally, the

neutral solution was freeze-dried for 48 hours for GPC and ^1H NMR analyses.

5.3. Results and discussion

5.3.1. Optimization of the pre-treatment of the cotton fabric

The immobilization of initiator is the first and utmost important step in entire synthesis process because each immobilized initiator molecule provides an initialization point for the polymer chains in the later stage. The number of polymer chain grafted is therefore highly dependent on the immobilization efficiency of the initiator. Therefore, in the following sections, the studies described that made to improve the initiator immobilization efficiency, based on several methods previously reported in the literature⁵⁻⁷ for modifying cellulose-based materials.

In order to improve the reactivity of the cotton fiber and obtain a higher grafting efficiency, the fabric was pre-treated with UV light using a PSD-UVT benchtop UV-cube⁸⁻¹⁰. To investigate the possible degradation of the cotton surface caused by this pre-treatment, FTIR-ATR analyses were performed on the pre-treated cotton fabric. As can be seen on Figure 5.1, the spectrum of the sample pre-treated for 10min (Figure 5.1b) is almost identical to the spectrum of the original cotton fabric (Figure 5.1a). The vibration band at 1635 cm^{-1} observed for both samples is attributed to the absorbed water¹¹⁻¹³. However, after exposure

to UV irradiation for 1 hour, the spectrum clearly shows some degradation. A new stretching vibration band was identified at 1718 cm^{-1} , which is attributed to carbonyl groups originated from the oxidation of the ether bonds or hydroxyl groups of the cellulose units at the cotton surface¹². A further evidence of degradation was the yellow color detected on the cotton fabric pre-treated for 1 hour with UV irradiation. The fabric remains white and shows no noticeable color change after the 10 min UV irradiation.

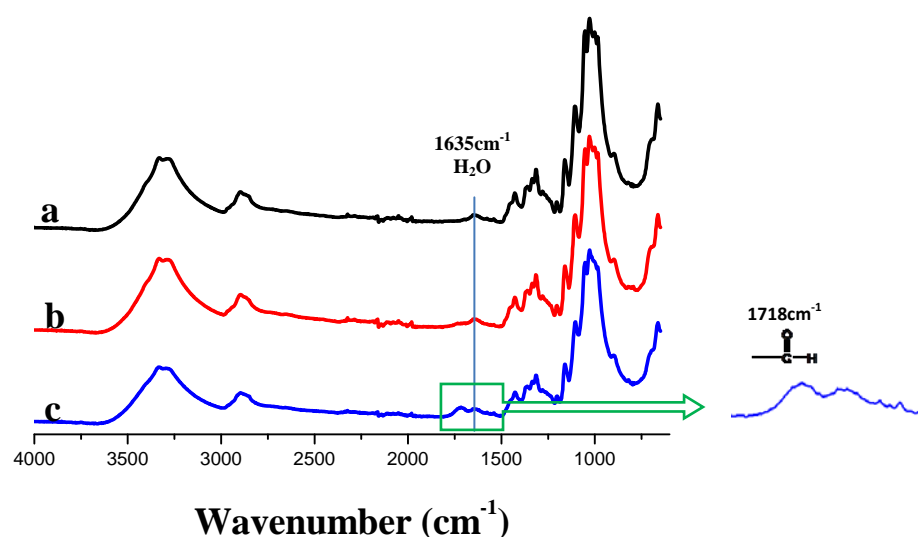


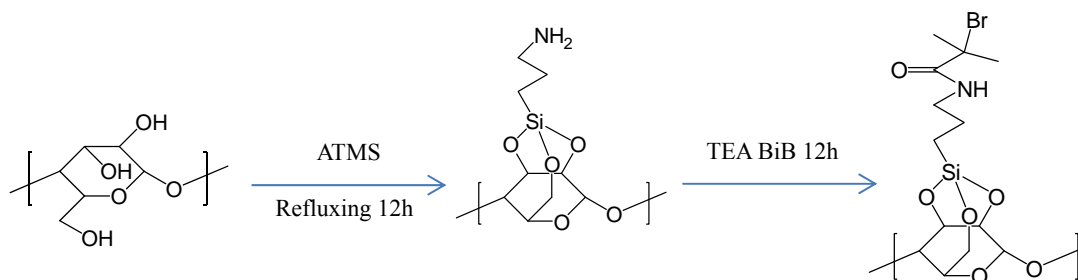
Figure 5.1. FTIR-ATR spectra of (a) untreated cotton sample, (b) UV pretreated for 10 min, (c) UV pretreated for 1 hour.

Based on the results described above, the FTIR results show that no significant degradation occurs on cotton fabric after 10 min UV irradiation. Therefore, unless otherwise stated, 10 min UV irradiation were the conditions used for the pre-treatment of all the samples in the following discussion.

The fabrics with and without UV treatment were both modified with Aminotriethoxymethylsiloxane (ATMS) in order to immobilize amine initiators and based on previous work in the literature¹⁴⁻¹⁶. Aminopropyl trimethoxysilane (ATMS) was immobilized on the cotton surface (Cotton-ATMS), to provide amine groups at the cottons surface for the further linking of the ATRP bromine initiator.

The ATMS modified cotton fabric was further reacted with 2-Bromoisobutyryl bromide (BiB) to get the macromolecular initiator –Br. To confirm the success of the immobilization procedure, the cotton samples were analyzed by FTIR-ATR Spectroscopy. Figure 5.2 shows the comparison of the FTIR spectra of the bare cotton fabric and the Cotton-ATMS-Br initiator with and without UV pre-treatment. The spectrum of the un-treated Cotton-ATMS-Br sample (Figure 5.2b) is similar to the bare cotton fabric (Figure 5.2a). This result is consistent with the FTIR results obtained for the low-grafting cotton fabric (Cotton-PNIPAAm-L) shown in Chapter 3. In the spectrum of the UV pre-treated Cotton-ATMS-Br, the typical amide band II stretching vibration at 1540 cm^{-1} expected for the amide bond formed upon reaction with ATMS molecules is absent (Figure 5.2c). On the other hand, a new vibration band at 1735 cm^{-1} which is attributed to the stretching vibration of the carbonyl group was observed. These results may indicate that the BiB did not react with the amine group of ATMS as expected (see Scheme 5.1), but with the active hydroxyl groups on the cellulose molecules. Furthermore, it was also observed that after the initial

treatment with ATMS, the cotton fabrics become slightly yellow. These results seem to indicate that the fabrics were degraded after longtime exposure in the solvent refluxing conditions used to graft ATMS molecules on the cotton surface.



Scheme 5.1. Immobilization of Cotton-ATMS-Br initiator at low temperature.

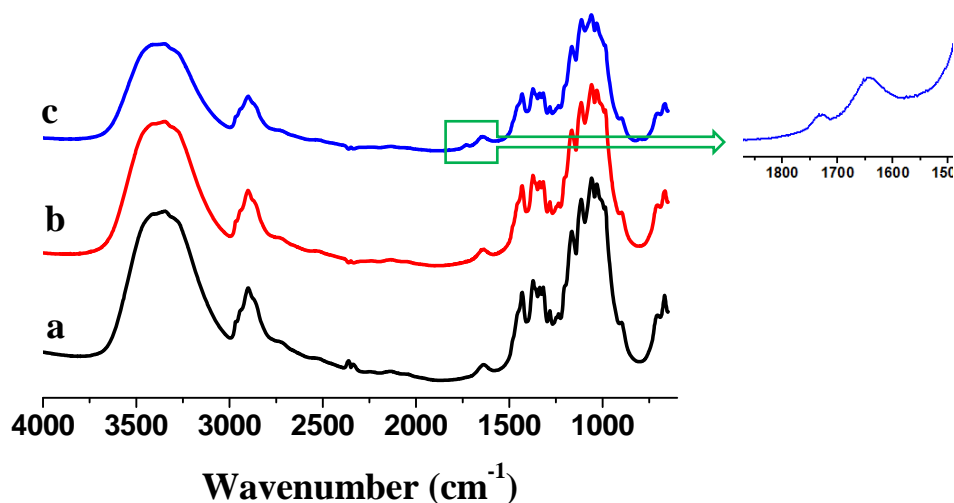


Figure 5.2. FTIR spectra of (a) bare cotton sample, (b) Cotton-A-Br without UV pretreatment, (c) Cotton-A-Br with UV pretreatment.

As mentioned in the previous discussion, the UV pre-treatment is beneficial for the activation of the cotton cellulose surfaces. The mechanism of

this activation can be understood as an oxidation process of the cellulose molecules. The hydroxyl groups of the pyranose ring are oxidized into carbonyl and carboxyl groups, and this process is accompanied by opening of the pyranose ring⁵. Among these two oxidation processes, the pyranose ring opening reaction requires higher UV energy or longer exposing time. As more carbonyl and carboxyl groups are produced, the fabric becomes yellowish because these groups are chromophores. The FTIR result in the beginning of this part (Figure 5.1) shows that after 1h irradiation, a new band can be identified at 1718 cm^{-1} which is attributed to the stretching vibration of the carbonyl group. Therefore, it is presumed that the opening of pyranose ring dominated the reaction in this stage. It is also presumed that during the first 10mins irradiation the oxidation of the hydroxyl dominates because no new stretching vibration could be found in FTIR spectra and the color of fabric keeps white. Although the UV pre-treatment enhances the reactivity of cellulose fiber, the grafting efficiency of ATMS is still too low to be detected, and more over, it seems to promote some degradation of the cotton fabric. Therefore, another immobilization method was investigated in which the BiB initiator was directly grafted onto an UV pre-treated cotton fabric instead of using ATMS as the bridging molecule.

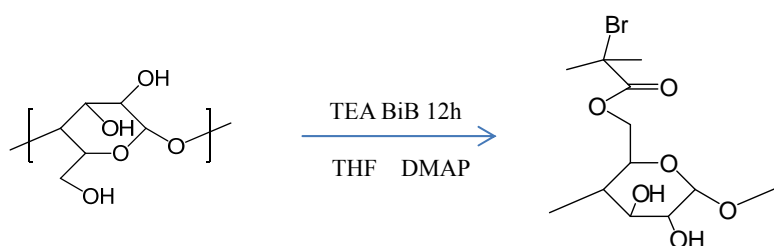
5.3.2 Optimization of the immobilization of the polymerization initiator on the cotton fabric: synthesis and characterization

5.3.2.1 Low temperature method

The immobilization procedure at low temperature is similar to that has been described in Section 5.3.1.

5.3.2.2 Room temperature method

In order to achieve a high grafting efficiency and use a simpler grafting process a new immobilization route was investigated, based on the work of literatures^{1,2,17}. The preparation procedure was showed in Scheme 5.2. However, in this case the cotton fabric pre-treated with UV irradiation was directly immersed in a THF solution in the presence of DMAP, TEA and the BiB initiator.



Scheme 5.2. Immobilization of Cotton-R-Br initiator at room temperature.

Figure 5.3 clearly shows that the spectrum of fabric without UV pre-treatment (Figure 5.3b) is identical to the untreated cotton fabric sample (Figure 5.3a). This result is consistent with the FTIR result of the sample

prepared at low temperature (Figure 5.2a,b). However, it is interesting to see that for the fabric pre-treated with UV (Figure 5.3c), there is an absorption band at 1735 cm^{-1} which is attributed to the ester bond between the cellulose units and the initiator. The appearance of this ester bond provides a strong evidence of the covalent bonding between substrate and the initiator confirming the successful immobilization of the initiator at the cotton surface. As compared to the low temperature method (Figure 5.2c), the fabric with the initiator immobilized at room temperature remains white, the intensity of vibration of ester bond increases (Figure 5.3c), and the immobilization process was simplified. Therefore, the immobilization method at room temperature was considered better than the one made at low temperature.

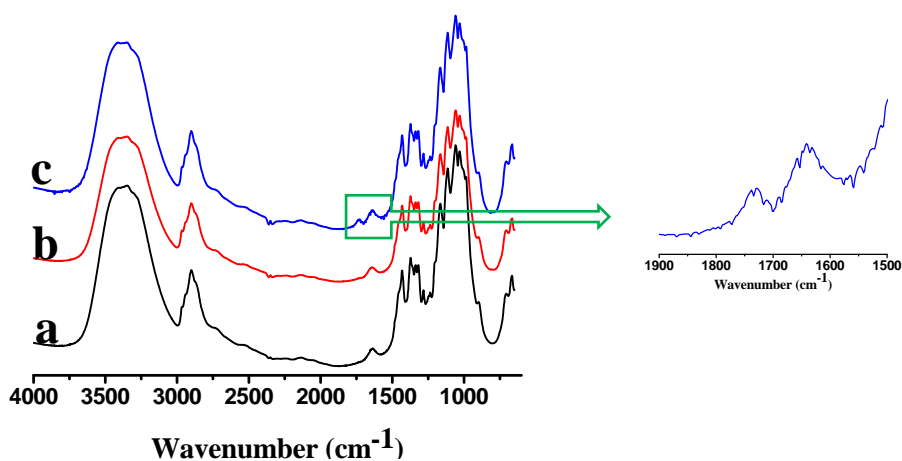
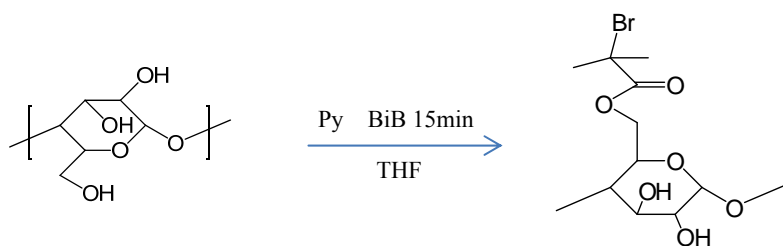


Figure 5.3. FTIR spectra of (a) untreated cotton fabric sample, (b) Cotton-R-Br without UV pretreatment, (c) Cotton-R-Br with UV pretreatment.

5.3.2.3 High temperature method

In the previous discussion, the efficiency of the low-temperature and room-temperature immobilization methods have been compared and analyzed. The sample pre-treated with UV irradiation and immobilized using the room-temperature method shows the best results so far, based on FTIR-ATR and color of the fabric. In this section, the immobilization of the initiator made at high temperature is described.

The UV pre-treated bare cotton fabric was immersed in THF in the presence of Py and the BiB initiator and the reaction was carried at the reflux temperature (see scheme 5.3). For comparison, the cotton with initiator ATMS (Cotton-A) was used as blank reference instead of bare cotton fabric.



Scheme 5.3. Immobilization of Cotton-F-Br initiator at high temperature.

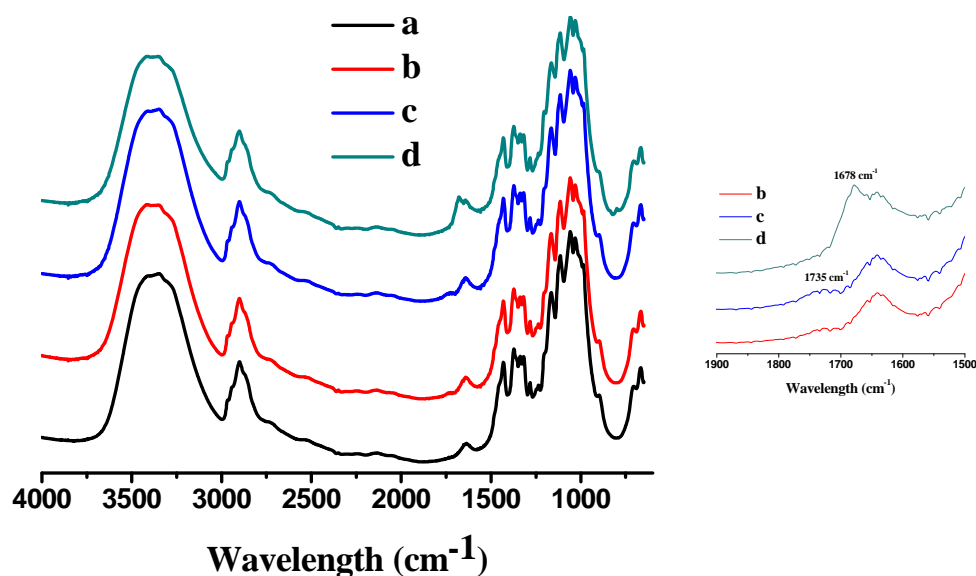


Figure 5.4. FTIR spectra of (a) bare cotton sample, (b) Cotton-F-Br without UV pre-treatment, (c) Cotton-F-Br with UV pre-treatment, (d) Cotton-A-F-Br with UV pre-treatment.

From Figure 5.4 it can be seen that in this case the sample without UV pre-treatment (Figure 5.4b) also shows the presence of ester bonds vibration at 1735 cm^{-1} after the reaction, in spite of their low intensity. This can be attributed to the increase of active reaction at higher temperature. However, the immobilization efficiency of the fabric with UV pre-treatment (Figure 5.4c) is lower than that obtained from the room-temperature method (Figure 5.3c), which is unexpected. Although the intensity of the ester peak is slightly higher than the untreated sample (Figure 5.4b), the grafting efficiency is still rather low. For the sample cotton-A-F-Br (Figure 5.4c), the peak at 1678 cm^{-1} might be attributed to the vibration of amid band I. However, this assignment is dubious because of the

absence of N-H bending (amid band II) at 1540 cm^{-1} .^{18,19} The color of the samples prepared by the high-temperature method (Figure 5.4b,c,d) become yellowish. Hence, it is considered that the high-temperature treatment may cause degradation to the fiber cellulose molecules.

In this section, all the cotton-initiator samples that prepared by different immobilization methods have been shown, presented no ester bonds vibration at 1735 cm^{-1} , without UV pre-treated. Therefore, UV pre-treatment seems to be beneficial for increasing initiator immobilization efficiency. Amongst all, the room temperature method was considered to be the best results in terms of immobilization of the initiator, because of its simplicity, highly efficiency and less damaging (the color of fabric was light after the reaction) to the cotton substrate.

5.3.3 Synthesis and characterization of the highly-grafted fabric (Cotton-PNIPAAm-H) via Surface-Initiated Atom Transfer Radical Polymerization (SI-ATRP)

In Chapter 3, the procedure to graft PNIPAAm brushes onto a cotton fabric was described. In that procedure, the solid and liquid components were degassed separately in order to remove any traces of oxygen. The liquid components were then transferred into the flask containing the solid components. This transfer process has to be made very carefully because any leakage will introduce oxygen into the system and deactivate the catalyst very rapidly. In the new procedure, in

order to avoid leakages, all the components were mixed at once and immediately frozen, instead of using the injection method. The reaction medium was further degassed by several vacuum-argon cycles. This new procedure was expected to increase the efficiency of de-oxygenation and as a result to increase the polymer grafting efficiency. The reactions were carried out in a sealed Schlenk flask at room temperature for 24 hours. After this period the reaction was terminated by exposure to air.

The Cotton-R-Br sample, showing the best results for the initiator immobilization as described before, was chosen to be the cotton-macro-initiator for grafting the PNIPAAm via SI-ATRP with the new method.

After the polymerization reaction, the resulting Cotton-PNIPAAm-H sample was extensively extracted by Soxhlet to remove the non-reacted monomer, non-bonded polymer and catalyst complex. The extracted Cotton-PNIPAAm-H fabric was characterized further by FTIR-ATR, XPS and SEM.

5.3.3.1 FTIR Spectroscopy

Figure 5.5 shows the FTIR-ATR spectra of the bare cotton fabric, the initiator grafted cotton fabric and the cotton fabric grafted with initiator and PNIPAAm. For simplicity, these three samples will be referred to as bare cotton, Cotton-R-Br and Cotton-PNIPAAm-H, respectively, in the following discussion.

The spectrum of Cotton-R-Br reveals a noticeable peak at 1735 cm^{-1} , which is not present in the spectrum of the bare cotton. As discussed before, this peak is assigned to the stretching vibration of the carbonyl groups. This is a strong evidence of the formation of ester bonds between the initiator and the cotton substrate. Figure 5.5c shows the FTIR spectrum of Cotton-PNIPAAm-H sample. The amide bands I and II at 1648cm^{-1} and 1543cm^{-1} can be clearly identified in the spectrum.^{18,19} Differently from the FTIR spectrum of the low grafting efficiency sample Cotton-PNIPAAm-L shown in Chapter 3, the intensity of amide bands I and II increased significantly. Moreover, the bands at 1388 cm^{-1} and 1365 cm^{-1} which are assigned to the bending vibration of the carbon-hydrogen bond of the isopropyl groups in NIPAAm molecule are also observed²⁰. It should be noticed that since the Cotton-PNIPAAm-H fabric was Soxhlet extracted, there is no residual monomer or free polymer left, hence the polymer identified is most likely chemically bonded to the cotton fiber. The presence of all these peaks strongly suggests the success of the polymerization reaction and a significant increase of grafting efficiency.

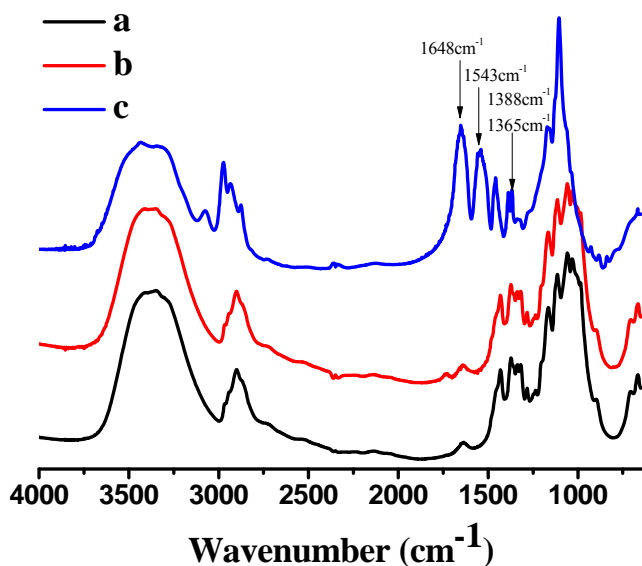


Figure 5.5. FTIR spectra of (a) bare cotton, (b) Cotton-R-Br and (c) Cotton-PNIPAAm-H.

5.3.3.2 XPS

In addition to FTIR, X-Ray Photoelectron Spectroscopy (XPS) was used to characterize the composition of the fabrics surfaces. Figure 5 a, 5b and 5c show the XPS wide-scan spectra of the bare cotton, Cotton-R-Br and Cotton-PNIPAAm-H samples, respectively. For bare cotton (figure 5.6a), only C 1s and O 1s signals are observed, whereas in the spectrum of Cotton-R-Br (figure 5.6b), Br 3d and Br 3p signals with band energy (BE) of 70eV and 189eV can be clearly identified. The Br signal originates from the BiB initiator molecules which are introduced by the immobilization reaction. It should be noticed that, for the Cotton-A-Br initiator sample synthesized using the method described in Chapter 3, it was not possible to detect by XPS the presence of the Br element on the surface of the modified fabrics, because of the low immobilization yield.

The peak at 402 eV in Figure 5.6c is assigned to the N 1s from PNIPAAm molecules. This result confirms what was observed by the FTIR spectra, which indicated that the PNIPAAm molecules were successfully grafted onto the cotton substrate via SI-ATRP. Furthermore, comparing the intensity ratio of oxygen to carbon O 1s /C 1s in Figure 5.6a and 5.6c, one can find that, the ratio of the sample Cotton-PNIPAAm-H is dramatically lower than that of bare cotton sample. This is attributed to the contribution from the polymerized PNIPAAm chains, which has lower oxygen content comparing to cellulose molecules.

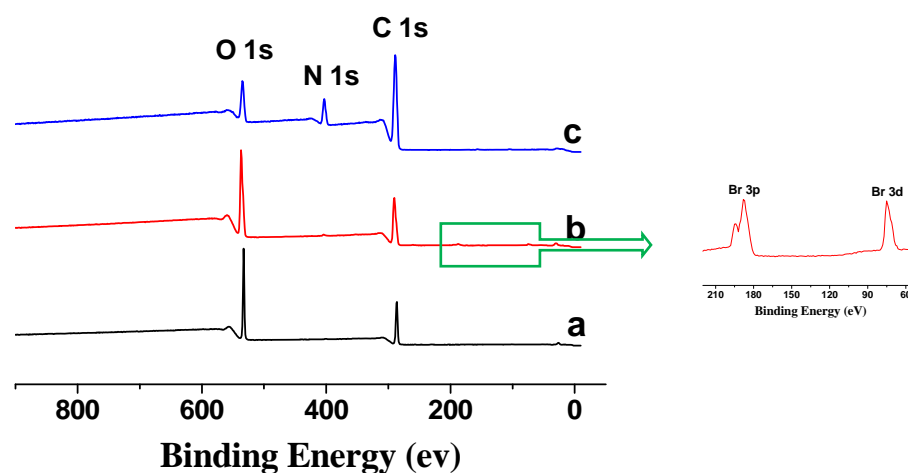


Figure 5.6. XPS wide-scan and Br 3d spectra of (a) bare cotton, (b) Cotton-R-Br and (c) Cotton-PNIPAAm-H .

5.3.3.3 Grafting efficiency and the product compositions

The grafting yield of PNIPAAm and weight uptake of the cotton fabric was measured by different methods and the results are given in Table 5.1.

Table 5.1. Grafting yield and weight uptake percentage of the Cotton-PNIPAAm-H sample obtained from weighting, NMR and TGA methods.

Sample	Gravimetric method		¹ NMR		TGA
	#Weight uptake (%)	*Grafting yield (%)	&Monomer conversion (%)	^s Weight uptake (%)	Weight uptake (%)
Cotton-PNIPAAm-H	460	12.7	12.5	454	143.2

[#] The weight uptake is calculated from Equation 5.1:

$$\text{weight uptake} = \frac{M_{\text{grafted}}}{M_{\text{fiber}}} \times 100 \% \quad (\text{Eq. 5.1})$$

where M_{grafted} is the mass of the grafted PNIPAAm calculated by $M_{\text{final}} - M_{\text{fiber}}$, and M_{fiber} is the initial mass of the Cotton-R-Br fiber used.

^{*} The grafting yield was calculated from Equation 5.2:

$$\text{grafting yield} = \frac{M_{\text{grafted}}}{M_{\text{put in}}} \times 100 \% \quad (\text{Eq. 5.2})$$

where M_{grafted} is the mass of the grafted PNIPAAm, and $M_{\text{put in}}$ is the mass of the NIPAAm monomers which were put initially into the reaction flask.

[&] The monomer conversion was calculated from ¹H NMR experiments using Equation 5.3:

$$\text{monomer conversion} = \left(1 - \frac{C_t}{C_0}\right) \times 100 \% \quad (\text{Eq. 5.3})$$

where C_t is the monomer concentration in the solution at the end of the reaction and C_0 is the initial monomer concentration.

[§] The weight uptake is calculated from Equation 5.4:

$$\text{weight uptake} = \frac{M_{\text{put in}} \times \text{monomer conversion}}{M_{\text{fiber}}} \times 100 \% \quad (\text{Eq. 5.4})$$

where $M_{\text{put in}}$ is the mass of the NIPAAm monomers which were put initially into the reaction flask, monomer conversion is from result of Eq. 5.3 and M_{fiber} is the initial mass of the Cotton-R-Br fiber used.

5.3.3.3 NMR Spectroscopy

The monomer concentration in the solution can be quantified by ^1H NMR using an inert solvent as an internal reference. Since the reference solvent does not take part in the reaction, its concentration can be taken as constant throughout the reaction provided that we have a sealed medium (NMR tube). The monomer intensities are then normalized to the internal reference intensity and plotted against the reaction time. Deuterated methanol and heavy water were used as solvents and *N,N*-Dimethylformamide (DMF) was used as a internal reference. Figure 5.7 shows a NMR spectrum of the reaction medium. The normalized monomer concentration was plotted against the reaction time and shown in Figure 5.8. Each monomer concentration determined at specific times of reaction

is an average of 5 spectra collected. The NMR spectrum shows the DMF resonances at peak a and d. Peak b and c are assigned to vinyl group of NIPAAm monomer. As the reaction time increases, the monomer is continuously grafted onto the Cotton-R-Br surface and the concentration of the remaining monomer in solution decreases.

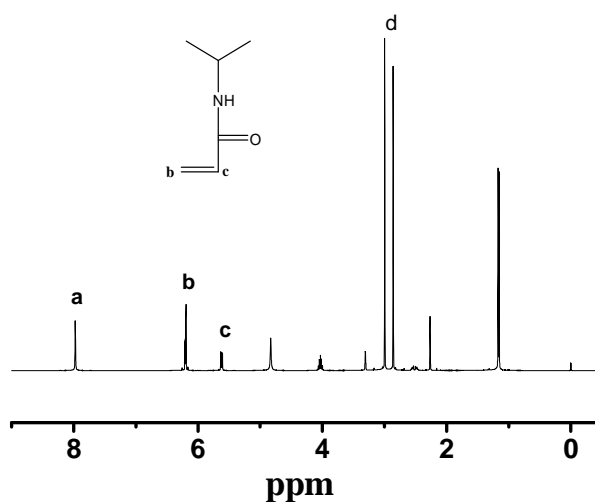


Figure 5.7. NMR spectra of the extracted solution from the reactor. DMF is used as an internal reference for quantification of the monomer concentration.

The monomer conversion (figure 5.8) shows the kinetics of the polymerization reaction. The intensity of NIPAAm monomers drops rapidly in the initial stage of the reaction indicating a fast monomer consumption. . A plateau was reached after c.a. 20 h reaction time, and the intensity decreased by 12.5 % after 24 hours. This result fits very well with the grafting yield calculated from weighting method. With these results, it can be estimated that about 454 %

(wt %) of the PNIPAAm was grafted onto the cotton surface.

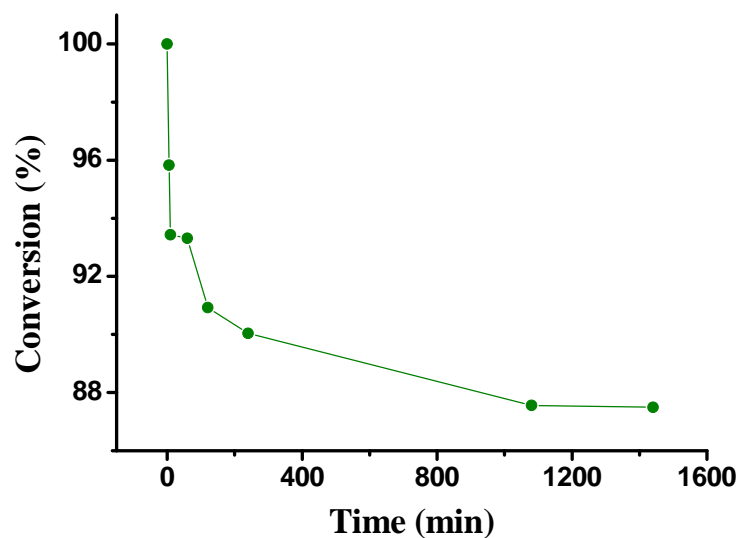


Figure 5.8. Monomer conversion *versus* time of reaction given by the monomer peak intensities (b and c in Figure 5.7) on samples taken at different reaction times.

5.3.3.4 TGA

TGA was performed to study the composition and thermal stability of the modified cotton fabrics. Figure 5.9 shows the decomposition behavior of bare cotton, PNIPAAm and Cotton-PNIPAAm-H. Both the bare cotton and pure PNIPAAm samples show a single-step degradation with onset temperature of 330 °C and 387 °C, respectively. However, the PNIPAAm grafted fiber presented two decomposing steps. As shown in Figure 5.10, the first decomposing onset at 334 °C corresponds to the decomposition of cotton cellulose, and the second one at 378 °C corresponds to the decomposition of PNIPAAm. The weight loss during the first decomposition was 36.1%, and the

second one is 51.7%.

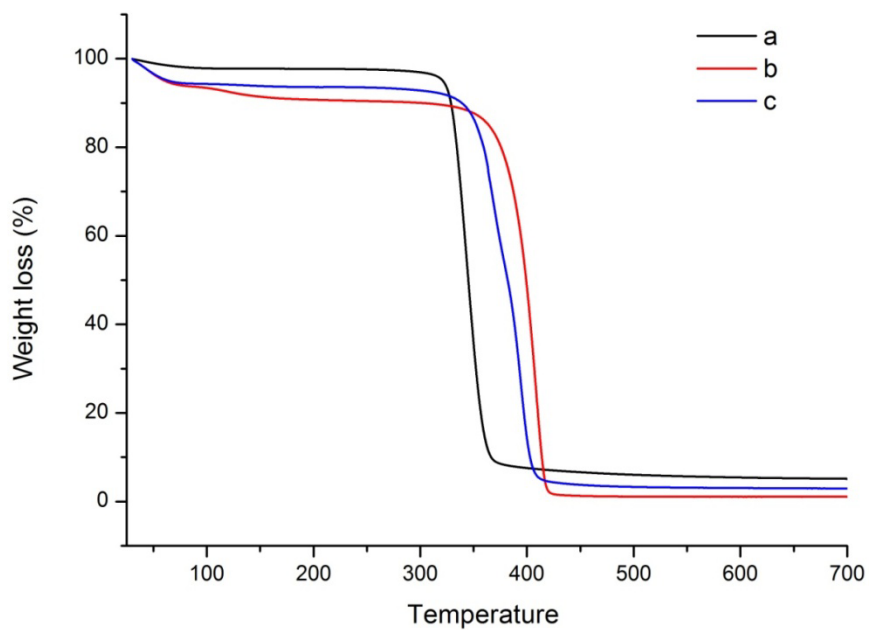


Figure 5.9. Thermogravimetric analysis (TGA) curves of (a) bare cotton, (b) Pure PNIPAAm, (c) Cotton-PNIPAAm-H

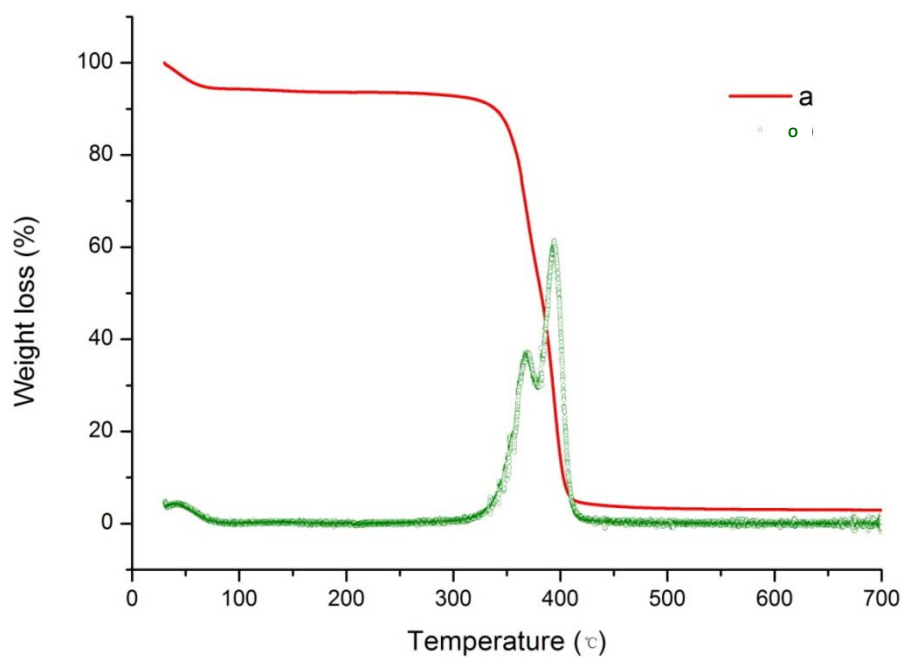


Figure 5.10. Cotton-g-PNIPAAm TGA (a) and DTGA (b) curves.

From these data, the weight uptake result calculated from TGA is 143.2%. This value is much smaller than that calculated from NMR and weighting methods, both of which give a weight uptake value of ca. 460%. This is understandable in the sense that the decomposition temperatures of the two components are so close to each other that the two decomposition processes overlap in a certain temperature range, resulting in a significant calculation error.

5.3.3.5 GPC

To determine the molecular weight and PDI of the grafted polymer, the PNIPPA_m was cleaved from the cotton substrate. A NaOH aqueous solution was used as catalyst to accelerate the hydrolysis reaction of the ester bonds. The detailed information about the hydrolysis procedure was described in the experimental section 5.2.6. The molecular weight of polymer cleaved from the Cotton-PNIPAA_m-H fabric was characterized by GPC. As shown in Figure 5.11, the M_n of the polymer is about 31000, and the PDI is 2.77. The M_n obtained was much higher than the expected value of 11 300 (based on the theoretical values). This may be due to the initial assumption that all the hydroxyl groups in the cellulose molecules are active in the reaction. However, only the surface layer of –OH groups will be active and can be grafted with PNIPAA_m. The PDI is also rather broad, which may be due to the weak controllability of the complex agent PMDETA or the degradation of cellulose substrate during the hydrolysis process. The controllability of agent PMDETA will be discussed in next chapter. In fact,

the characterization of the grafting yield of a polymer from an organic surface has been a common difficulty for a long time^{1,2,21}, especially when the grafting efficiency is low. Hydrolytic demolition of the cellulose^{5,22} or selective cleavage of the ester bond might be a possible solution²³, but these treatments can easily bring in the fragments of cellulose polymer.

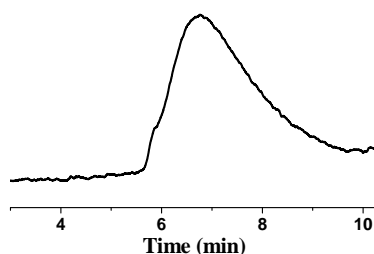


Figure 5.11. Gel Permeation Chromatography of the cleaved PNIPAAm from the PNIPAAm-cotton sample.

5.3.3.6 SEM

In Figure 5.12 the SEM images show the surface morphology of bare cotton and as-prepared Cotton-PNIPAAm-H samples. The diameter of the bare cotton fibers is about 10 μm , and their surfaces are smooth and flat. The polymerization of NIPAAm monomer by the optimized SI-ATRP method produced a thick layer of PNIPAAm on the cotton surface (Cotton-PNIPAAm-H) (Figure 5.12 c,d), which is rather different from the previous low-grafted sample (Cotton-PNIPAAm-L) reported in Chapter 3. The diameter of the cotton fiber

increases to about 40 μm . The morphology of the fiber surface becomes much rougher. The magnified image of the Cotton-PNIPAAm-H surface is shown in figure 5.12d. Polymer particles with diameter of about 800nm are densely packed in a good order on the surfaces of cotton fibers. This surface roughness in the submicron scale gives to this sample a high potential to be a temperature-controllable super-amphiphilic material.

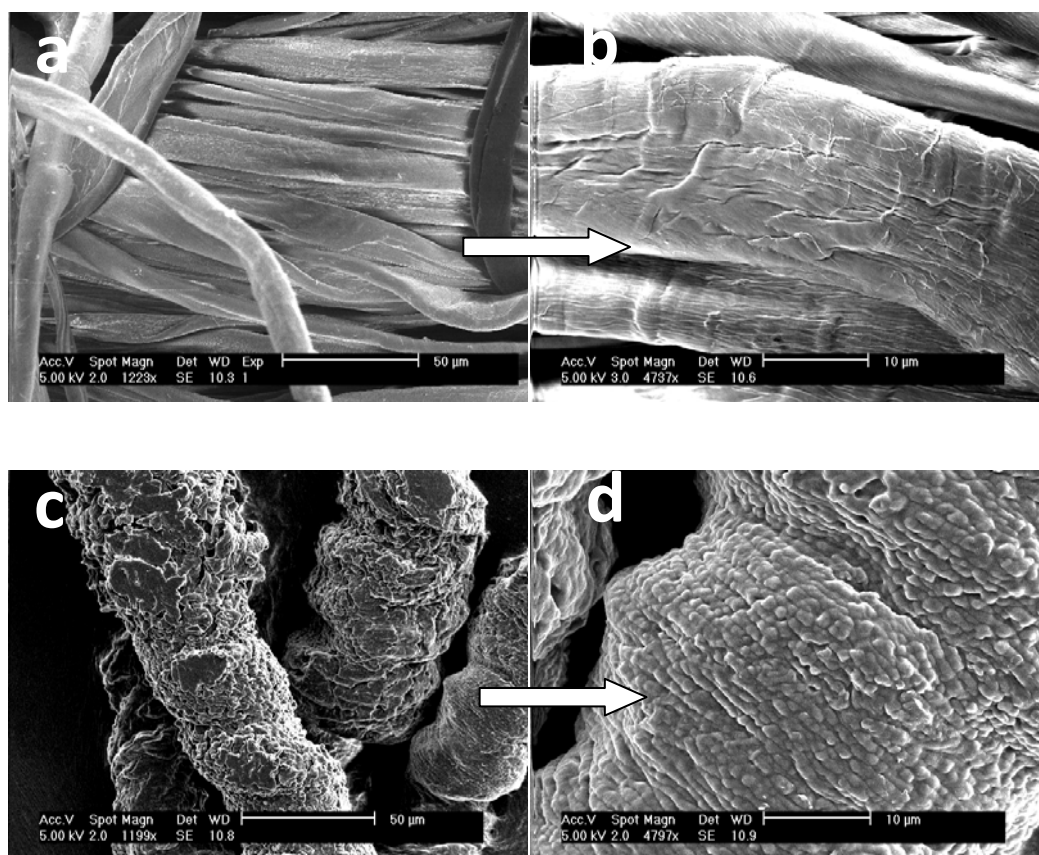


Figure 5.12. SEM images of (a) Cotton and (c) Cotton-PNIPAAm-H. (b) and (d) the magnified image of (a) and (c), respectively.

5.3.3.7 OM

Figure 5.13 shows the optical microscope images of the bare Cotton and as-prepared Cotton-PNIPAAm-H samples recorded at room temperature, in the dry state and after being pre-wet with water. The dried cotton fibers (Figure 5.13a) are smooth with diameters of about 10 μm . Upon water saturation (figure 5.13b), the diameter increases slightly to ca. 15 μm (averaged from 5 measurements), and the fiber becomes translucent under the microscope. Moreover, the morphology of the water saturated bare Cotton fiber is quite similar to that of the dry sample. Figure 5.13c shows the optical microscope image of the dry Cotton-PNIPAAm-H sample. The fiber surface is covered by a thick polymer layer, and the diameter of the sample increases to about 40 μm (averaged by 5 measures) as compared to the bare cotton. After water saturation, the Cotton-PNIPAAm-H fibers swell dramatically (figure 5.13d), and the diameters of the water saturated fibers become approximately 75 μm (average from 5 measurements). Moreover, from the image of the water-saturated Cotton-PNIPAAm-H sample (figure 5.13d), it is also possible to identify the interface between the cotton fiber (the inner dark area) and the polymer layer on the edge. The diameter of the cotton fiber in the Cotton-PNIPAAm-H is larger than in the water saturated bare Cotton fibers.

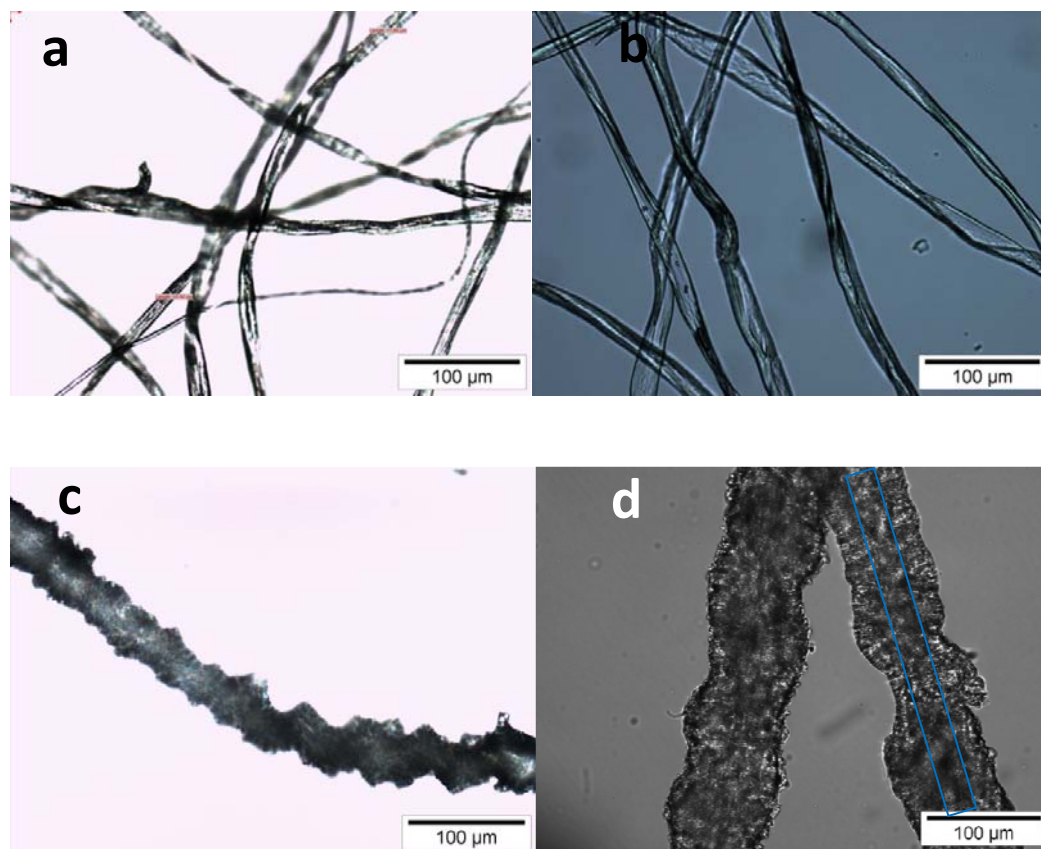


Figure 5.13. Optical microscope images of (a) bare cotton fibers, (b) pre-wet bare cotton fibers, (c) Cotton-PNIPAAm-H fibers, (d) pre-wet Cotton-PNIPAAm-H fibers. The images were recorded at room temperature (20 °C).

5.4. Conclusion

The primary concern of this work was to improve the grafting efficiency of the temperature-responsive polymer on the cotton fabric. In order to achieve this goal, the first step of immobilization of the ATRP initiator onto the cotton fabric surface needed to be improved. Short-time UV pre-treatment coupled with a room temperature immobilization method proved to be the most efficient way to increase the immobilization efficiency of ATRP-initiator. After this treatment, a

much higher polymer grafting efficiency was achieved, as compared to the un-treated sample, or the low-grafted fabrics reported in Chapter 3. The grafting yield was evaluated by three different methods: NMR, TGA, and gravimetry. The NMR and gravimetry results are rather consistent with each other, whereas the TGA method tends to underestimate the grafting yield due to the overlapping between the decomposition processes, from the cellulose and PNIPAAm. The cotton fabric grafted with PNIPAAm was characterized by FTIR, XPS, NMR, TGA, SEM and OM. It was shown that cotton fibers were covered with PNIPAAm brushes with a high grafting efficiency. SEM and OM images show a significant increase of the diameter of the cotton fibers upon grafting with the new method and a dramatic difference in the surface morphology.

5.5. References

- 1 Carlmark, A. & Malmstrom, E. E. ATRP grafting from cellulose fibers to create block-copolymer grafts. *Biomacromolecules* **4**, 1740-1745, (2003).
- 2 Carlmark, A. & Malmstrom, E. Atom transfer radical polymerization from cellulose fibers at ambient temperature. *J. Am. Chem. Soc.* **124**, 900-901, (2002).
- 3 Malešič, J. *et al.* Photo-induced degradation of cellulose. *Polym. Degrad. Stabil.* **89**, 64-69, (2005).
- 4 Puls, J., Wilson, S. & Höltner, D. Degradation of Cellulose Acetate-Based Materials: A Review. *Journal of Polymers and the Environment* **19**, 152-165, (2011).
- 5 Margutti, S. *et al.* Physical–chemical characterisation of acrylic polymers grafted on cellulose. *Polymer* **43**, 6183-6194, (2002).
- 6 Guthrie, J. T. & Tune, P. D. The preparation, characterization, and application of cellulose–MMA graft copolymers. I. The aqueous-based preparation of cellulose–MMA graft copolymers. *Journal of Polymer Science Part A: Polymer Chemistry* **29**, 1301-1312, (1991).
- 7 Hu, J.-L., Liu, B.-H. & Liu, W.-G. Temperature/pH Dual Sensitive N-isopropylacrylamide/ Polyurethane Copolymer Hydrogel-grafted Fabrics. *Textile Research Journal* **76**, 853-860, (2006).

- 8 Kang, E. T., Tan, K. L., Kato, K., Uyama, Y. & Ikada, Y. Surface modification and functionalization of polytetrafluoroethylene films. *Macromolecules* **29**, 6872-6879, (1996).
- 9 Ron, H., Matlis, S. & Rubinstein, I. Self-assembled monolayers on oxidized metals. 2. Gold surface oxidative pretreatment, monolayer properties, and depression formation. *Langmuir* **14**, 1116-1121, (1998).
- 10 Kolar, J., Strlic, M., Pentzien, S. & Kautek, W. Near-UV, visible and IR pulsed laser light interaction with cellulose. *Appl. Phys. A-Mater. Sci. Process.* **71**, 87-90, (2000).
- 11 Fengel, D. & Strobel, C. FTIR SPECTROSCOPIC STUDIES ON THE HETEROGENEOUS TRANSFORMATION OF CELLULOSE-I INTO CELLULOSE-II. *Acta Polym.* **45**, 319-324, (1994).
- 12 Lojewska, J., Miskowicz, P., Lojewski, T. & Proniewicz, L. M. Cellulose oxidative and hydrolytic degradation: In situ FTIR approach. *Polym. Degrad. Stabil.* **88**, 512-520, (2005).
- 13 Hatakeyama, H., Nagasaki, C. & Yurugi, T. RELATION OF CERTAIN INFRARED BANDS TO CONFORMATIONAL-CHANGES OF CELLULOSE AND CELLULOSE OLIGOSACCHARIDES. *Carbohydr. Res.* **48**, 149-158, (1976).
- 14 Xia, F. *et al.* Dual-Responsive Surfaces That Switch between Superhydrophilicity and Superhydrophobicity. *Advanced Materials* **18**, 432-436, (2006).

- 15 Wong, A. K. Y. & Krull, U. J. Surfaces for tuning of oligonucleotide biosensing selectivity based on surface-initiated atom transfer radical polymerization on glass and silicon substrates. *Anal. Chim. Acta* **639**, 1-12, (2009).
- 16 Wang, W., Yang, J. X., He, B. & Gu, Z. W. A novel method to prepare crosslinked polyethyleneimine hollow nanospheres. *Chin. J. Polym. Sci.* **25**, 431-435, (2007).
- 17 Hansson, S., Östmark, E., Carlmark, A. & Malmström, E. ARGET ATRP for Versatile Grafting of Cellulose Using Various Monomers. *ACS Applied Materials & Interfaces* **1**, 2651-2659, (2009).
- 18 Lindqvist, J. *et al.* Intelligent Dual-Responsive Cellulose Surfaces via Surface-Initiated ATRP. *Biomacromolecules* **9**, 2139-2145, (2008).
- 19 Kim, D. J. *et al.* Formation of Thermoresponsive Gold Nanoparticle/PNIPAAm Hybrids by Surface-Initiated, Atom Transfer Radical Polymerization in Aqueous Media. *Macromolecular Chemistry and Physics* **206**, 1941-1946, (2005).
- 20 Ruiz, J.-C. *et al.* Polypropylene grafted with smart polymers (PNIPAAm/PAAc) for loading and controlled release of vancomycin. *European Journal of Pharmaceutics and Biopharmaceutics* **70**, 467-477, (2008).
- 21 Castelvetro, V., Geppi, M., Giaiacopi, S. & Mollica, G. Cotton Fibers Encapsulated with Homo- and Block Copolymers: Synthesis by the Atom Transfer Radical Polymerization Grafting-From Technique and Solid-State NMR Dynamic

- Investigations. *Biomacromolecules* **8**, 498-508, (2006).
- 22 Fernández-García, M., Fuente, J. L. d. l., Cerrada, M. a. L. & Madruga, E. L. Preparation of poly(tert-butyl acrylate-g-styrene) as precursors of amphiphilic graft copolymers. 1. Kinetic study and thermal properties. *Polymer* **43**, 3173-3179, (2002).
- 23 Prucker, O. & Rühle, J. Synthesis of Poly(styrene) Monolayers Attached to High Surface Area Silica Gels through Self-Assembled Monolayers of Azo Initiators. *Macromolecules* **31**, 592-601, (1998).

Chapter 6

The superamphiphilic switch behavior and humidity collecting ability of the highly grafted cotton fibers

Abstract

The surface wettability of a highly grafted smart cotton fabric was studied in this chapter. It exhibits superhydrophobicity with a water contact angle (CA) up to 140° at 40 °C, and superhydrophilicity with a water CA of 0° at room temperature. Because of this special superamphiphilic property, this fabric surface was used to capture moisture from atmosphere at lower temperature and release water at higher temperature. The DSC results show a completely reversible conversion between superhydrophobicity and superhydrophilicity can be achieved in a short time. The concept reported in this chapter may provide a new insight into solutions for fresh water conversion and purification.

6.1 Introduction

While the deserts and arid areas constitute approximately one-third of the earth's land surface¹, the capture of fresh water becomes a serious problem in the twentieth century. However, easily ignored, there are real “sky rivers” in earth's atmosphere full of clean and fresh water. Collecting humidity from the air and releasing water to the soil may be a perfect idea to solve easily and efficiently the water depletion problem².

Namib Desert beetles, can collect and drink water from humid air^{3,4} due to a carapace which combines hydrophilic and hydrophobic domains at its surface. Similarly to these desert beetles, some spider silks are also capable of capturing humidity, by the presence of spindle-knots and joints on their surface^{5,6}.

Inspired by nature, a smart humidity collection and release cotton fabric was designed which could respond to temperature changes. The cotton fabric was modified with temperature sensitive Poly(N-isopropylacrylamide) (PNIPAAm) polymer brushes grafted directly from the hydrophilic cotton surface. In comparison with bare cotton fabric, the PNIPAAm modified fabric demonstrates remarkably superior humidity collection at low temperatures (23 °C), up to 340 % weight increase.

In many deserts and arid areas where the rainfall is scarce, like the Namib Desert, the temperature fluctuates considerably between day and night. It

experiences extreme high temperatures in day time (up to 40 °C) and cools down significantly overnight (below 20°C), originating very often a early-morning fog^{7,8}. The beauty of the cotton fabric reported here is that it can collect water from the atmosphere overnight or early morning, and automatically release to the dry soil during the day, as the temperature goes up, alleviating the water scarceness in these particularly arid areas. Moreover, such humidity collecting and release fabrics can be used in smart water-trapping or uni-directional water transporting textiles, for clothes, home textiles, tents, geotextiles such as building covers, to name but a few.

6.2 Experiment

6.2.1 Materials

N-isopropylacrylamide (NIPAA, Aldrich 97 % purity) was recrystallized twice in *n*-hexane and dried under vacuum for 24 hours at room temperature. Ethyl-2-bromopropionate (EBP, Aldrich 99 %), Triethylamine (TEA, Aldrich 99 %), 2-bromisobutyryl bromide (BiB, Aldrich, 98 %), Pentamethyldiethylenetriamine (PMDETA, Aldrich 99 %), Copper (I) Bromide (CuBr, Aldrich, 99 %), tetrahydrofuran (THF, WRT, 99.8 %), methanol (MeOH, WRT, 99.8 %) were used as received without any further modification.

6.2.2 Instruments

Contact angle (CA) measurements were measured with an OCA20

equipment (Data Physics, Germany) at different temperatures. The humid atmosphere was created using NaCl saturated salt solution.

Optical microscopy (OM) analyses were performed with a Polyvar optical microscope (Reichert Hung). The cotton samples were sandwiched between two glass slides and the temperature was precisely controlled using a Linkam temperature-cell. The heating rate was 10 °C/min, and all the samples were hold for 5 min at the target temperature. All the values of fiber diameters are averages of 5 measurements.

Differential Scanning Calorimetry (DSC) experiments were performed on a Q2000 equipment from TA instruments, using a heating rate of 5 °C/min, in the temperature range 5 °C – 60 °C. Typically, samples of 5-6 mg of PNIPAAm samples were pre-wet with 30 µL of distilled water and sealed on aluminum T0-Hermetic pans (from TA instruments).

The molecular weight and molecular weight distribution (polydispersity index, PDI) of the copolymers were measured on a size exclusion chromatography (SEC) instrument (Equipped with Waters 2414 refractive index detector and Waters 1525 Binary HPLC Pump, using Waters Styragel HT2, HT3, HT4 THF 7.8 ×300 mm²columns.). THF was used as eluent with a flow rate of 1 mL/min. Polystyrene (PS) standards were used for calibration.

6.2.3 Synthesis of pure PNIPAAm

NIPAAm (2.2035 g, 19.5 mmol), PMDETA (41 μ L, 0.195 mmol), Ethyl-2-bromopropionate (EBP, 29 μ l, 0.195 mmol), methanol/H₂O (3:1 v/v, 4 ml) and CuBr (0.0286 g, 0.195 mmol) were added into a Schlenk flask. The solution was frozen by liquid nitrogen and degassed by three vacuum-Argon cycles to remove oxygen. After this procedure the Schlenk flask was sealed and kept at room temperature for 24 h. After the reaction, the copper catalyst was removed from the product by filtration through an activated (alkali) alumina column, and the remaining NIPAAm monomer was removed by precipitating twice in diethyl ether. The solvent was evaporated using a rotary evaporator. The remaining white solid (PNIPAAm) was collected and dried under vacuum at room temperature for 24 h.

6.2.4 Humidity collection experiments

The as-prepared dry PNIPAAm-cotton fibers (typically ~ 12 mg) were placed in a small open-aluminum (DSC type) pan. The pan was left floating on a glass vial (20,00 mL capacity) filled with a small amount of water (10.00 μ L). The vial was sealed with a plastic cap and the fibers were exposed to the humid environment inside the vial for 3 days, at three different temperatures (23, 34 and 40 °C). The weight of the PNIPAAm-cotton fibers was accurately measured, before (W_0) and after the 3-day period (W_h) of humidity environment exposure.

6.3 Results and Discussion

6.3.1 The superamphiphilic property of Cotton-PNIPAAm-H

6.3.1.1 Phase transition between superhydrophilicity and superhydrophobicity

Wettability is a very important property governed by both chemical composition and the geometrical micro-structures of a surface⁹⁻¹¹. In general, the surface roughness dramatically enhances the water contact angle (CA) on a hydrophobic surface but decreases the CA on a hydrophilic surface because of the capillary effect. This phenomenon suggests that superhydrophilicity and/or superhydrophobicity can be achieved by tuning the hierarchical micron/nano-scale structure on the surface^{12,13}. If the surface roughness concept is applied to a responsive material, a stimulus-responsive smart interfacial material which can switch between superhydrophilicity and superhydrophobicity can be developed.

Figure 6.1 shows the CAs of Cotton-PNIPAAm-H measured at temperatures below and above the PNIPAAm LCST temperature. A reversible change from superhydrophilicity at 23 °C, to superhydrophobicity at 40 °C is observed and the reversible cycles can be stably repeated many times (5 cycles were tested). At 23 °C, the Cotton-PNIPAAm-H surface is superhydrophilic with

a CA of 0° (Figure 6.1a). It should be pointed that at the same temperature, the CA of a film of pure PNIPAAm is 40° (Figure 6.2a). As the temperature is raised up to 40°C , the fiber surface switches to superhydrophobic with a final CA of 140° (Figure 6.1b). As expected, this value is much higher than the CA of the pure PNIPAAm film, which is 50° at 40°C (Figure 6.2b).

As mentioned before, the CA of a solid surface is determined by both the surface chemical composition^{14,15} and surface roughness¹⁶⁻¹⁸. According to Wenzel's law¹⁹:

$$\cos \theta_w = r \cos \theta \quad (1)$$

where r is surface roughness ($r \in (1, -\infty)$), θ_w and θ are the apparent and intrinsic contact angles on rough and smooth surfaces, respectively. Decreasing the value of r will result in a larger apparent contact angle. Thanks to the rough surface of the cotton textile substrate, a superhydrophobic surface of the Cotton-PNIPAAm-H was fabricated.

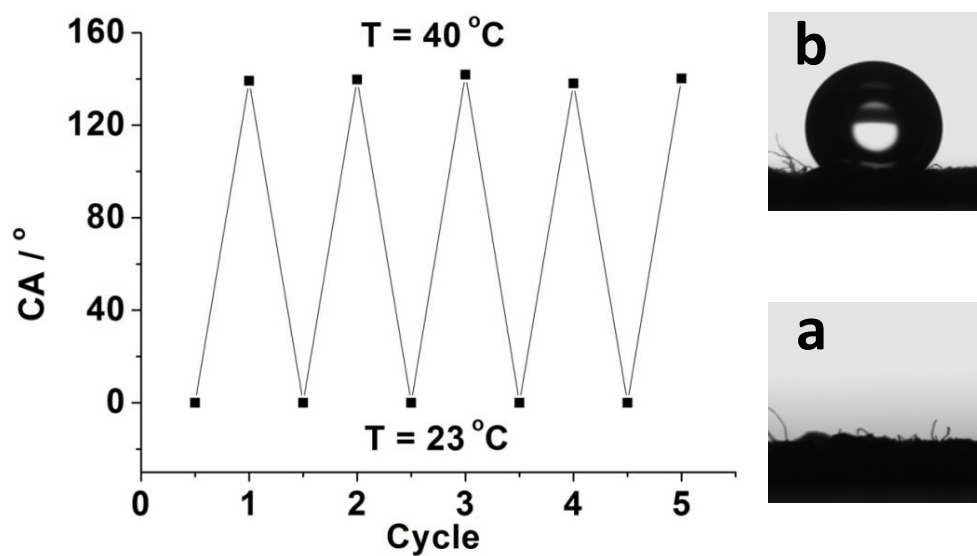


Figure 6.1. Water CAs at two different temperatures for a Cotton-PNIPAAm-H surface. Half cycles: $T=23\text{ }^{\circ}\text{C}$, and integral cycles: $T=40\text{ }^{\circ}\text{C}$. (a) $23\text{ }^{\circ}\text{C}$ and (b) $40\text{ }^{\circ}\text{C}$

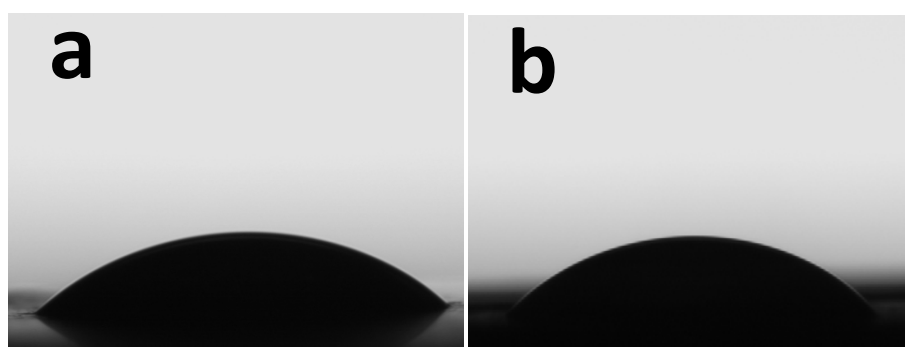


Figure 6.2. Water CAs at two different temperatures for a pure PNIPAAm film surface (a) $23\text{ }^{\circ}\text{C}$, and (b) $40\text{ }^{\circ}\text{C}$

In a short conclusion, a superamphiphilic intelligent surface was fabricated by combination of a temperature-responsive polymer and surface roughness. The hierarchical micro-scale structure makes the material surface more hydrophobic at higher temperature and more hydrophilic at lower temperature.

For further understanding of the superamphiphilic property, both the bare cotton and modified cotton fibers were put in the water. Upon increasing temperature, the modified cotton fiber surfaces are expected to switch into hydrophobic. As showed below (Figure 6.3), bare cotton fibers and Cotton-PNIPAAm-H fibers were put in bottle I and II respectively, and be filled with the same amount of pure water. At room temperature (Figure 6.3a), fibers in both bottles were sank at bottom. As the temperature raised to 40°C, bare cotton fibers (bottle I) stayed at the bottom, whereas the PNIPAAm modified cotton floated (bottle II). This phenomenon can be explained by the fact that the surface tension between PNIPAAm and water molecules increases significantly as the polymer turns into hydrophobic. This simple experiment is a clear and straight forward indication of hydrophilic/hydrophobic transition.

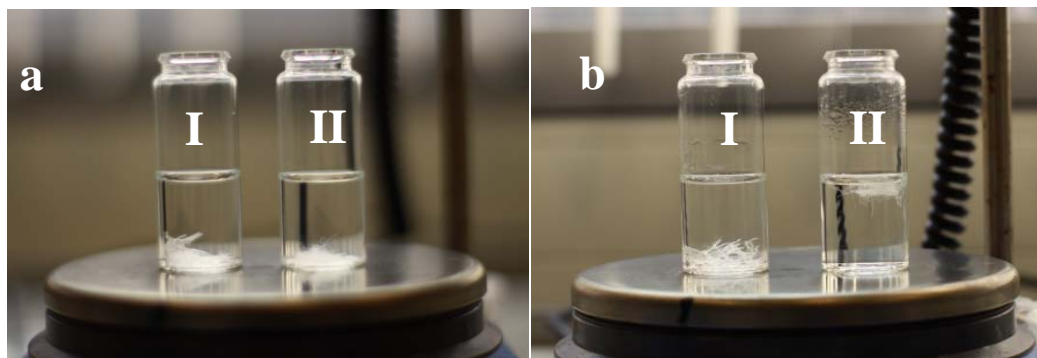


Figure 6.3. Photo pictures of fibers in pure water, (a) 23°C (I) bare cotton fibers, (II) Cotton-PNIPAAm-H fibers; (b) 40°C (I) bare cotton fibers, (II) Cotton-PNIPAAm-H fibers.

6.3.1.2 Thermal responsive property

The well-known LCST transition of PNIPAAm is a

hydrophilic-hydrophobic phase transition in nature²⁰. This process involves enthalpy exchange between the system and the environment which can be detected by DSC. Figure 6.4a shows the DSC exotherms and endotherms of Cotton-PNIPAAm-H sample. A typical endothermic peak around 34 °C and an exothermic peak around 31 °C were observed for heating and cooling scan, respectively. In order to investigate the reversibility of this phase transition process, 5 temperature cycles were recorded. Completely identical endotherms and exotherms were found for all the scans. This means the LCST transition of grafted PNIPAAm is fully reversible. The DSC results show that the LCST transition is an endothermic process during heating scan. At lower temperatures, the PNIPAAm molecules are hydrophilic, and the amide groups of PNIPAAm form intermolecular hydrogen bond with H₂O molecules. Therefore, the mobility of water molecules is restricted by the macromolecule chains. At elevated temperatures, the hydrophobic isopropyl group dominant the hydrophilicity of PNIPAAm molecules. Hydrogen bond between PNIPAAm and water molecules breaks down, and the PNIPAAm molecules becomes hydrophobic. Both enthalpy and entropy of the system increase in the heating process. Therefore, in thermodynamics, this hydrophilic/hydrophobic phase transition is an enthalpy-driven process.

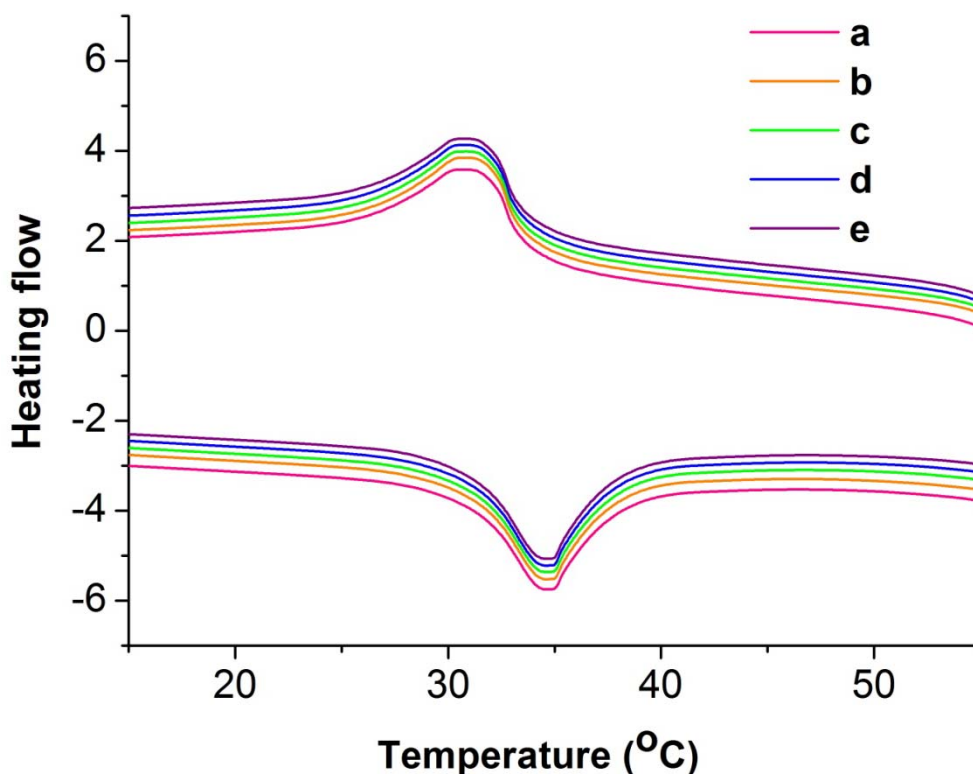


Figure 6.4. Recycling DSC curves of Cotton-PNIPAAm. (a) 1st cycle, (b) 2nd cycle, (c) 3rd cycle, (d) 4th cycle, (e) 5th cycle

6.3.1.3 Swelling and deswelling triggered by temperature

The swell and deswell transition is usually characterized by dynamic light scatter (DLS), and the contact angle methods.²¹⁻²³ In this work, optical microscopy (OM) was used to observe the morphology change during the phase transition. A direct evidence of this transition behavior may be obtained from the OM images. Figure 6.5 shows the temperature response of the water saturated Cotton-PNIPAAm-H fibers observed by optical microscope as the temperature raised up to 40 °C. The fibers are translucent at room temperature (Figure 6.5 a and b) with diameter of about 75 μm. Upon rising the temperature to 34 °C

(Figure 6.5 c and d), nearby the PNIPAAm LCST, the edge of the fibers becomes hazy, and the diameter of fibers begins to retract. The formation of air bubbles can be observed in the microscopic field, which is attributed to the condensation of water vapor released from the wet Cotton-PNIPAAm-H fibers. In order to observe the final stage of the water release process, the temperature was further increased to 40 °C (Figure 6.5e,f). The diameter of fibers reduces to 40 – 50 μm, which is comparable with the diameter of dry sample. The image of the fibers gets darker as the temperature increases, which indicates a more compact structure. These results indicate that the water release by the Cotton-PNIPAAm-H fibers is accompanied by a change in the structure and morphology of the polymer covering the cotton's surface, which is triggered by temperature.

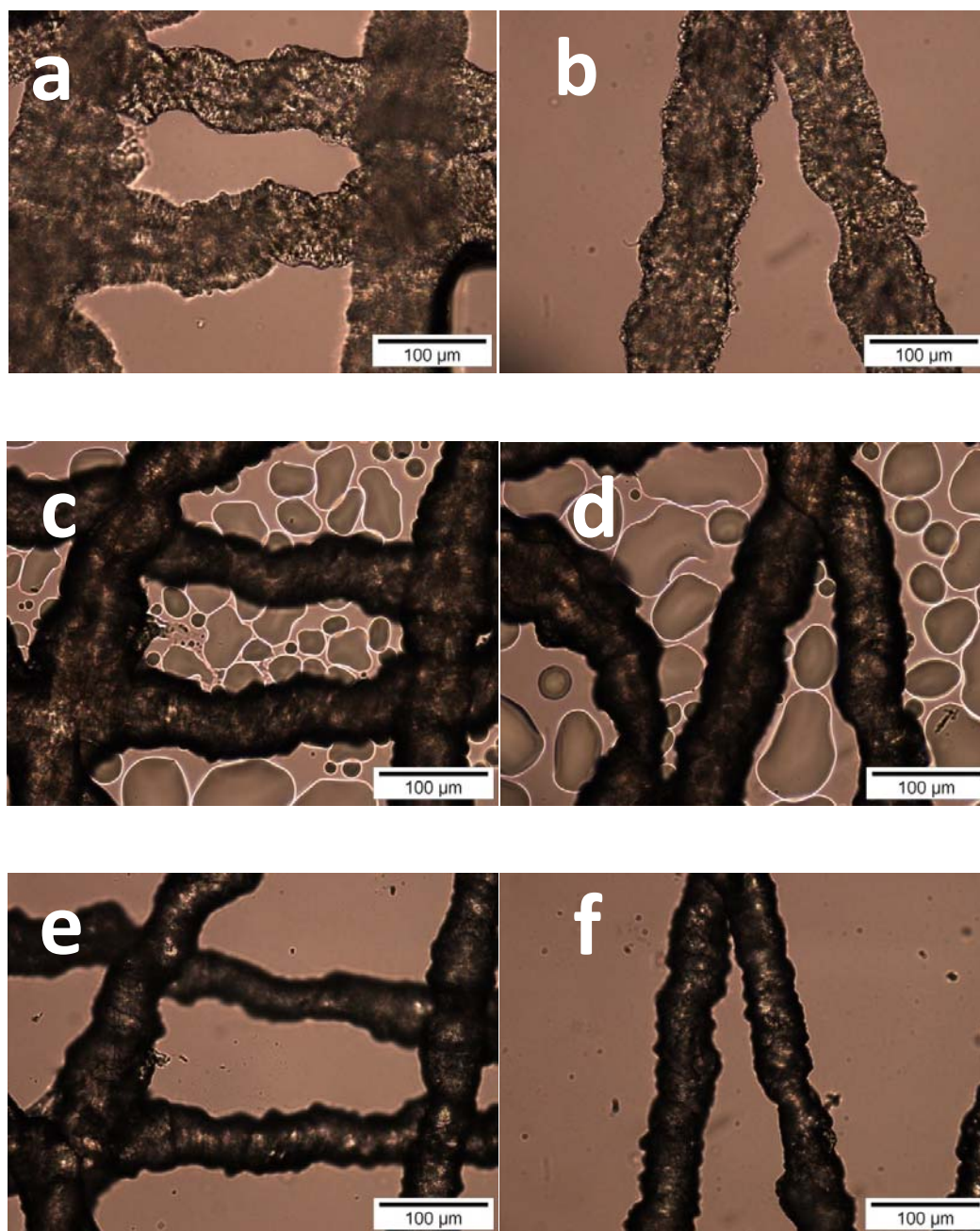
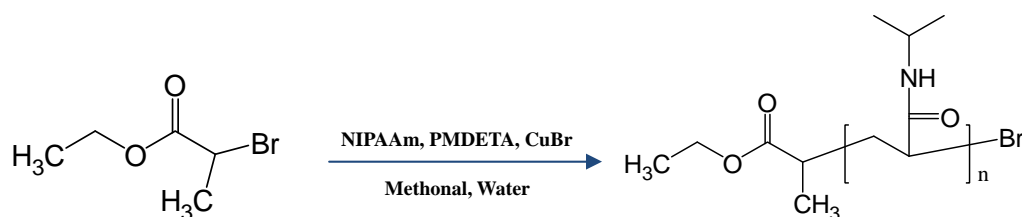


Figure 6.5. Optical microscope images of wetting Cotton-PNIPAAm-H under different temperatures: (a) and (b) at 22°C, (c) and (d) at 34°C, (e) and (f) at 40°C

6.3.2 Synthesis of pure PNIPAAm polymer

In order to have some general ideal about the molecular weight and molecular weight distribution of the grafted polymer on the cotton substrates,

pure PNIPAAm was synthesized using a small-molecule initiator and exactly the same polymerization conditions. Scheme 6.1 shows the polymerization process of the pure PNIPAAm by ATRP. Ethyl-2-bromopropionate (EBP) was used as an initiator and the reaction was terminated by exposure to the air. The dried product was dissolved in THF and eluted through an alumina column, and subsequently precipitated by adding the THF solution into diethyl ether. In this work, the theoretical polymerization degree of the PNIPAAm monomers is $n=100$ (polymerization degree can be calculated by the molar ratio between monomer and initiator).



Scheme 6.1. Small molecule initiated ATRP of NIPAAm monomer.

It is well known that the color of the solution is green during the ATRP reaction due to the presence of Cu^+ , and when the reaction is terminated by exposure to air in the end, the color of the solution becomes blue, because that Cu^+ has been oxidized to Cu^{2+} .^{24,25} All the ATRP reactions performed in Chapters 3 and 5 were in compliance with this common sense. However, when the cellulose macroinitiator is replaced by small molecule initiator EBP, the reaction solution turns into blue even at the beginning stage. It could be suspected that because of the effect of the cellulose molecules in the cotton fabric reduce the

Cu^{2+} to Cu^+ and therefore can achieve a narrow polydispersity of the product. Several attempts have been tried to improve the polymerization degree and narrow the PDI of the polymer products. Table 6.1 shows the parameters of all the experiments. Comparing the different preparation methods, one could find that the “transfer” of liquid component to another container results in a low grafting ratio. PNIPAAm sample 2#, 3#, 4# could not be collected by precipitation in diethyl ether. This means that the NIPAAm monomers were not polymerized or the polymerization degree was very low. Although the sample PNIPAAm 1# was precipitated from the solution, molecular weight of $M_n=2900$ (Figure 6.6a) is far less than the theoretical molecular weight of 11300. This low molecular weight of the PNIPAAm involved with “transfer” of reactant in the polymerization steps may be due to the leakage of air and therefore the reaction was terminated by the oxygen in the air. With the freeze and vacuum method, the polymerization degree can achieve M_n of 22600. However, the polydispersity is rather broad with PDI of 4.4 (Figure 6.6b), which means the ATRP is out of control, and the free radical polymerization mechanism dominates the reaction.

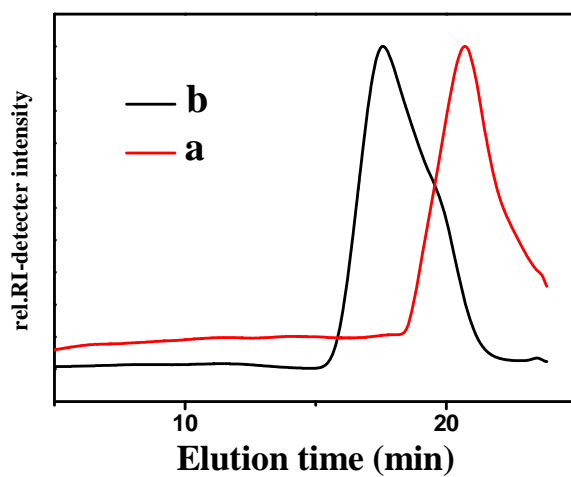


Figure 6.6. GPC curves of (a)PNIPAAm 1#, (b)PNIPAAm 5#

Table 6.1. Different operating methods of conducting the ATRP grafting.

Sample	PNIPAAm 1#	PNIPAAm 2#	PNIPAAm 3#	PNIPAAm 4#	PNIPAAm 5#
Procedure description	EBP + NIPAAm + PMDETA + Methanol + Water CuBr Vacuum argon 3times Argon bubbled for 2h Transfer	EBP + NIPAAm + water + Methanol + PMDETA + CuBr Vacuum argon 3times Argon bubbled for 2h Argon bubbled for 2h Transfer Transfer	CuBr + PMDETA EBP + NIPAAm + Methanol + Water Freeze Vacuum Melting 3 times Freeze Vacuum Melting 3 times Transfer	CuBr + EBP PMDETA + NIPAAm + Methanol + Water Freeze Vacuum Melting 3 times Freeze Vacuum Melting 3 times Transfer	EBP + NIPAAm + PMDETA + Methanol + Water + CuBr Argon bubbled for 2h Freeze Vacuum Melting 3 times
Color of the solution	Blue	Blue	Blue	Blue	First green then turns blue
Precipitate	Yes	No	No	No	Yes
Mn	2900				22600

From the above discussion, it can be concluded that freeze and vacuum conditions tends to increase the degree of polymerization, but the polydispersity of the polymer obtained from this methods rather broad. In order to quantify the molecular weight and molecular weight distribution of the grafted polymer, small-molecules sacrifice initiator EBP was added into the system before reactor, assuming that it has the same activity as the macro-initiator. The freeze and vacuum method was used to graft NIPAAm from cellulose initiator (Cotton-R-Br) to obtain a higher grafting efficiency. It is observed that the reaction solution still turns blue. The GPC result shows a broad PDI of 3.5, which is narrower than that of the PNIPAAm 5# (Figure 6.6b). The reason that the reactant solution turns blue when it contain small molecule initiator whereas keeps green when only macro initiator exists was not clear yet. It is considered this may be attributed to the lower active reaction of surface initiator than free initiator in solution, or due to the reduction property of the cellulose molecules. In order to compare the controllability if the ligand used in the ATRP reaction, another chemical Tris[2-(dimethylamino)ethyl]amine (M_{e6} TERN) was used. It was found that the color of solution kept green with the new ligand. Figure 6.7b shows a narrow and symmetric peak without a shoulder, which probably mean that no detectable coupling termination during the reaction. The PDI is a 1.2, which is much lower than that obtained by using PMDETA as a ligand.

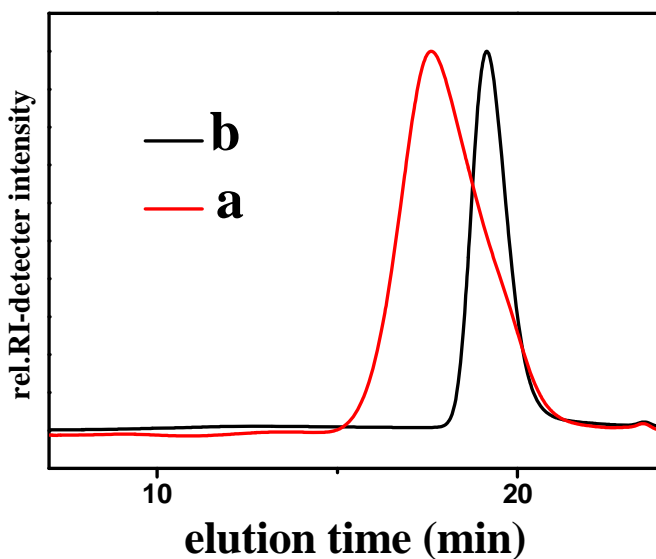


Figure 6.7. GPC curve of polymer obtained by (a) using PMDETA as ligand; (b) using M_{e6} TERN as legend.

It has been shown that the M_{e6} TERN exhibited superior controllable ability compare to PMDETA. However, the grafting efficiency of the cotton surface is decreased significantly as can be directly observed from the SEM results. Figure 6.8 shows the SEM images of the grafting surface. Comparing the images of Figure 5.12 in the previous chapter which using PMDETA as a ligand, fibers in Figure 6.8 were found to be thinner and the surface is only partially covered by PNIPAAm polymer. The diameter of the Cotton-PNIPAAm fiber was about $20\mu\text{m}$ which is comparable to the diameter of the original cotton fibers. CA measurements were also performed on this sample in order to study the surface properties. The reversible change from superhydrophilicity at low temperature to superhydrophobicity at high temperature was not observed for this sample.

Therefore, it can be concluded that with the ligand M_{c6} TERN the polydispersity can be controlled very well, but grafting efficiency is not satisfactory.

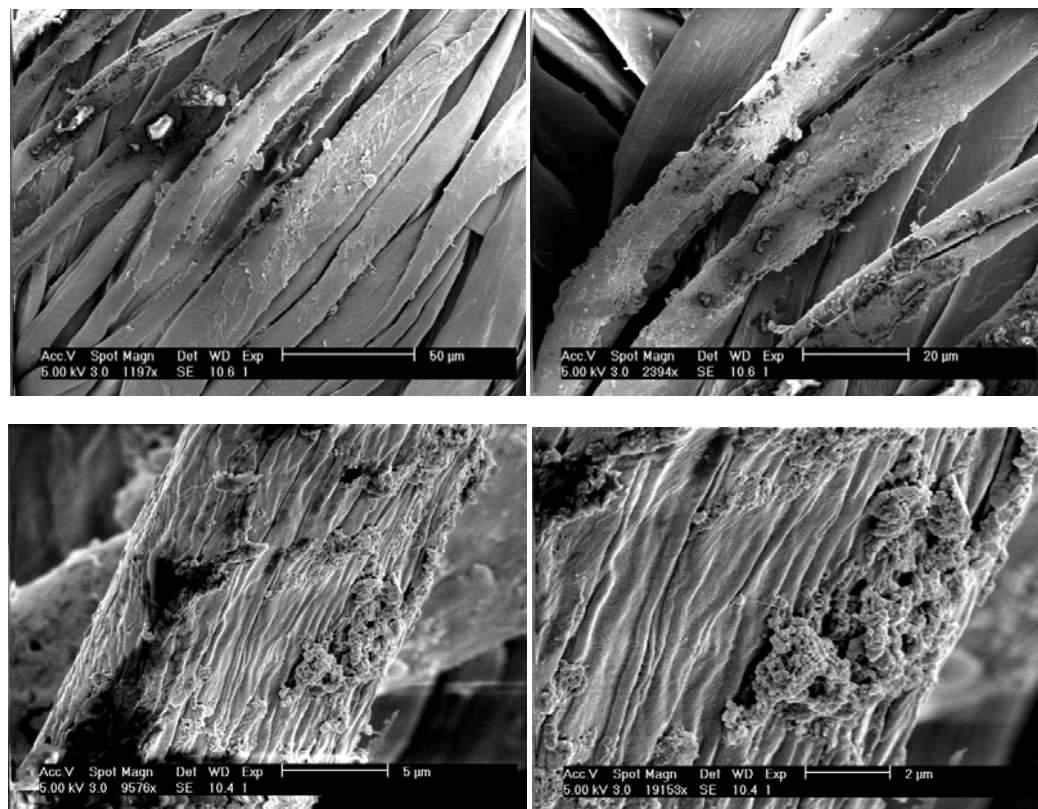


Figure 6.8. SEM images of Cotton-PNIPAAm synthesis by using M_{c6} TERN as ligand.

6.3.3 Humidity collecting ability of grafted cotton fiber

Figure 6.9 shows the water capture ability of the bare cotton fiber, pure PNIPAAm (PNIPAAm 5# in this experiment) and Cotton-PNIPAAm-H fiber samples, after being exposed to a 100% humidity environment and different temperatures, as the method described in Section 6.2.4. These experiments were repeated 3 times. The average value of the three experiments was used to describe the humidity collection ability of the cotton fibers.

At 40 °C the water uptake ratio of the bare cotton, PNIPAAm and the PNIPAAm-modified fiber are rather similar, with only a 25 % increase in relation to its respective original weight. When the temperature goes down to 23 °C, the water uptake of the pure PNIPAAm increases up to 100 %, while for the PNIPAAm-modified cotton its weight raises abruptly to 340 %.

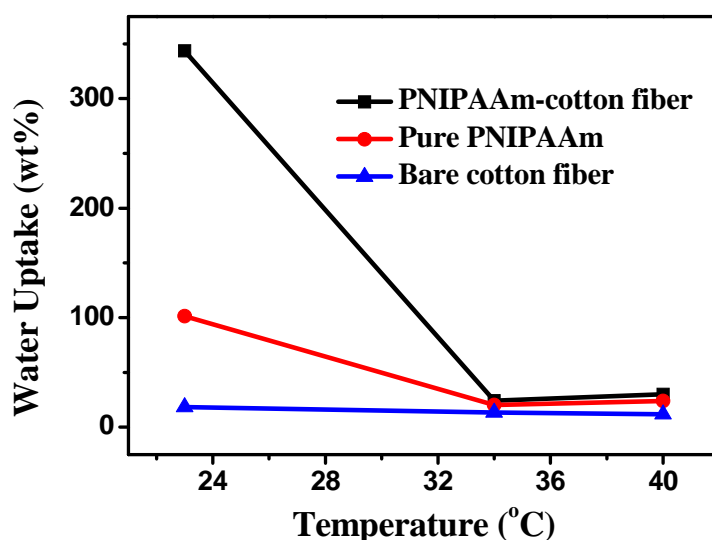


Figure 6.9. Humidity collection ability: water uptake (%) given by the weight increase in relation to the original weights of Cotton-PNIPAAm-H fiber, pure PNIPAAm and bare cotton fiber samples, when exposed to 100% humidity atmosphere, at different temperatures.

The humidity collection ability of bare cotton fiber is relatively low and almost keeps constant at all different temperatures. The low water uptake ratio of bare cotton can be easily understood in terms of its micro-phase structures. Each cotton fiber is composed of concentric layers. The most peripheral layer is constituted of cellulosic crystalline fibrils²⁶. Due to the densely packed molecular

structure of crystals, only the amorphous region in this layer is accessible to water molecules.

It is well known that PNIPAAm undergoes a coil-to-globule transition in aqueous solution at a certain temperature, which is denoted as the Lower Critical Solution Temperature (LCST)^{27,28}. When the temperature is above the LCST, PNIPAAm molecules tend to form intra-molecular hydrogen bonding with each other and the water bound to the polymer chain is released. Therefore, at a temperature higher than the LCST (34 °C and 40 °C), the pure PNIPAAm and the PNIPAAm-cotton fiber exhibit similar weight increase ratio as the bare cotton sample.

The superior humidity collection ability of Cotton-PNIPAAm-H as compared with the pure polymer may be attributed to the micro-scale structure on the material surface. Hence, due to the hydrophilic-hydrophobic transition behavior of the PNIPAAm molecules, it is expected that the water saturated Cotton-PNIPAAm-H sample will release water above the LCST temperature. This transition process of Cotton-PNIPAAm-H fibers at different temperatures was captured by optical microscope and shown in the previous section (see Figure 6.5).

6.4 Conclusion

In conclusion, a smart textile surface was designed and fabricated by

grafting a temperature sensitive polymer brush directly from a hydrophilic cotton fabric substrate. Importantly, this material exhibits a superamphiphilic property which can be easily triggered by changing the temperature above and below the LCST temperature. A fully reversible conversion between superhydrophobicity and superhydrophilicity can be achieved in a short time. More interestingly, as the LCST temperature of PNIPAAm is about 34 °C, the switch between superhydrophilic and superhydrophobic states can be automatically controlled by the alternating day and night temperatures in nature. It is believed that this material can be used to collect the atmosphere humidity into recyclable water and help to alleviate water scarcity in arid area. It may also be used for water purification in the littoral area. The never-ending temperature cycle in nature will continuously supply the power for the switch between hydrophobic and hydrophilic states, and in turn produces the precious fresh water.

6.5 Reference

- 1 Fredlund, D. G. & Rahardjo, H. in *Soil Mechanics for Unsaturated Soils* 1-19
(John Wiley & Sons, Inc., 2007).
- 2 Gindel, I. IRRIGATION OF PLANTS WITH ATMOSPHERIC WATER WITHIN
DESERT. *Nature* **207**, 1173-&, (1965).
- 3 Parker, A. R. & Lawrence, C. R. Water capture by a desert beetle. *Nature* **414**, 33-34,
(2001).
- 4 Hamilton, W. J. & Seely, M. K. Fog basking by the Namib Desert beetle, *Onymacris*
unguicularis. *Nature* **262**, 284-285 (1976).
- 5 Zheng, Y. *et al.* Directional water collection on wetted spider silk. *Nature* **463**,
640-643, (2010).
- 6 Bai, H. *et al.* Direction Controlled Driving of Tiny Water Drops on Bioinspired
Artificial Spider Silks. *Advanced Materials* **22**, 5521-5525, (2010).
- 7 Nicholson, S. E. in *Dryland Climatology* 385 (Cambridge University Press,
2011).
- 8 Gates, H. L. A., Kwame Anthony. in *Encyclopedia of Africa* 213 (Oxford
University Press, 2010).
- 9 Ichimura, K., Oh, S.-K. & Nakagawa, M. Light-Driven Motion of Liquids on a
174

- Photoresponsive Surface. *Science* **288**, 1624-1626, (2000).
- 10 Gallardo, B. S. *et al.* Electrochemical Principles for Active Control of Liquids on Submillimeter Scales. *Science* **283**, 57-60 (1999).
- 11 Crevoisier, G. d., Fabre, P., Corpart, J.-M. & Leibler, L. Switchable Tackiness and Wettability of a Liquid Crystalline Polymer. *Science* **285**, 1246-1249, (1999).
- 12 Jiang, L., Zhao, Y. & Zhai, J. A Lotus-Leaf-like Superhydrophobic Surface: A Porous Microsphere/Nanofiber Composite Film Prepared by Electrohydrodynamics. *Angewandte Chemie International Edition* **43**, 4338-4341, (2004).
- 13 Erbil, H. Y., Demirel, A. L., Avci, Y. & Mert, O. Transformation of a Simple Plastic into a Superhydrophobic Surface. *Science* **299**, 1377-1380, (2003).
- 14 Daniel, S., Chaudhury, M. K. & Chen, J. C. Fast Drop Movements Resulting from the Phase Change on a Gradient Surface. *Science* **291**, 633-636, (2001).
- 15 Chaudhury, M. K. & Whitesides, G. M. How to Make Water Run Uphill. *Science* **256**, 1539-1541, doi:10.1126/science.256.5063.1539 (1992).
- 16 Konrad, W. & Roth-Nebelsick, A. Sorting of droplets by migration on structured surfaces. *Beilstein Journal of Nanotechnology* **2**, 215-221, (2011).
- 17 Yang, J.-T., Yang, Z.-H., Chen, C.-Y. & Yao, D.-J. Conversion of Surface Energy and Manipulation of a Single Droplet across Micropatterned Surfaces. *Langmuir* **24**,

- 9889-9897, (2008).
- 18 Fang, G., Li, W., Wang, X. & Qiao, G. Droplet Motion on Designed Microtextured Superhydrophobic Surfaces with Tunable Wettability. *Langmuir* **24**, 11651-11660, (2008).
- 19 Wenzel, R. N. RESISTANCE OF SOLID SURFACES TO WETTING BY WATER. *Industrial & Engineering Chemistry* **28**, 988-994, (1936).
- 20 Pu, H., Ding, Z. & Ma, Z. Vol. 62 1529-1535 (Wiley Subscription Services, Inc., A Wiley Company, 1996).
- 21 Corten, C., Kretschmer, K. & Kuckling, D. Novel multi-responsive P2VP-block-PNIPAAm block copolymers via nitroxide-mediated radical polymerization. *Beilstein Journal of Organic Chemistry* **6**, 756-765, (2010).
- 22 Lindqvist, J. *et al.* Intelligent Dual-Responsive Cellulose Surfaces via Surface-Initiated ATRP. *Biomacromolecules* **9**, 2139-2145, (2008).
- 23 Mittal, V., Matsko, N. B., Butté, A. & Morbidelli, M. PNIPAAm Grafted Polymeric Monoliths Synthesized by the Reactive Gelation Process and their Swelling/Deswelling Characteristics. *Macromolecular Reaction Engineering* **2**, 215-221, (2008).
- 24 Wang, J.-S. & Matyjaszewski, K. Controlled/"Living" Radical Polymerization. Halogen Atom Transfer Radical Polymerization Promoted by a Cu(I)/Cu(II) Redox

- Process. *Macromolecules* **28**, 7901-7910, (1995).
- 25 Edmondson, S., Osborne, V. L. & Huck, W. T. S. Polymer brushes via surface-initiated polymerizations. *Chemical Society Reviews* **33** (2004).
- 26 Pastore, C. M. & Kiekens, P. in *Surfactant Science* (CRC Press, New York, 2000).
- 27 Stuart, M. A. C. *et al.* Emerging Applications of Stimuli-Responsive Polymer Materials. *Nat. Mater.* **9**, 101-113 (2010).
- 28 Ono, Y. & Shikata, T. Hydration and Dynamic Behavior of Poly(N-isopropylacrylamide)s in Aqueous Solution: A Sharp Phase Transition at the Lower Critical Solution Temperature. *J. Am. Chem. Soc.* **128**, 10030-10031 (2006).

Chapter 7

Conclusions and suggestion for future work

7.1 Conclusions

In this thesis, cotton fabric surfaces were successfully modified with thermo-responsive PNIPAAm brushes using a surface-initiated ATRP method.

7.1.1 Low grafting efficiency sample

For low grafting efficiency sample, the polymer was confirmed by the combined results from FTIR, XPS, SEM and Solid-State NMR experiments. The grafting efficiency is rather low because of the low density of hydroxyl group available to the ATRP reaction. The structure and dynamics of the PNIPAAm brushes were investigated by both static and MAS ^1H NMR techniques. It has been shown that PNIPAAm molecules are immobilized by the covalent bond with the cotton surface. The mobility of PNIPAAm molecules is significantly restricted even at higher temperature (329 K).

In spite of the low-grafting efficiency of the sample Cotton-PNIPAAm-L, the structure and dynamics of the PNIPAAm brushes were investigated by both static and MAS ^1H NMR techniques, while still grafted on the cotton fabric. NMR results from D_2O saturated samples showed that while the temperature is below the LCST of PNIPAAm, the resonance peak intensity of PNIPAAm molecules increases with the increasing temperature. This was attributed to the hydrophilic-hydrophobic phase transition of PNIPAAm. The LCST of the PNIPAAm brushes grafted on the cotton fabric was estimated by VT- ^1H MAS

spectra to be 307 K (34 °C).

7.1.2 Improve the grafting efficiency

To improve the grafting efficiency of the temperature-responsive polymer is the primary concern of Chapter 4. In order to achieve this goal, the initiator need to be immobilized onto the cotton fabric surface as much as possible. Short-time UV pretreatment coupling with room temperature immobilization method was proved to be the most efficient way to increase the grafting efficiency of ATRP-initiator. After this treatment, a much higher grafting efficiency compared to that of the untreated sample was achieved. The grafting yield was evaluated by three different methods: NMR, TGA, and Gravity. The NMR and Gravity results are rather consistent with each other, whereas the TGA method tends to underestimate the grafting yield due to the overlapping between the decomposition processes. The cotton fabric grafted with PNIPAAm was characterized by FTIR, XPS, NMR, TGA, SEM and OM. It is shown that cotton fibers were covered with PNIPAAm brushes with a high grafting efficiency. SEM and OM images show a significant increase of the diameter of the cotton fibers and a dramatic difference in the surface morphology after being grafted with PNIPAAm.

7.1.3 High grafting efficiency sample

This highly grafted material exhibits a superamphiphilic property which

can be easily triggered by changing the temperature above and below the LCST temperature. A fully reversible conversion between superhydrophobicity and superhydrophilicity can be achieved in a short time. More interestingly, as the LCST temperature of PNIPAAm is about 34 °C, the switch between superhydrophilic and superhydrophobic states can be automatically controlled by the alternating day and night temperatures in nature. We believe that this material can be used to collect the atmosphere humidity into recyclable water and help to alleviate water scarcity in arid area. It may also be used for water purification in the littoral area. The never-ending temperature cycle in nature will continuously supply the power for the switch between hydrophobic and hydrophilic states, and provide us the precious fresh water.

7.2 Future work suggested

The surface modification and functionalization have been an ever-lasting research topic since the last century. Although many methods are available in literature to incorporate new functional materials onto various (organic or inorganic) substrates, only few scattered applications in industry can be found nowadays. The bottle-neck for the limited application in industry is apparently the high production cost. It is well-accepted that the ATRP is a robust technique to anchor a functional polymer onto a solid surface because with this technique, the molecular weight and molecular weight distribution (PDI) of the polymer can be very well controlled. However, the reaction condition of this method is

extremely demanding and consequently it will contribute to the production cost significantly. Therefore, in the near future, seeking a cheaper functional polymer substitute and exploring a less-demanding reaction condition are the most important issue from the industry point of view. To find a cheaper way of grafting the functional polymer, free radical polymerization method may be a promising candidate. This technique has been widely applied in industry because of its high polymerization efficiency and mild reaction condition. However, an apparent disadvantage of this method is that the molecular weight distribution (PDI) of the product can be very broad. Therefore, how the molecular weight and PDI of the grafted polymer affect the surface property of the substrates is still to be understood.

As it have discussed in Chapter 6, the ligand M_{e6} TERN exhibited superior controllable ability compared to PMDETA. However, the grafting efficiency of the cotton surface is decreased significantly, and the CA measurements showed no reversible change from superhydrophilicity at low temperature to superhydrophobicity at high temperature. To increase the grafting efficiency of polymer in presence of M_{e6} TERN will be an interesting topic in future work.

Comparing with the bare cotton and pure PNIPAAm polymer, grafted fiber Cotton-PNIPAAm can collect water from the atmosphere in low temperature, and automatically release in high temperature. As which measured in Chapter 6, the fiber weight will increase up to 340 % after collecting humidity. This moisture

absorption ability might be improved after grafting some superhydrophilic chains.

The cotton fiber with block copolymer chains which combined with superhydrophilic and temperature responsive polymers might exhibit superior humidity collection and controlled release ability.